Uncovering the molecular mechanisms of Joka2-mediated plant immunity

Gonzalo Arellano Dominguez

Imperial College of Science, Technology and Medicine

(Imperial College London)

Department of Life Sciences

A thesis submitted for the degree of Doctor of Philosophy

January 2025

Declaration of originality:

I declare that this thesis is a result of the author's own work. All the data and conclusions have been analysed and formulated by the author. Any external contributions are indicated and acknowledged appropriately. This study has been conducted at Imperial College London, between October 2020 and January 2025, and it has not been submitted for any other degree.

Abstract

Autophagy is a conserved eukaryotic mechanism essential for cellular homeostasis and immunity. In plants autophagy serves as a crucial defense layer against pathogens. The autophagy cargo receptor Joka2 plays a vital role in plant immunity, particularly in defense against *Phytophthora infestans*, although its precise mechanisms remain poorly understood.

This thesis investigates the molecular mechanisms through which Joka2 contributes to plant immunity. Using biochemical and cell biological approaches, I characterized three distinct aspects of Joka2 function. First, I demonstrated that Joka2 acts as a scaffolding protein for MAP kinase signaling cascades. Through detailed domain mapping, I showed that MAPK3, MAPK6, and MEK2 all bind to a specific region encompassing the NBR1, bZN, and ZZ domains. The NBR1 domain proved essential for MAPK6 phosphorylation, suggesting Joka2 facilitates signal transduction during immune responses. Second, I uncovered a novel redox-dependent property of Joka2 mediated by its newly identified helical bundle (HB) domain. Unlike its mammalian ortholog p62, Joka2 becomes more soluble under oxidizing conditions. This behavior is triggered by both direct oxidation and pathogen-associated molecular pattern (PAMP) treatment, suggesting a role in early immune responses. Finally, I established that Joka2 regulates defense-related gene expression during immunity. RNA-sequencing and subsequent validation revealed several Joka2-dependent defense genes, including key transcription factors. This regulation requires the NBR1 domain. I also discovered that the resistance Joka2 conferrs against *Phytophthora infestans* is independent of both the HB domain's redox sensitivity and conserved phosphorylation sites. Surprisingly, I found that

Joka2 maintains simultaneous interactions with both autophagy machinery and MAP kinases regardless of immune activation, suggesting parallel rather than switching functions.

Together, these findings reveal Joka2 as a multifunctional protein that integrates autophagy, signal transduction, and transcriptional regulation during plant immunity. This work provides new insights into plant defense mechanisms and suggests potential strategies for enhancing crop resistance to pathogens.

Table of contents

Table of contents **4**

List of tables and figures **8**

Acknowledgements **11**

Chapter 1 - Introduction **12**

1.1. The role of filamentous pathogens in food security 13

1.2 *P. infestans*, its mechanisms of infection and its effectors 13

1.3. Plant Immunity 17

1.4. Macroautophagy and defence-related autophagy 19

1.5 Subversion of autophagy by plant pathogens 21

1.6 Structure of Joka2 and its relationship to homologs 22

1.7 Aims 25

Chapter 2 - Materials and methods **27**

2.1 Biological material growth and maintenance conditions 28

2.2 Gene cloning 28

2.3 Agroinfiltration and co-immunoprecipitation (co-ip) 30

2.4 SDS-Page gels and western blotting 32

2.5 Confocal microscopy and FRAP 33

2.6 RNA extraction, cDNA synthesis and qPCR quantification 34

2.7 P. infestans preparation and PAMP treatment 34

2.8 Analysis of cell death 35

2.9 In planta infiltration and in vitro treatments of hydrogen peroxide 35

2.10 P. infestans infection assays 36

Chapter 3 - Understanding the binding of MAP kinase members and PAL to Joka2 ... 37

3.1 Introduction 38

3.1.1 The role of MAPKs in plant immunity 38

3.1.2 The role of PAL in immunity 40

3.2 Aims 41

3.3 Results 42

3.3.1 The NBR1 domain and adjacent regions are critical for Joka2-MAPK associations 42

3.3.1.1 Colocalization of Joka2 and MAPK3 occurs regardless of any individually missing domain 42

3.3.1.2 MAPK6 requires the NBR1-bZN-ZZ region for binding with Joka2. 45

3.3.1.3 The KR mutation in MAPK3 does not affect binding with Joka2 47

3.3.1.4 Lack of the NBR1 domain causes a reducction in phosphorylation of MAPK6 50

3.3.2 PAL associates with the UBA domains when binding to Joka2 independently of their ubiquitin binding ability 52

3.4 Discussion 56

Chapter 4 - The effect of redox on Joka2 solubility 61

4.1 Introduction 62

4.1.1 Redox signaling in plant immunity and stress responses 62

4.1.2 Thiols and their role in redox control and signaling 63

4.1.3 P62's s redox-dependent ability to aggregate is necessary for its function 64

4.2 Aims 65

4.3 Results 67

4.3.1 Joka2 responds to different oxidation states by changing solubility 67

4.3.2 Hydrogen peroxide exposure enhances Joka2 solubility 71

4.3.3 Redox-dependent solubility of Joka2 is independent of the ZZ domain 73

4.3.4 The HB domain mediates Joka2's temporal response to oxidative conditions 75

4.3.5 Recovery of insoluble Joka2 from pellet fractions under oxidizing conditions 77

4.3.6 Microscopic analysis confirms time-dependent changes in Joka2 puncta formation under oxidative stress 80

4.3.7 Joka2 and NPR1 exhibit distinct responses to oxidative stress and salicylic acid 83

4.3.8 PAMP-triggered immunity induces Joka2 reorganization in a HB domain-dependent manner 86

4.3.9 Fluorescence Recovery After Photobleaching reveals altered Joka2 mobility under oxidative conditions 89

4.3.10 The ΔHB mutant retains ATG8-binding functionality 91

4.4 Discussion 93

Chapter 5 - The role of Joka2 on gene expression and signalling 99

5.1 Introduction 100

5.1.1 Transcriptional regulation of plant defense 100

5.1.2 The role of p62 and NBR1 in signalling and gene expression 101

5.2 Aim 102

5.3 Results 103

5.3.1 Joka2 is responsible for the upregulation of certain genes associated with defence 103

5.3.2 Joka2 regulates several genes during the exposure of *N. benthamiana* to PAMP treatment. 105

5.3.3 ΔNBR1 is not able to rescue gene levels after being infiltrated into Joka2 silence plants 106

5.3.4 Removal of the HB domain does not decrease resistance towards P. infestans 109

5.3.5 None of the conserved phosphorilated residues in Joka2 have an effect on resistance. 110

5.3.6 PAMP treatment does not cause a shift in the colocalization of Joka2 between MAPK6 and ATG8 113

5.3 Discussion 115

Chapter 6 – General discussion and future perspectives 119

Appendix 126

R code 126

Fiji Macros 128

References 129

List of Tables and Figures

Figure 1.1: Cartoon representation of *P. infestans* infection and effector secretion. 17

Figure 1.2: Cartoon representation of Joka2 and its human and fungal homologues..... 23

Figure 3.1:Representative images of MAPK3:MkoK and several Joka2 truncates co-expressed in *N. benthamiana* leaves 43

Figure 3.2: Quantification of punctas between Joka2 truncates and MK3 show no difference with the exception of ΔPB1. 44

Figure 3.3: MAPK6 associates with all domains of Joka2 between ZZ and NBR1 46

Figure 3.4: MAPK is able to bind to Joka2 irrespective of which domain within the ZZ and NBR1 region is lacking. 47

Figure 3.5: The KR mutation in MAPK3 does not affect binding to Joka2. 48

Figure 3.6: MEK2kr binds all regions between ZZ and NBR1 with higher binding in NBR1…. 49

Figure 3.7: Removal of the NBR1 domain causes a reduction in the phosphorylation levels of MAPK6 51

Figure 3.8: PAL is able to bind the UBA domains of Joka2, irrespectively of ubiquitin binding ability. 52

Figure 3.9: PAL is unable to bind any other domain of Joka2 besides the UBA domain. 53

Figure 3.10: PAL is able to bind both ΔHB and ΔPB1/UBA. 54

Figure 4.1: Joka2 shows an increased solubility when exposed to media containing a lower amount of reducing agent 67

Figure 4.2:Joka2 shows an increased solubility when exposed to media containing a lower amount of reducing agent. 68

Figure 4.3:The change in solubility the Joka2 experiences is not linked to the HB domain of Joka2. 69

Figure 4.4: The shift in Joka2 is linked to the HB domain but not to the ZZ domain of Joka2
..... 71

Figure 4.5: Joka2 shows an increased solubility when exposed to media containing a higher amount of oxidizing agent. 73

Figure 4.6: The ZZ domain is not responsible for the shift in solubility when under increased oxidation conditions 74

Figure 4.7: Removal of the HB domain eliminates the solubility shift seen under increased oxidation conditions 76

Fig 4.8: When there is DTT present within the extraction media, pellets extracted with hydrogen peroxide or water exhibit no difference in the amount of Joka2 present.. 78

Fig 4.9: Removal of DTT from the extraction media, causes a significant difference in the band size when pellets are exposed to either water or hydrogen peroxide 79

Fig 4.10: Full length Joka2 and ΔZZ both respond to hydrogen peroxide with an increase in puncta numbers and a decrease in puncta size.. 81

Fig 4.11: ΔHB puncta size and number do not change when exposed to hydrogen peroxide 83

Figure 4.12: NPR1 oligomerizes upon response to exposure to salicylic acid. 85

Figure 4.13: Joka2 does not oligomerize upon exposure to salicylic acid 86

FIG 4.14:Joka2's response to PAMP extract cannot be determined using western blotting.
..... 87

Figure 4.15: Full length Joka2 and ΔZZ both respond to PAMP treatment with an increase in puncta numbers and a decrease in puncta size. 88

Figure 4.16: PAMP extract causes Joka2 puncta to recover faster after photobleaching but has no effect on ΔHB puncta recovery 90

Figure 4.17: ΔHB is still able to bind ATG8 similarly to full length Joka2 92

Figure 5.1: Joka2 alters gene expression when the plant is exposed to PAMP treatment…. 104

Table 5.1: Selected genes that are significantly upregulated by Joka2 during PAMP treatment. 105

Figure 5.2: Silencing of Joka2 causes differences in gene expression levels during PAMP treatment. 106

Figure 5.3: Agroinfiltration of Joka2 is able to restore gene expression levels so there is no significant difference between GUS and Joka2 silenced plants during PAMP treatment except for the protein of unknown function. 107

Figure 5.4: Agroinfiltration of ΔNBR1 is not able to restore gene expression levels so there is a significant difference between GUS and Joka2 silenced plants during PAMP treatment. 108

Figure 5.5: Removal of the HB domain does not reduce resistance to P. infestans. 109

Fig 5.6: Joka2 and its homologs share five conserved residues that are possible phosphorylation targets 111

Fig 5.7: Mutation of conserved phosphorylated residues did not result in lower necrosis levels upon P. infestans infection. 112

Fig 5.8: Joka2 does not associate differently between ATG8 and MAPK6 when exposed to PAMP treatment 113

Figure 6.1: Summary figure of the role of Joka2 during immunity 121

Acknowledgements

First and foremost, I would like to thank my parents as well as my siblings for their unwavering support throughout this long journey. Without that support, this thesis would not have been possible.

I would then like to thank all of my labmates, Yasin Tümtaş for his never ending patience in showing me the ropes, Tarhan Ibrahim for his immense knowledge and great amount of tips and tricks in the lab, Eleonora Moratto for her sense of humour (Kneecap!) and her empathy, Enoch Yuen for his brain teasers and crosswords breaks, Freddie King for his mid-morning coffee breaks and bioinformatic skills and Cristina Vuolo for her endlessly good vibes and immaculate memes. As well as my students Cecilia Longoni and XinYi Yang, whom I assure have a wonderful future ahead in science. I also want to thank my supervisor Tolga Bozkurt I also need to thank Giorgos Kourelis and Bernadette Byrne, for their gargantuan help during some of my lowest moments, as well as Blanca Landa del Castillo for her help from abroad.

I cannot thank enough all of my friends who have helped me through this journey, including Öykü Ozçan, Renata Oliveira de Vasconcelos, Mar Ferrando Marco, Alba Jimenez, Alex Taylor, Vanda Adamkova and Jovan Esmenos. I am immensely grateful for their moral support and their oddly large ability to tolerate my nonsense.

I would also like to thank the Imperial College boardgame society, more explicitly, I would like to thank all of the members of the Magic: The Gathering club, who made my Thursday nights unimaginably enjoyable and made me discover a new hobby that will stay with me for a long time.

Chapter 1 - Introduction

1.1. The role of filamentous pathogens in food security

Filamentous plant pathogens are one of the most prolific plant pathogens. This group of eukaryotes, consisting of both fungi and oomycetes, contain some of the most notorious disease causing organisms and are estimated to cause hundreds of billions of dollars in both lost crop and overall yield reduction (Anand & Rajeshkumar, 2022) One of the most prolific members of this group is *Phytophthora infestans*, the causative agent of late potato blight in members of the Solanacee family and the main pathogen in this study. This pathogen is amongst the most prolific plant pathogens, as it was the cause behind the Irish potato famine in the 1800s, a period which led to widespread social and economic devastation including the deaths of approximately one million people (Yoshida et al., 2013). Current strategies to control the pathogen mostly fall into one of two categories: resistance gene based, such as the use of the *Rpi-blb1* gene from the wild potato species *Solanum bulbocastanum*, or chemical based (Rakosy-Tican et al., 2020). Both of these approaches are currently not adequate enough to manage the *P. infestans* problem, as gene based approaches are often short lived due to *P. infestans* quickly evolving resistances to them and chemical approaches can only be used prophylactically since the pathogen is mostly intracellular and as such is shielded from exposure by the host. (Coomber, Saville & Ristaino, 2024; Ivanov, Ukladov & Golubeva, 2021) Therefore, the discovery of new and improved methods to both control and prevent the spread of this pathogen further is crucial for the survival of our crops.

1.2 *P. infestans*, its mechanisms of infection and its effectors

For *P. infestans*, the infection cycle begins with a motile zoospore traveling through wind or mist in conditions of high ambient humidity. Once this spore lands on the

adaxial side of a host leaf, it begins to germinate. The spore first develops into a cyst by discarding their flagella and forming a cell wall around them (Whisson et al., 2016) and then forms an appressorium. This appressorium will then through mechanical forces break both the plant cuticle and epidermis, opening a point of entry (Bronkhorst et al., 2022). After going through this point of entry, the first cell that *P. infestans* encounters is killed and a primary infection vesicle is formed within it. From here onwards the pathogen growth becomes apoplastic, with the formation of long filaments named hyphae extending from the originally infected cell. (Whisson et al., 2016)

Hyphae then branch into smaller, finger-like projections named haustoria. Haustoria serve as a means for the pathogen to colonize new cells and proliferate throughout the plant, and are responsible for both nutrient uptake and the release of pathogen produced virulence factors known as effectors.(Wang, S. et al., 2018) *P. infestans* releases hundreds of effectors both cytoplasmic and apoplastic to manipulate host physiology and undermine host defence. Although the exact methods for the exchange of effectors and nutrients throughout the haustoria are yet unknown, there is evidence pointing towards the presence of sugar transporters within them (Mendgen & Nass, 1988). There is also evidence that hyphae may be able to transport other macromolecules such as RNA such as in the case of parasitic plants that also use hyphae (Shahid et al., 2018).

Once haustoria reach an uncolonized cell and begin penetration, a new host-derived lipid bilayer continuous with the plasma membrane known as the extra haustorial membrane (EHM) forms around the finger-like structures. (Lu et al., 2012) The origin

of this membrane is unknown, it has a different composition than that of the plant's own plasma membrane, lacking most of its associated proteins. There are, however, some exceptions to this rule, with proteins present in both the EHM and the plasma membrane, including the vesicle fusion protein SYNAPTOTAGMIN1 and the membrane associated protein Remorin1.3 (Bozkurt et al., 2014).

Further investigation into the EHM points to it being a highly specialized structure that is specifically tailored for each pathogen to develop its own infection strategy rather than it being a static structure, since the composition of the EHM varies depending on the invading pathogen. Examples include the early endosomal marker Rab5 being present during *P. infestans* infection in *Arabidopsis thaliana* (Lu et al., 2012), but not being present during infection by the fungal pathogen *Colletotrichum higginsianum* (Inada et al., 2016). Variation of the EHM is not only limited to proteins, but also phospholipids, with the EHM containing increased levels of $PI(4,5)P_2$ compared to the plasma membrane during powdery mildew infection (Qin et al., 2020). One final difference between EHMs from different pathogens is the way in which the plant responds to them, upon detection of an invading haustoria, most plants deposit callose around the EHM in a process known as focal immunity (Caillaud et al., 2014). The extent of cover of this callose, however, varies depending on the pathogen type. In the case of *P. infestans* most of the haustoria lack this callose encasings, although the mechanism for this remains unknown (Bozkurt et al., 2014).

The space between the haustoria and the EHM is named the extra haustorial matrix (EHMx) and it serves as the main site of exchange between the pathogen and the

host. The main method of transport is through the use of extracellular vesicles (EVs) (Micali et al., 2011). These vesicles are used by both pathogen and host and serve as a two-way site of communication, with the pathogen using them for the transport of effectors and the host for molecules pertaining to its defence strategy, including small RNA molecules (Baldrich et al., 2019; Cai, Q. et al., 2018; Wang, S. et al., 2017). The origin of these plant EVs varies in their intracellular origin, with three current subpopulations in *A. thaliana* determined by the presence of different markers (TET 8, PEN1 and exocyst positive EVs) (Cai, Q. et al., 2021; Liu, G. et al., 2021; Rutter & Innes, 2017).

As mentioned before, *P.* infestans releases a set of small proteins capable of immunomodulation known as effectors. Most oomycete effectors contain an RXLR motif prior to the N-terminal secretion signal (Bozkurt et al., 2012). This motif is necessary for secretion but not for its role inside the plant cell. However, the mechanism of translocations is yet unknown, even more so with the recent realization that RXLR effectors like the plasmodium PEXEL effectors both undergo cleavage of their motifs inside their respective pathogens before being released into the host (Boddey et al., 2016; Wawra et al., 2017).

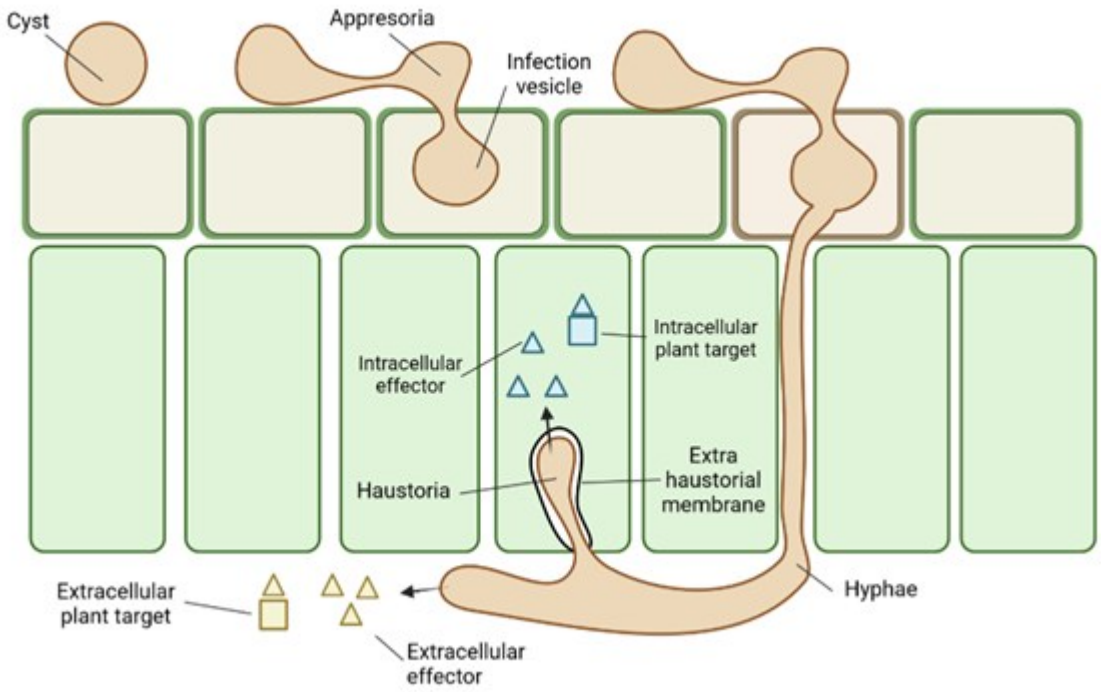

Figure 1.1: Cartoon representation of *P. infestans* infection and effector secretion. After germination of the zoospore at the surface of the host, an appressorium is formed. The cell adjacent to the appressoria, is the colonised and an infection vesicle is formed inside it. From this infection vesicle, hyphae then extend into the apoplastic space, and smaller haustoria which branch from the main hyphae are used to colonise individual cells.

1.3. Plant Immunity

Plants lack motile cells. As a result, once pathogens have penetrated the physical barriers that plants have as a first line of defence, their main defence strategy relies upon different kinds of receptors that allow for pathogen detection. These can broadly be characterised into two different subsets (Dodds & Rathjen, 2010). Pattern recognition receptors (PRRs) are usually located on the exterior part of the plasma

membrane and are responsible for the detection of pathogen or damage-associated molecular patterns (PAMPs / DAMPs) These receptors usually take the form of receptor like kinases (RLKs) or receptor like proteins (RLPs) (Giraldo & Valent, 2013; Giraldo et al., 2013).

Upon detection of the conserved motifs, PRRs trigger pattern triggered immunity (PTI). However, pathogens have specialized a way to overcome this immunity through the use of the aforementioned effectors, which commonly suppress the mechanisms by which this immunity is carried out . As a response, plants evolved the second layer of defence which relies on the detection of these effectors through nucleotide binding leucine rich repeats (NB-NLRs) (Cui, Tsuda & Parker, 2015). These NLRs can be further classified through the domain found in their N-terminus. The three main types are coiled coil (CC-NLRs), RESISTANCE TO POWDERY MILDEW 8 (RPW8-NLRs) and toll/interleukin-1 receptor-type (TIR-NLRs) (Contreras et al., 2023). The collective response from these receptors is termed effector triggered immunity (ETI).

Both PTI and ETI, although orchestrated by different effectors, generally overlap in terms of the downstream response they produce, resulting in the upregulation of defence gene expression, reactive oxygen species production, calcium spiking and defence hormone production. Both of these responses are closely associated with stronger immune responses such as the hypersensitive response (HR) (Cui, Tsuda & Parker, 2015; Giraldo et al., 2013).

Besides ETI and PTI, there is another layer of defence in focal imunity. Focal immunity is the collective term that results from the reorganization of the plant's cytoskeleton resulting in the localization of defences alongside the point of entry of

the pathogen into the cell. This includes the previously mentioned callose deposition around the haustorial interface, as well as the formation of cell wall papillae (Li, P. et al., 2020).

One of these focal immune responses includes the re-routing of autophagosomal vesicles into the infection site.

1.4. Macroautophagy and Defence-related autophagy

Autophagy is a conserved eukaryotic self-eating catabolic mechanism through which cargo is sequestered and degraded by its delivery into the lytic organelle. (Gatica, Lahiri & Klionsky, 2018). Autophagy was first described in rat liver cells, but the genes responsible for the expression of proteins controlling this process were documented first in *Saccharomyces cerevisiae* (Yang, Z. & Klionsky, 2010). It can currently be divided into three large categories: macroautophagy and microautophagy, which is present in all eukaryotes; and chaperone mediated autophagy, only present in animals. (Yamamoto & Matsui, 2024) In this study I will be focusing mostly on macroautophagy, the most well studied of the three.

Macroautophagy (hereafter referred to as autophagy) consists in a *de novo* formation of a double-membrane vesicle known as the autophagosome, and used to sequester intracellular cargo. This vesicle is then used to deliver cargo into the litic organelle (Lysosomes in animals and the vacuole in plants). (Yamamoto & Matsui, 2024)

This process, originally thought to be a bulk degradation process, is now thought to be highly selective. This specificity is conferred by proteins lining the inside of the

autophagosome known as cargo receptors.(Adriaenssens, Ferrari & Martens, 2022) These cargo receptors then bind the autophagosome through either ATG8 in plants or through its animal analogue LC3. Both proteins are found on the interior membrane of the autophagosome and utilize special motifs to allow cargo receptors to bind them. ATG8 uses the ATG8 interactive motif (AIM) while LC3 uses the LC3 interactive region (LIR) (Rogov et al., 2023).

Like ATG8, there exist about forty other known autophagy related (ATG) proteins found in plants that are responsible for the correct working of the autophagic process. ATG proteins oversee the main four stages of autophagosome formation (initiation, nucleation, elongation and completion) as well as the autophagosome-lysosome or autophagosome-vacuole fusion process (Nishimura & Tooze, 2020).

The role of autophagy in pathogen clearance is well-documented in mammals, with studies showing increased susceptibility to *Mycobacterium tuberculosis* (Golovkine et al., 2023) and several *Streptoccocus* species in autophagy deficient cells (Shi et al., 2024). However, recently new evidence has emerged that autophagy also plays a role in defence against plant pathogens. An example of this is how cassava plants (*Manihhot esculenta*) use WRKY20 to upregulate *ATG8* transcription during *Xanthomonas axonopodis* infection, with silenced plants resulting in increased disease succeptibility (Yan et al., 2017).

In plants, autophagy plays a dual role in defense, acting as both a pro-survival and pro-death mechanism depending on the context. In PTI, autophagy regulates key immune components, such as PRRs (pattern recognition receptors), ensuring proper

degradation and turnover. For instance, it prevents over-accumulation of FLAGELLIN-SENSING 2 (FLS2), a critical receptor in bacterial flagellin recognition, thereby modulating basal immune responses (Yang, F. et al., 2019). In ETI, autophagy supports the containment of hypersensitive response-programmed cell death (HR-PCD), preventing its spread beyond the infection site, which is essential for limiting pathogen proliferation (Liu, Y. et al., 2005).

With this duality, autophagy is able to improve defence against both biotrophic and necrotrophic pathogens. Examples include infection from the biotroph *Pseudomonas syringeae* in *A. thaliana*, against which, silencing of *ATG* genes create enhanced susceptibility in the host (Üstün et al., 2018). On the other hand, the necrotrophic pathogens *Alternaria brasssicicola* and *Botrytis cinerea* both result in increased necrotic infection in autophagy-impaired plants (Hofius et al., 2011).

1.5 Subversion of autophagy by plant pathogens

Since autophagy is now understood to be a key defence mechanism against disease, many pathogens actively target the autophagic machinery as part of their invasion strategy. One of the most common ways is through the use of effectors such as the Cauliflower mosaic virus P6 protein binding and activating the negative autophagy regulator TARGET OF RAPAMYCIN (TOR) in *A. thaliana* (Zvereva et al., 2016).

Although the use of effectors does not necessarily entail the suppression of autophagy, other pathogens like *Ralstonia solanacearum* inhibit TOR through their AWR5 effector to increase the rate of autophagy, but then use this to their advantage through the use of metabolic re-routing facilitating nutrient acquisition before their

transition to the necrotrophic phase (Popa et al., 2016). Autophagy can also be used indirectly to gain an advantage during infection like how poleroviruses use the P0 protein to trigger ARGONAUTE1 degradation, reducing the amount of RNA-silencing complexes within the cell (Csorba et al., 2010).

Although effectors are the most common method to subvert autophagy, pathogens can also use phytotoxins to prevent autophagy like in the case of *Sclerotina sclerotiorum* who secretes oxalic acid as a method to overcome autophagy, with oxalic acid deficient mutants not showing pathogenicity (Zhu et al., 2024).

1.6 Structure of Joka2 and its relationship to homologs

Joka2 is an autophagy cargo receptor and as such is responsible for determining some of the cargo the autophagosomes carry and then degrade (Zientara-Rytter et al., 2011). As a result it plays a vital role in the defence of the plant but is also targeted by pathogen effectors as a way to prevent successful defence.

The structure of Joka2 from N to C terminus consists of a phox/Bemp1p (PB1) domain that is used in self-oligomerization, a zinc finger domain (ZZ), a neighbor of BROCA1 (NBR1) domain of unknown function and two ubiquitin association domains (UBA) that are able to bind ubiquitinated cargo, a common protein tag used to denote cargo that should be degraded. In the first alpha helix of the second UBA domain is where the AIM motif is located (Zientara-Rytter et al., 2011).

Joka2 structure is highly resemblant of its *A. thaliana* counterpart, and resembles both of its human homologs NBR1 and p62 (Figure 1.2). The fungal ATG19 although slightly less similar to Joka2 with the loss of the ZZ domain has also been demonstrated to be a Joka2 homolog (Kraft, Peter & Hofmann, 2010).

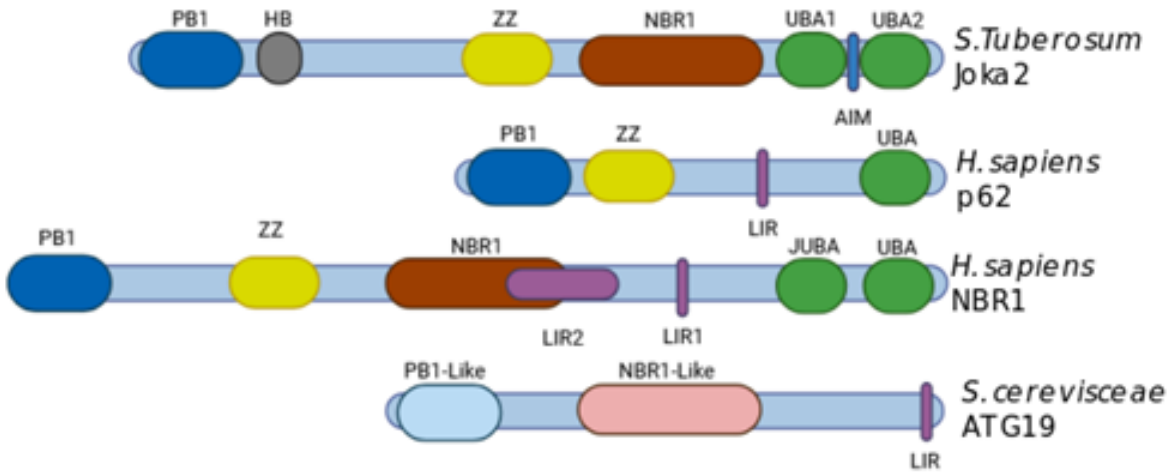

Figure 1.2. Cartoon representation of Joka2 and its human and fungal homologues. PB1:phox/Bemp1p, UBA: Ubiquitin-binding domain, Juba: Amphipathic helical domain, ZZ: ZZ-type zinc finger domain, NBR1: Neighbour of BRCA1 gene, HB: Helical bundle, LIR: LC3 interacting region, AIM: ATG8 interacting motif.

One of the examples of Joka2 contributing to immunity is in the invasion by the cauliflower mosaic virus (CaMV) . Joka2 interacts with the P4 capsid protein of CaMV leading to viral autophagy and removal of the viral particles (Hafrén et al., 2017). CaMV is then able to fight back against the pant defences by producing inclusion bodies to prevent recognition. CaMV is also able to modulate non-selective autophagy, meaning autophagy that does not targuet specific molecules, leading to less plant senescence giving the virus a longer time frame from which to be picked up by aphids and transported to a new host.

Joka2 also plays an antagonizing role to the Turnip mosaic virus (TuMV) through its interaction and subsequent degradation of the helper component proteinase (HCpro) (Hafrén et al., 2018). This interaction seems to be carried out through the ubiquitinated potyvirus- induced granules (PGs), as the removal of the UBA domains from Joka2 lowers the percentage colocalization of Joka2 and HCpro and leads to

more susceptibility. In order to circumvent this defence, TuMV secretes the effector VPg which manipulates the host autophagy machinery into degrading itself, leading to autophagy deficient cells with an inability to degrade the viral particles (Huang, X. et al., 2020).

The final pathogen that is known to target Joka2 is *P. infestans*. Although the mechanism behind the increased resistance towards *P. infestans* is not fully known yet, it is understood that the AIM motif of Joka2, the region responsible for ATG8 binding as Joka2 is important for this interaction, since AIM mutants were unable to contribute to immunity (Dagdas et al., 2018). *P. infestans* takes advantage of this and uses the PexRD54 effector, which also contains an AIM motif that has a higher binding affinity to ATG8 than that of Joka2, resulting in Joka2 being outcompeted and *P. infestans* being able to subvert the autophagic process and redirect autophagosomes towards the haustoria in order to obtain nutrients from the host. PexRD54 effectors with non-functioning AIMs do not enhance virulence (Dagdas et al., 2016). Recent discoveries have also yielded that the NBR1 domain is necessary for *P. infestans* resistance, possibly because NBR1 serves as a scaffolding protein for the members of the MAPK family, and NBR1 serves as the domain that interacts with MAPK3 (Tumtas *et al*, Unpublished).

Joka2 human homolog NBR1 also plays a role in prevention of human disease, a good example of this being its role against influenza A. However, it also serves as a target for viral manipulation similarly to Joka2, with the H7N9 strain using its PB1 protein to associate with NBR1 causing it to degrade the Mitochondrial antiviral-signalling protein, which would otherwise antagonize the virus (Zeng et al., 2021).

NBR1 in humans is also associated with diseases caused by protein aggregation, which is especially true when NBR1 is mutated or otherwise unable to perform its role in protein aggrephagy. Examples of this include: sporadic inclusion body myostitis (sIBM), a progressive degenerative myopathy where lack of phosphorialtion of NBR1 at Thr586 results in NBR1 not being able to degrade ubiquitinated cargo and instead aggregating alongside p62 and LC3, resulting in large accumulations of misfolded proteins within muscle cells (D'Agostino et al., 2011; Nicot et al., 2014), hereditary myophathy with early respiratory failure, where a mutation in NBR1 prevents it from binding the serine/threonine kinase domain in titin, making it unable to recruit p62 and MURF2 and causing both p62 and MURF2 to agreggate (Lange et al., 2005) as well as Parkinson's disease, where NBR1 is found inside Lewy bodies and in alcoholic steatohepatitis where both NBR1 and p62 are found within Mallory bodies (Kirkin et al., 2009; Odagiri et al., 2012).

1.7 Aims

The goal of my PhD was to dissect the functional principles of defence-related autophagy in order to understand how it is able to contribute to disease resistance. To do so, I focused on the autophagy cargo receptor Joka2, which has been demonstrated to increase immunity against *P. infestans*, although the mechanism for which has not been elucidated. I have employed a multidisciplinary approach including both cell biology and biochemistry to study how Joka2 mediates autophagy, as well as to investigate other non-autophagy related mechanisms through which Joka2 is able to contribute to immunity. To achieve this goal I pursued the following objectives:

1. **To determine the role of Joka2 when binding members of the MAPK family and other defence related proteins**. Preliminary data has already shown how Joka2 is able to bind MAPK3 and MAPK6 and that the NBR1 domain of Joka2 is responsible for the binding of MAPK3. I hypothesised that Joka2 could serve as a scaffolding protein for members of the MAPK family, as such I investigated the distinct regions that Joka2 uses to bind the MAPKs as well as PAL, another important enzyme in defence.

2. **To understand how a change in the redox potential of the environment leads to changes in Joka2 solubility.** The serendipitous discovery that Joka2 reacts to changes in redox potential by shifting solubility could imply that it undergoes phase transition within the cell. The characterization of this mechanism and its causes could yield some insights into how Joka2 is responsible for resistance against pathogens.

3. **To discover how Joka2 and its domains are responsible for immunity against pathogens.** Joka2 has already been shown to contribute towards *P. infestans* immunity in *N. benthamina*. However the mechanism for this is unknown, and as such, I wanted to elucidate weather the previous interactions between Joka2 and the MAPKs as well as the apparent phase transition of Joka2 play a role in this resistance. I also wanted to research whether this resistance was also true for pathogens besides *P. infestans*

Chapter 2 - Materials and methods

2.1 Biological material growth and maintenance conditions

N. benthamiana plants were grown in a mixture of 3:1 made of organic mixture and vermiculite respectively. Plants were grown under constant conditions with a 16 hour photoperiod. Daytime conditions consisted of 50% humidity and 24 ºC and nighttime conditions consisted of 65% humidity and 22 ºC.

P. infestans cultures were grown in rye sucrose agar plates which were kept in the dark and at 18 ºC. *P. infestans* plates were used for experiments 3 to 4 weeks after the plates were inoculated.

2.2 Gene cloning

Designated primers with overhangs designed for Gibson assembly were added to cDNA extracted from *N. benthamiana* plants and the subsequent mixture was amplified *via* PCR through the use of Phusion proof-reading DNA polymerase (New England Biolabs). Promega's PCR clean up kit was then used to purify the end result of this reaction. Genes were N terminally fused to a protein marker (GFP or 3xHA) which had already been inserted into the pJK7WGF2 plasmid. The addition of this marker was done by plasmid excision with the restriction endonuclease EcoRV. After an initial plasmid digestion, a new segment was inserted into the plasmid containing the designated marker, as well as a linker region and a secondary EcoRV restriction site.

Plasmids were digested for a second time before being mixed with the purified PCR product and Gibson assembly mix, containing 5x Isothermal reaction buffer (25% PEG-8000, 500 mM Tris-HCl, 50 mM MgCl2, 50 mM DTT, 1 mM adenine, guanine,

cytosine and thymine each and 5 mM NAD), T5 exonuclease (Epicentre), Phusion DNA polymerase (New England Biolabs) and Taq DNA ligase (New England Biolabs). This mixture was incubated for 2 hours at 50 °C, and then preserved at 4 °C until it was needed.

Vectors were transformed into chemically competent DH5α cells by heat shock at 42 °C for 90 seconds followed by immersion into ice for 2 minutes. Cells were resuspended in antibiotic free LB media and allowed to recover for 2 hours through incubation at 37 °C whilst shaking at 700rpm. Cells were seeded on LB agar plates containing 50 µg/mL kanamycin and allowed to grow at 37 °C for 1-2 days until colonies were visible. Recombinant colonies were then detected through colony PCR using the vector specific primers 35sF and Rev2.

Single recombinant colonies were then used to create overnight cultures from which plasmids were isolated, by using Promega's Pure yield plasmid miniprep kit and sent for sequencing. After obtaining positive sequencing results, electrocompetent GV3101 *Agrobacterium tumefaciens* bacteria were transformed using Bio-Rad's micropulser, which were then allowed to recover in antibiotic free LB media for 2 hours and subsequently plated in LB agar plates containing 50 µg/mL kanamycin and 20 µg/mL gentamycin. Single colonies were then isolated and used to create glycerol stocks consisting of 50% glycerol and 50% overnight *A. tumefaciens* culture. These were then stored in -80 °C for long term usage.

2.3 Agroinfiltration and co-immunoprecipitation (co-ip)

A. tumefaciens bacteria containing the gene of interest were harvested form LB plates and resuspended into 1mL of distilled water and centrifuged twice at 4000 rpm

(1500g) for 5 minutes. This washing step was repeated twice more until the cells were finally resuspended in 1 mL of agroinfiltration buffer (10 mM MgCl2, 5 mM 2-(N-morpholino)-ethanesulphonic acid (MES), pH 5.6). The OD600 of the resultant mixture was obtained and adjusted to 0.2 for all constructs except for Joka2, which required 0.3. 4-5 week old *N. benthamiana* plants were infiltrated on the abaxial side of the leaf, with the help of a 10 mL syringe, until the whole leaf turned a dark green colour, indicating all of it was infiltrated. Leaves were left attached to the plant for two days, after which, they were detached, weighed and subsequently flash frozen in liquid nitrogen inside 50mL Falcon tubes. For easier handling and processing, the weight of all leaves was equalised before they were flash frozen. This depended on the biomass of the leaves infiltrated, but usually varied between 1.5 and 2.5 g of wet tissue.

Flash frozen leaf tissue was then ground to a fine powder using a mortar and pestle which had been previously chilled to avoid defrosting. Grinded tissue was placed into new 50mL tubes, and twice the volume of the sample was added as elution buffer (GTEN (10% glycerol, 25 mM Tris-HCl pH 8.3, 1 mM EDTA and 150 mM NaCl), 10 mM DTT, 0.5% protease inhibitor cocktail (Sigma-Aldrich), 2% w/v polyvinylpolypyrrolidone (PVPP), 1 mM phenlymethylsulphonylfluoride (PMSF) and 0.1% w/v IGEPAL). The mixture was vortexed vigorously for 1 minute and immediately after centrifuged at 3500g at 4 °C for 20 minutes. Once this had been completed, without disturbing the pellet, the supernatant was the passed through 22-25 µm pore size miracloth (Merck Millipore). Filtrate was recentrifuged with the same conditions as before and the resultant supernatant was re-collected in 5 mL Eppendorf tubes.

At this point 55 µL of every supernatant was extracted and kept at -20°C until they would be later run on an SDS-Page gel as part of the “Input’’ series. The supernatants that were not reserved for later, were then incubated for either 1 hour or overnight at 4 °C along with a mixture of 12 µL agarose beads containing anti-GFP antibodies (GFP trap (Chromotek)) and 188 µL of IP buffer (GTEN and 0.1% w/v Tween 20).

Once the time had transpired, the mixture was then centrifuged for 1 minute at 800g, and the supernatant was discarded with the use of a syringe and needle. Beads were resuspended in 1mL of IP buffer and transferred to 1.5 mL tube and inverted 30 times. This washing step was repeated twice and in the final step, no more IP buffer was added. Instead, the tubes were centrifuged again, in order to remove any residuum from the walls, and needles were used to eliminate any final drops.

Finally, in order to extract the proteins from the beads, 25 µL of Elution Buffer (25% 4x Laemmli buffer (2% w/v SDS, 10 mM DTT, 10% w/v glycerol, 60 mM Tris and 0.01% w/v bromophenol blue), 20% of DTT and 55% distilled water) was added to the beads and they were then left on a heating block for 10 minutes at 70 °C. After this, they were centrifuged for 5 minutes at 4000 g and 10-15 µL of the remaining supernatant, loaded into an SDS gel.

For the ‘’Input’’ series that I had set aside before, 20 µL of DTT and 25 µL of Laemmli buffer (2% (w/v) SDS, 10 mM DTT, 10% (v/v) glycerol, 60 mM Tris and 0.01 % (w/v) bromophenol blue) were added, and 20 µL of the resulting mixture, loaded into an SDS-Page protein gel.

2.4 **SDS-Page gels and western blotting**

The SDS gel used, consisted of two main parts, a 4% acrylamide w/v top layer, named the stacking phase. (625 µL of 1.5M pH 8.3 Tris buffer, 250 L of 40% acrylamide:bis acrylamide 13 solution (37.5:1; Bio-Rad), 1585 µL of distilled water, 25 µL of 10% SDS solution, 12.5 µL of 10x ammonium persulfate solution (APS) and 2.5 µL TEMED (N,N,N',N'-tetramethylethylene-diamaine) (Bio-Rad) and a bottom layer called the separating phase, consisting of a mixture of 8% acrylamide w/v. (625 µL of 0.5 M pH 6.8 Tris buffer, 500 µL of 40% acrylamide:bis acrylamide solution (37.5:1; Bio-Rad), 1335 µL of distilled water, 25 µL of 10% SDS solution, 12.5 µL of 10x APS and 2.5µL TEMED) and 16% acrylamide w/v. (625 µL of 0.5 M pH 6.8 Tris buffer, 1000 µL of 40% acrylamide:bis acrylamide solution (37.5:1; Bio-Rad), 835 µL of distilled water, 25 µL of 10% SDS solution, 12.5 µL of 10x APS and 2.5 µL TEMED)

To assemble the gel, a serological pipette was used to obtain 2.2mL of the 8% solution, followed by 2.2 mL of the 16% solution. Then, an air bubble was passed through this mixture, in order to obtain a homogenous gradient from top to bottom. This was then lowered into two glass slides and left to solidify. A layer of isopropanol was added, as to avoid the creation of bubbles. Once the first part of the gel had fully solidified, the isopropanol was removed and 2.2 mL of the 4% mixture was added and a comb used to remove any final bubbles and to mark the position of the wells.

The gel was run on SDS-Page running buffer, initially starting at 80 V, and once the proteins had passed by the stacking gel, increasing the voltage to 100 V and 45 minutes after this point increasing it again to 110 V.

Once a total of 1.5 hours had passed since the first voltage was applied to the gel, the current was stopped, and the gel removed. The stacking phase was then discarded. Two stacks of 5 Wypall x70 cloths were submerged in Bjerrum Schafer-Nielsen Buffer (48 mM Tris Base, 39 mM glycine, 1.3 mM SDS (0.00375% w/v) and 10% w/v ethanol). In the meantime, a polyvinylidene difluoride (PVDF) membrane was soaked in absolute methanol to activate it.

The setup is then assembled on a tray of the semi-dry Trans-Blot Turbo transfer system, by placing one of the Wypall stacks at the bottom, followed by the membrane, the separating portion of the gel and finally another stack of Wypall on top. The standard Bio-Rad transfer protocol was used for the transfer (Constant 25 V, 1.0 A for 30 minutes).

2.5 Confocal microscopy and FRAP

Leaf discs from *N. benthamiana* leaves using a cork borer of size 3 were mounted on microscope slides with the use of Carolina observation gel (Carolina Biological Supply Company). The abaxial side of the live tissue was performed using a Leica SP5 resonant inverted confocal microscope (Leica Microsystems) using a 63x water immersion objective or a Leica SP8 with a 40x water immersion objective. GFP and mKOk fluorophores were excited using 488 and 561 nm laser diodes and their fluorescent emissions detected sequentially at 495-550 and 570-620 nm respectively. Images were then compressed as maximum intensity projections of Z-stack confocal images. For FRAP, candidate puncta of 3.5μm ±0.1 were bleached with 488nm laser (Ar, 65 mW) at 100% for 30 seconds (zoom=6.00), then imaged at 10 second intervals for 6 minutes (zoom=3.59, gain intensity=3.9%), manually adjusting the z-plane to keep the full puncta visible. Individual images were processed for analysis using ImageJ (FIJI) and Inkscape

2.6 RNA extraction, cDNA synthesis and qPCR quantification

Genetic material was extracted from liquid nitrogen flash frozen leaf discs using the RNAeasy plus mini kit (Quiagen) followed by the removal of DNA using the TURBO DNA-free™ Kit (Thermo Fisher). RNA quality was then determined through both nanodroping and running the sample through a 1% agarose gel. Once purity was deemed acceptable, first strand cDNA was synthesised through the use of Roche's Transcriptor First strand cDNA synthesis kit. RT-qPCR was then performed in the LightCycler® 480 II. RNA expression data was then normalised to the control

glyceraldehyde-3-phosphate dehydrogenase (GAPDH) housekeeping gene analysed using the LightCycler480 software (Version 1.5.1.62 SP2).

2.7 *P. infestans* preparation and PAMP treatment

P. infestans hyphae were collected from RSA plates with the use of a scalpel and scraped into 10mL of glass distilled water. The resultant suspension was then incubated for 10 min at 90 ºC inside a water bath to neutralise any living tissue. The resulting solution was then filtered through miracloth and subsequently filtered using a 0.45µm filter to remove any large particles still present. The resulting liquid was kept at -20 ºC until the time for infiltration. This *P. infestans* extract was then infiltrated into *N. benthamiana* plants in order to trigger PTI due to the PAMPs present within the extract. Protein levels and other effects of the infiltration of this extract were then measured though either western blotting or RT-qPCR.

2.8 Analysis of cell death

Cell death was achieved through infiltration of both autoactive MEK2DD recombinant proteins and PAMP extract into leaf tissue. In order to measure the amount of necrosis within the cell, I measured the fluorescence of the tissue at 800nm using the LI-COR Odyssey Fc Imaging System, images were then further processed with the Image studio Light software.

2.9 *In planta* infiltration and *in vitro* treatments of hydrogen peroxide

Two days post agroinfiltration a 100 µM solution of hydrogen peroxide was infiltrated into the abaxial side of *N. bentahmiana* leaves until the infiltrated area reached the extent of a full or half-full leaf depending on the experiment to be achieved. Leaves were then left to incubate while still attached to the plant until the incubation time (between 15 - 60 minutes depending on the experiment) had elapsed. After this, leaves were harvested as described above for the relevant experiments.

2.10 *P. infestans* infection assays

Firstly, leaves to be infected were detached from their respective plants and placed inside a plastic container that had fully soaked blue roll sheets at the bottom so that the moisture of their environment was adequate. 5 mL of Ice cold glass distilled water was added to 3-4 week old *P. infestans* plates and using a bacterial spreader to break the surface tension, the water was evenly spread throughout the plate. Plates were then incubated at 4 ºC for up to 2 hours, after which, the water was collected into a 15mL falcon tube. In order to test for spore quality, 10 µL of sample liquid were placed in a hemocytometer under a light microscope to check the spore density. If this density surpassed 10 zoospores per mm^2 it was deemed adequate for infection, plates that yielded less than the desired amount, were re-incubated once more, and if the yield was still unsatisfactory, a new plate was used. Once I had

obtained a solution with sufficient spores, 6 drops of 10 µL of this solution were placed on the adaxial side of *N. benthamiana* leaves. These drops were evenly spread throughout the leaf with both left and right half leaves having 3 droplets each. Once all the leaves had been infected, the plastic trays that contained the leaves were parafilmed shut to both keep the moisture level constant. Leaves were then incubated for 5-8 days at 23 ºC rooms with a 16 hour photoperiod away from direct light to avoid condensation inside the trays. Leaves were then imaged using both natural light with a Canon EOS 700D camera with an EF-S 18-55 mm IS lens, and with the LI-COR Odyssey Fc Imaging System at the 800 nm channel.

Chapter 3 - Understanding the binding of MAP kinase members and PAL to Joka2

3.1 Introduction

3.1.1 The role of MAPKs in plant immunity

Previous studies have already shown how under infectious conditions, Joka2 increasingly associates with members of the mitogen-associated protein kinases (MAPKs). MAPKs are serine or threonine kinases that are essential for the transduction of the immune stimuli into an intracellular response (Colcombet & Hirt, 2008; Cristina, Petersen & Mundy, 2010).

MAPKs are regulated by upstream MAPK kinases (MAPKKs), which in turn are regulated by further upstream MAPKK kinases (MAPKKKs) (Hamel et al., 2006). Activation of MAPKs is usually done through the phosphorylation of a threonine and a tyrosine residue in a Thr-X-Tyr activation motif, whilst MAPKK activation can be done through phosphorylation of any combination of two serine or threonine amino acids in a Ser/Thr-X_{3-5}-Ser/Thr activation motif. Plant MAPKs usually contain either a Thr-Glu-Tyr activation motif like the mammalian extracellular receptor kinases (ERK) subclass of MAPKs or a motif only found in plants consisting of Thr-Asp-Tyr (Cristina, Petersen & Mundy, 2010; Taj et al., 2010).

Another difference between plant and other eukaryotic systems is the greatly expanded number of each of the three components present, with *A. thaliana* having 20 MAPKs, 10 MAPKKs and 60 MAPKKKs (Mohanta et al., 2015). The higher number of components is associated with greater specificity of the transduced signal, since MAPK signaling is not exclusive to the immune response, having been linked to a variety of both developmental causes as well as biotic and abiotic stressors. Including wounding,

temperature, drought, salinity and UV irradiation (Krysan & Colcombet, 2018; Liu, X. et al., 2017).

MAPK signalling cascades are present both during PTI and ETI. During PTI they are responsible for transducing the signals from PRRs downstream. Some of these PRRs include FLS2, wich recognises the flg22 conserved region of bacterial flagellin (Felix et al., 1999; Gómez-Gómez & Boller, 2000) , the EFR receptor that recognises the elongation factor EF-Tu (Zipfel et al., 2006), and the chitin receptor CERK1 (Miya et al., 2007).

During ETI, in tobacco, SIPK (salicylic acid-induced protein kinase) and WIPK (wound-induced protein kinase) (analogous to MAPK3 and MAPK6 from *N. benthamiana*) are activated in response to the fungal effector Avr9 being detected by its cognate receptor Cf9 (Romeis et al., 2000). Both of the kinases, alongside their upstream regulator MEK2, have been associated with resistance to tobacco mosaic virus (TMV) resistance through the use of gene silencing experiments(Kobayashi et al., 2010) .

The consequence of signal transduction after PTI and ETI by MAPKs results in many of the defence responses that have been associated with these pathways, including phytoalexin and defence hormone production, defence gene activation, stomatal closure, ROS production and HR induced cell death (Meng & Zhang, 2013).

Pathogens can target several of the key points in this signalling network in order to prevent a successful defence form the host or as a means to further enhance either virulence. Examples of this include *Pseudomonas syringae* who in arabidopsis both releases the AvrPto effector that targets the FLS2 receptor and prevents PTI activation (Block & Alfano, 2011), as well as the HopAI1 effector that de-phosphorilates MAPK3, 4

and 6 (Dahale et al., 2021). *Agrobacterium tumefaciens,* on the other hand, does not suppress this network, but rather uses it to its advantage by activating MAPK3 form *A. thaliana*, which makes it able to hijack the VIP1 transcription factor in order to deliver its T-DNA into the cell's nucleus whilst preventing detection by the sending VIP1 for degradation using its VirF effector (Djamei et al., 2007; Li, S. et al., 2021).

3.1.2 The role of PAL in immunity

Phenylalanine ammonia-lyase (PAL) is an enzyme responsible for the non-oxidative deamination of phenylalanine into an ammonium ion and *trans*-cinnamic acid. *Trans*-cinnamic acid is the precursor to the phenylpropanoid synthesis pathway and therefore is the precursor to phytohormones, phytoalexins, lignin, flavonoids and anthocyanins (Wang, R., Wang & Ning, 2019). As a result PAL has been extensively studied for both its role in normal development as well as biotic and abiotic stressors in plants.

One of the main products of the phenylpropanoid pathway is salicylic acid (SA). SA is produced via isochorismate synthase (ICS) (Torrens-Spence et al., 2024), and is important for both normal regulation of plant development as well as pathogen defence, although it is mostly associated with defence against biotrophic pathogens whilst other hormones like jasmonic acid and ethylene are more associated with necrotrophic pathogens (Gondor et al., 2016).

SA is often linked with a plant's systemic acquired resistance and as a result the suppression of PAL through gene silencing or its inhibition through chemical means such as its inhibitor 2-aminoindan-2-phosphonic acid results in lower levels of

systemic acquired resistance resulting in lower defence against the oomycete *Hyaloperonospora parasitica* in tobacco plants (Mauch-Mani & Slusarenko, 1996). Similarly, knockdown transgenics of either ICS or PAL in soybean plants resulted in lower resistance against *Psudomoas syringae* (Huang, J. et al., 2010), and knockdown of PAL in pepper resulted in susceptibility to *Xanthomonas campestris (Kim & Hwang, 2014)*.

Rice contains nine PAL genes, of which eight are induced in response to pathogen attack. Suppression of the PAL4 gene results in susceptibility to all three of *Magnoportha oryzae*, *Rhizoctonnia solani* and *Xanthomonas oryzae* (Tonnessen et al., 2015).

3.2 Aims

In this chapter, my goal was to determine the binding sites of Joka2 to members of the MAPK family as well as PAL. Previous data has already shown the association of Joka2 and these proteins through a proteomic screen, and from there it has been shown that the NBR1 domain is responsible for the binding of Joka2 to MAPK3. However it has not been determined whether this is also true for MAPK6 or its upstream component MEK2. There is also some preliminary evidence pointing towards PAL binding the UBA domains of Joka2, although further testing is still required.

3.3 Results

3.3.1 The NBR1 domain and adjacent regions are critical for Joka2-MAPK associations.

3.3.1.1 Colocalization of Joka2 and MAPK3 occurs regardless of any individually missing domain

As previously stated, Joka2 interacts with members of the MAPK family, although their association does not lead to MAPK depletion. This finding goes against the idea that MAPK is the cargo of Joka2. Previous experiments done by Tumtas et al demonstrated the interaction of the importance of the NBR1 domain in the Interaction between Joka2 and MAPK3. To validate this claim, I decided to perform confocal microscopy on mKOK tagged MAPK3 by co-expressing it with several GFP tagged Joka2 truncates. The truncates all lacked a particular domain of Joka2, (ΔPB1, ΔZZ, ΔNBR1 or ΔUBAs). I also co-expressed Joka2 with an EV:GFP control and a truncate lacking the region between NBR1 and ZZ (ΔbZN) (Figure 3.1) (Figure 3.2). ΔPB1 showed no puncta at the time of detection, although that was expected since this domain is responsible for the self-oligomerization of Joka2. Besides ΔPB1, there were no significant differences in the amount of colocalization between any of the other truncates and Joka2. This is even though ΔUBAs showed an increase in the overall number of puncta compared to the full length Joka2 control. These findings suggest that there is not a singular domain that might be responsible for the binding of MAPK3 to Joka2, but rather it could be due to a combination of domains.

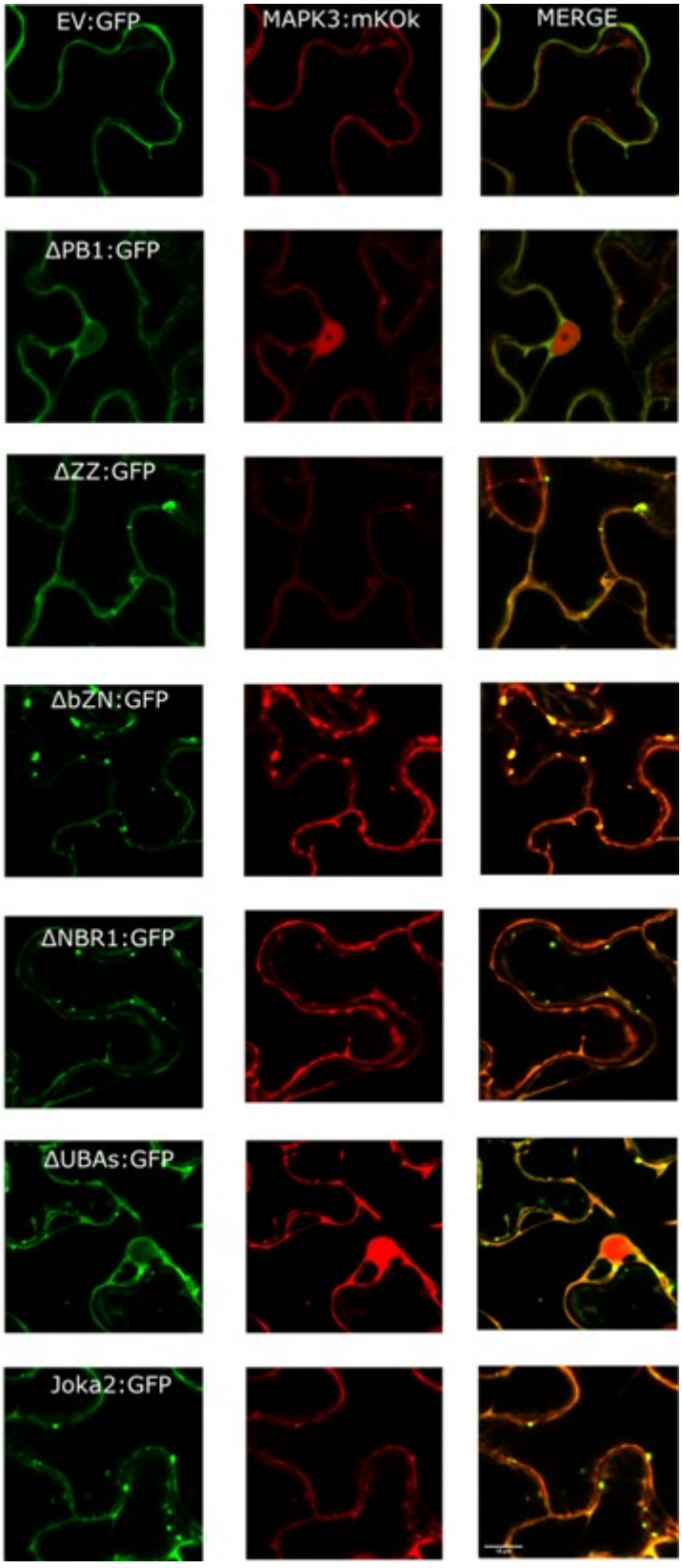

Figure 3.1:Representative images of MAPK3:MkoK and several Joka2 truncates co-expressed in *N. benthamiana* leaves (A-G): Confocal microscopy of MkoK

tagged MAPK3 and GFP tagged full length Joka2, ΔPB1, ΔZZ, ΔbZN, ΔNBR1, ΔUBAs or EV. All Joka2 truncates were able to show puncta formation and colocalization with MK3 with the exception of ΔPB1 since it lacks Joka2's oligomerization domain (B). All images are shown as maximum projections with 1µm steps. Images taken at 3dpi post infiltration.

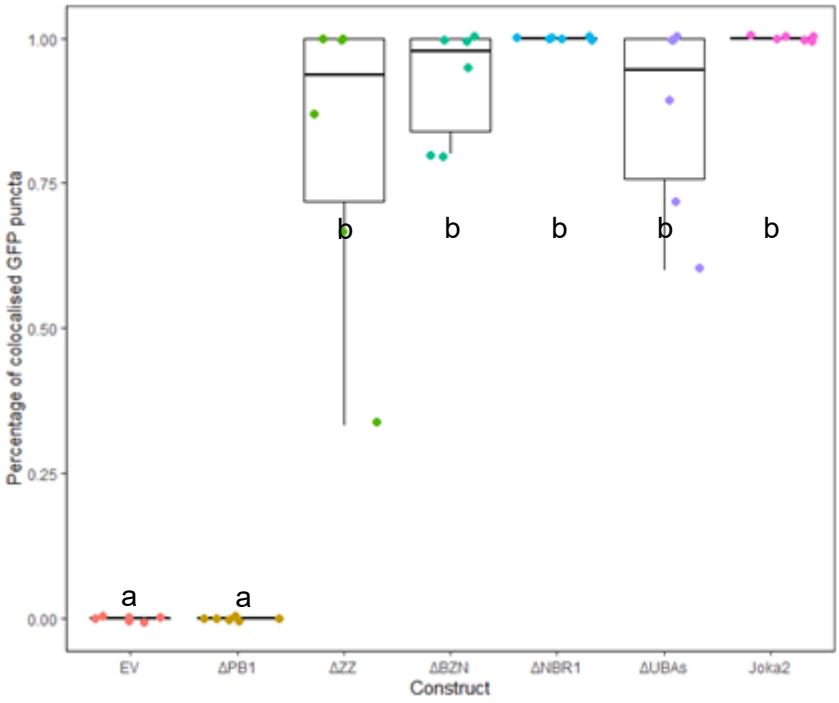

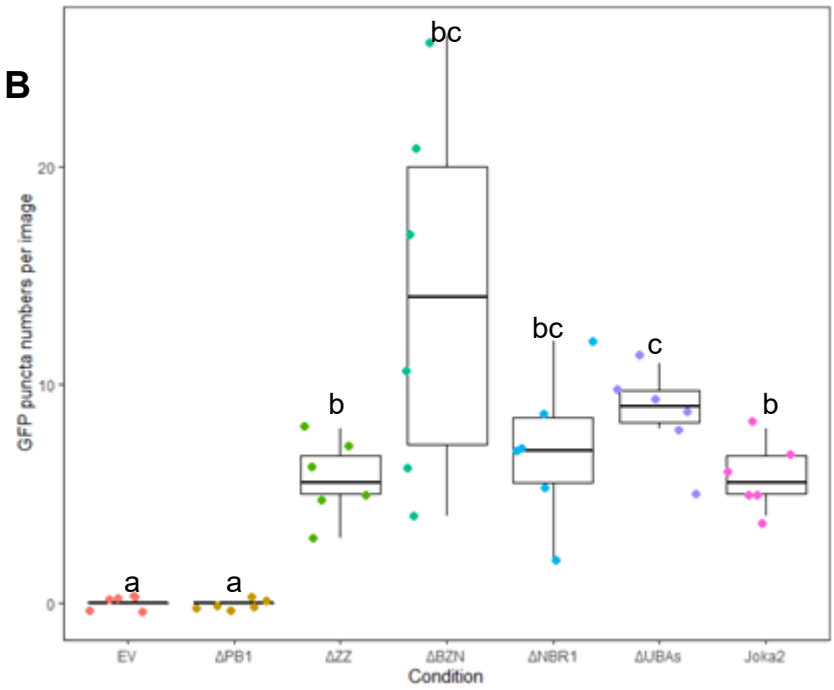

Figure 3.2: Quantification of punctas between Joka2 truncates and MK3 show no difference with the exception of ΔPB1. *N. benthamiana* leaf discs containing GFP labelled Joka2 truncates and and mKOk labled MPK3 were imaged 3 days post infiltration. Each point represents the mean number of puncta shoun in 3 technical repeats of a biological repeat.mKOk and GFP localization is reported as a percentage of total GFP puncta (a), whilst absolute numbers are reported in (b). A GFP empty vector and full length Joka2 controls were added. Constructs not sharing a letter have statistical significance. (student's t-test with p value < 0.05)

3.3.1.2 MAPK6 requires the NBR1-bZN-ZZ region for binding with Joka2.

Similarly to how Joka2 binds MAPK3, I was interested in the interaction between Joka2 and MAPK6. In order to understand which domains were responsible for binding, a co-immunoprecipitation was performed between the individual domains of Joka2 tagged with GFP and a 3xHA tagged MAPK3. Only the ZZ, bZN and NBR domains were used, since preliminary data pointed at the NBR1 and surrounding regions as being responsible for this interaction. Full length Joka2 and EV were used as positive and negative controls respectively (Figure 3.3). Weaker bands on the positive Joka2 control can be attributed to increased degradation of Joka2 within the cell The data suggests that MAPK6 is able to independently bind all three of the tested domains at similar intensities, supporting the hypothesis that MAPK6 binds all three domains.

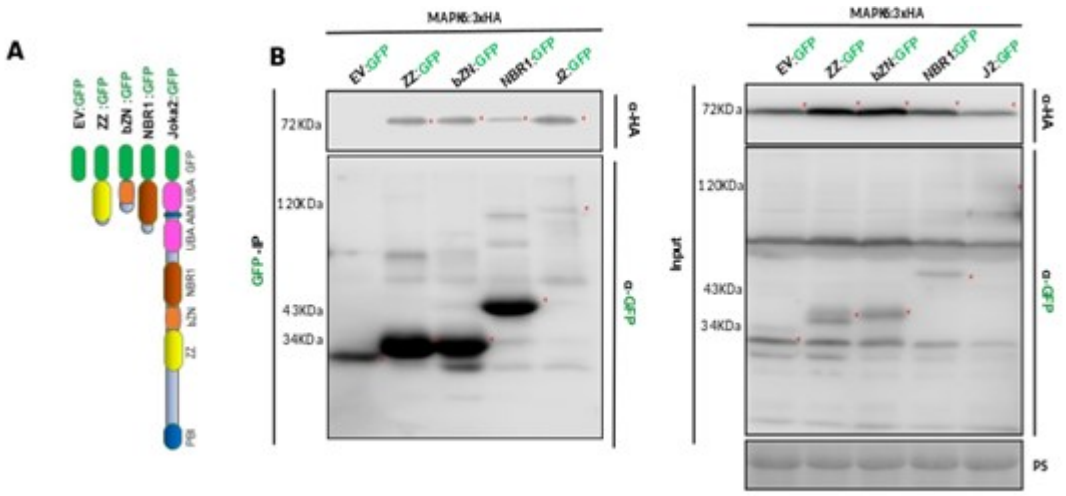

Figure 3.3: MAPK6 associates with all domains of Joka2 between ZZ and NBR1. A) Cartoon representation of the domain organization of Joka2 and the Joka2 domains used to pull down HA tagged MAPK6. B) *In planta* coimmunoprecipitation of HA tagged MAPK6 and GFP tagged Joka2 and Joka2 domains. Proteins were expressed in 4 week old *N .benthamiana* plants and samples were extracted 2 days post inoculation with *A. tumefasciens*. Immunoprecipitation (IP) was obtained by using anti-GFP antiserum and total protein extracts were immunoblotted with appropriate anti-HA and anti-GFP antisera. Red asterisks indicate protein bands of the expected molecular weight.

In order to confirm this, a second co-ip consisting of full length Joka2 truncates lacking the aforementioned domains was performed (Figure 3.4). Results also indicated that no one particular domain was responsible for Joka2 binding

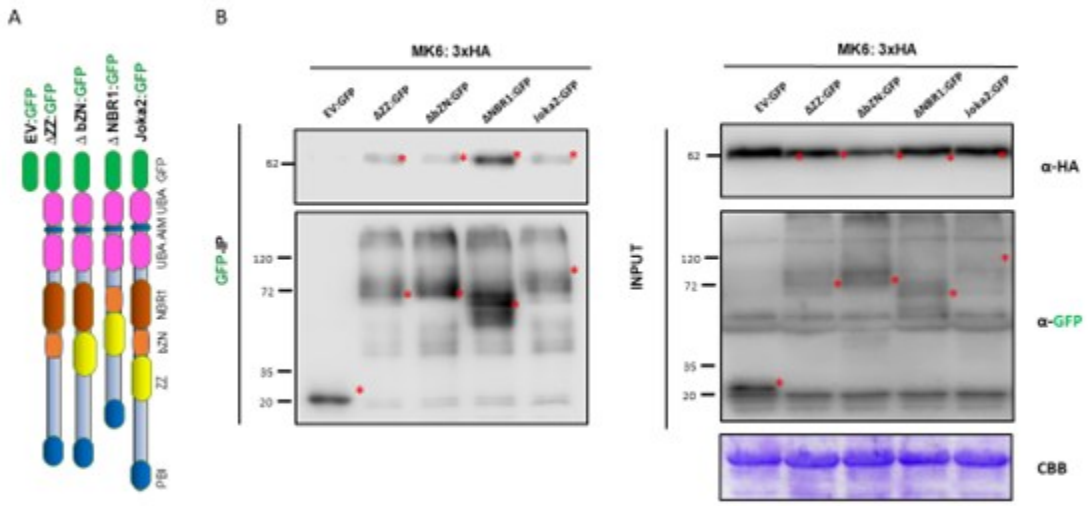

Figure 3.4: MAPK is able to bind to Joka2 irrespective of which domain within the ZZ and NBR1 region is lacking. A) Cartoon representation of the domain organization of Joka2 and the Joka2 truncates used to pull down HA tagged MAPK6. B) In planta coimmunoprecipitation of HA tagged MAPK6 and GFP tagged Joka2 and Joka2 truncates. Proteins were expressed in 4 week old *N .benthamiana* plants and samples were extracted 2 days post inoculation with *A. tumefasciens*. Immunoprecipitation (IP) was obtained by using anti-GFP antiserum and total protein extracts were immunoblotted with appropriate anti-HA and anti-GFP antisera. Red asterisks indicate protein bands of the expected molecular weight.

3.3.1.3 The KR mutation in MAPK3 does not affect binding with Joka2

The next step in my investigation was to determine the binding site of the upstream component of both MAPK3 and MAPK6, that is MEK2. However, agroinfiltration of MEK2 results in strong HR making the acquisition of tissue suitable for co-immunoprecipitation very hard. As a result I decided to introduce a mutation that would

remove the ability of MEK2 to perform its kinase role. To investigate whether the mutation resulted in altered changes to binding, the kinase dead mutant, referred to as the KR mutant (form he change to the amino acid composition), of MEK3 was tested against the fully working MAPK3 to see if there were any changes in the binding to Joka2 (Figure 3.5). I observed no changes in the binding of MAPK3kr compared to that of wild type, therefore I concluded that the KR mutation did not affect binding to Joka2

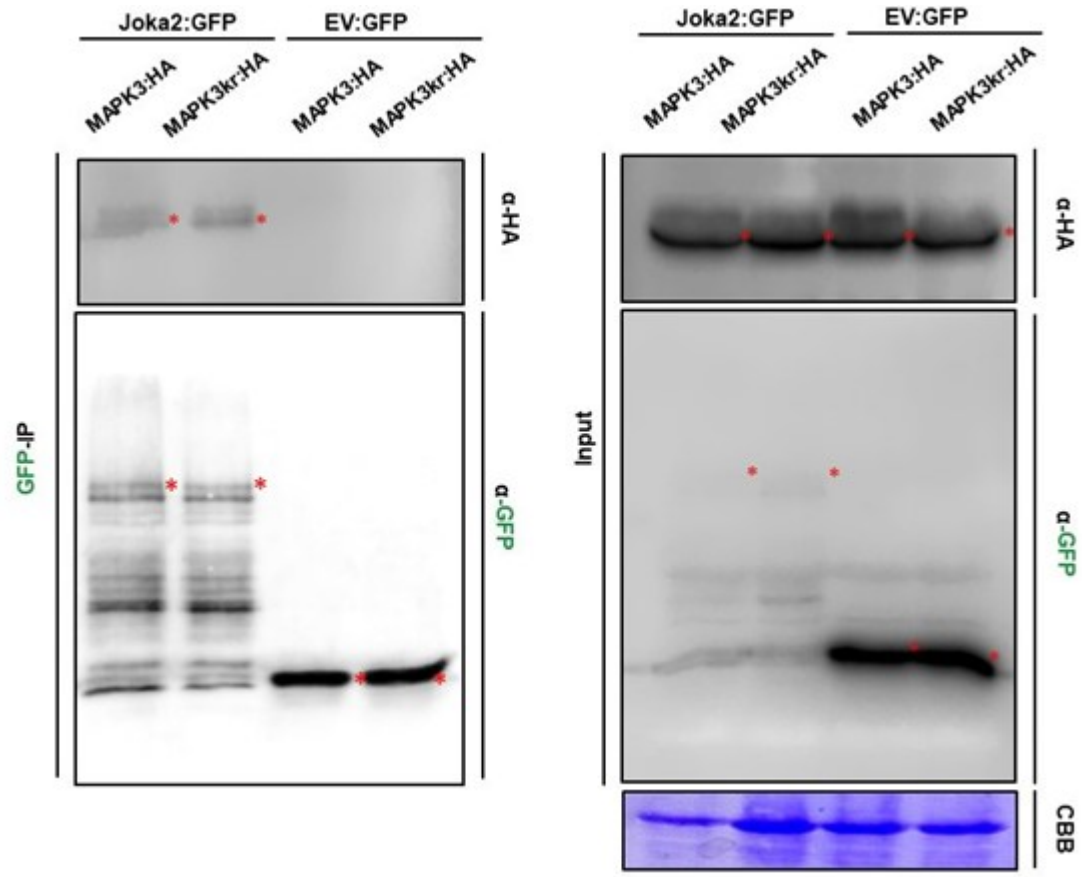

Figure 3.5: The KR mutation in MAPK3 does not affect binding to Joka2. *In planta* co-immunoprecipitation of MAPK3 and MAPK3kr with GFP tagged Joka2 and EV. Proteins were expressed on 4 week old *N. benthamiana* leaves and extracted 2 days post inoculation with *Agrobacterium*. Immunoprecipitation (IP) was obtained by using anti-GFP antiserum and total protein extracts were immunoblotted with appropriate anti-HA and anti-GFP antiser. Red asterisks indicate protein bands with expected molecular weight.

Since I observed no changes to the binding pattern of MAPK3kr compared to wild type, I decided that the same would be applicable to MEK2. Therefore, I decided to agroinflitrate MEK2kr along with Joka2 truncates in order to establish the binding site of Joka2 (Figure 3.6). From the results of this experiment I can see that MEK2 is able to bind to the NBR1, bZN and ZZ domains similarly to how I saw with MAPK3

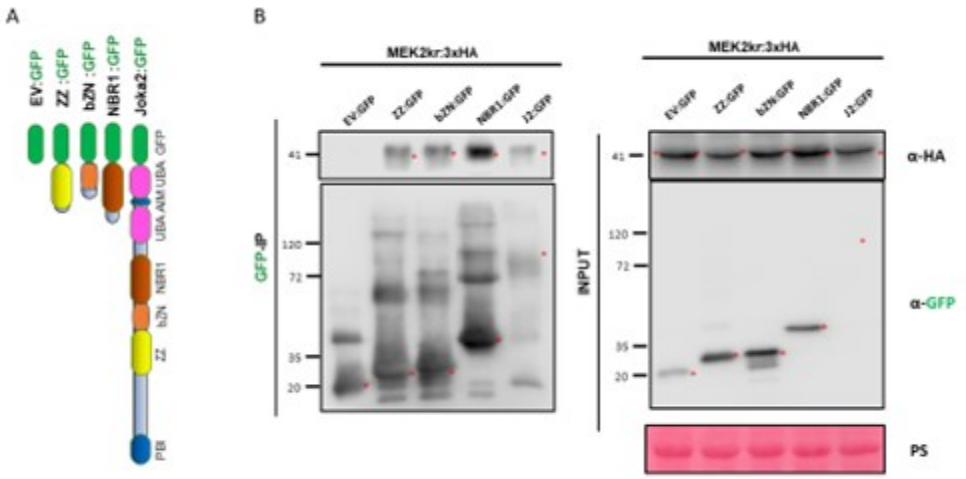

Figure 3.6: MEK2kr binds all regions between ZZ and NBR1 with higher binding in NBR1. A) Cartoon representation of the domain organisation of GFP tagged proteins used to pull down HA-tagged MEK2kr. B) In planta co-immunoprecipitation of HA tagged MEK2kr and GFP tagged Joka2 and Joka2 domains.. Proteins were expressed in 4 week old *N .benthamiana* plants and samples were extracted 2 days post inoculation with *A. tumefasciens*. Immunoprecipitation (IP) was obtained by using anti-GFP antiserum and total protein extracts were immunoblotted with appropriate anti-HA and anti-GFP antisera. Red asterisks indicate protein bands of the expected molecular weight.

3.3.1.4 Lack of the NBR1 domain causes a reducction in phosphorylation of MAPK6

After observing that both MAPK3 and 6 as well as their upstream component MEK2 bind Joka2 all within the same regions, I hypothesised that Joka2 could be acting as a scaffolding protein for the MAP kinases. Scaffolding proteins aid in the placement of the kinases facilitating their phosphorylation of one another, are common within MAPK signalling. To test this, I decided to test the levels of MAPK6 phosphorylation after coexpressing it with either full length Joka2 or the ΔNBR1 truncate, an EV control was also included as a negative control (Figure 3.7). Whilst at time point 0 MAPK6 shows similar levels of phosphorylation with full length Joka2, ΔNBR1 and EV, PAMP treatment leads to an increase in MAPK6 phosphorylation compared to the EV. ΔNBR1 however, does not show this change and exhibits a much smaller increase in phosphorylation when compared to the full length Joka2. This is indicative that the NBR1 domain is necessary for the PAMP-triggered phosphorylation of MAPK6.

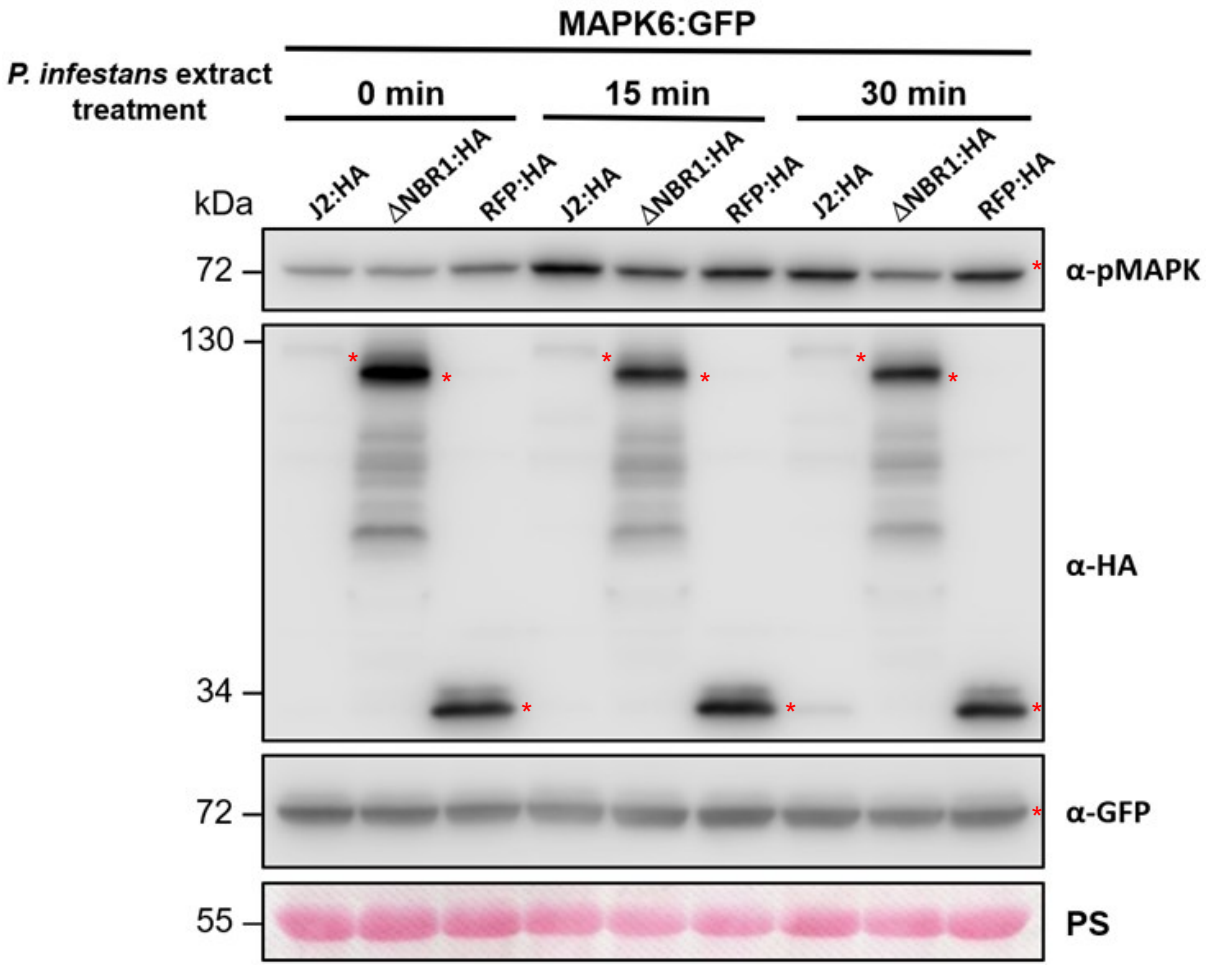

Figure 3.7: Removal of the NBR1 domain causes a reduction in the phosphorylation levels of MAPK6. *In planta* western blot of HA tagged Joka2 and empty vector and GFP tagged MAPK6. Timepoints within the graph represent time after PAMP inoculation of the plant. Proteins were expressed in 4 week old *N. benthamiana* plants and samples were extracted 2 days post inoculation with *A. tumefasciens*. Red asterisks represent bands of expected size. Results obtained with the help of Cecilia Longoni

3.3.2 PAL associates with the UBA domains when binding to Joka2 independently of their ubiquitin binding ability

Phenyl ammonia lyase is another important enzyme in plant defence. It is responsible for the production of cinnamic acid and plays a vital role in the cross linking of callose, and has been established as a binding partner of Joka2 through a proteomics screen. As a result I wanted to see if I could uncover which of the domains of Joka2 were responsible for its binding. I had some preliminary data pointing towards the UBA domains being the binding site for this protein (Tumtas *et al,* Unpublished), consequently I started by performing a Co-ip between PAL and different Joka2 truncates including just the UBA domains, UBA1 and UBA2 alone, and a modified version of the UBA domains lacking the ability to bind ubiquitin. I also included EV:GFP as a negative control (Figure 3.8). From the results I can observe that PAL was able to bind all of the proteins and truncates that I exposed it to, irrespective of ubiquitin binding ability or the presence of only one or both of the UBA domains.

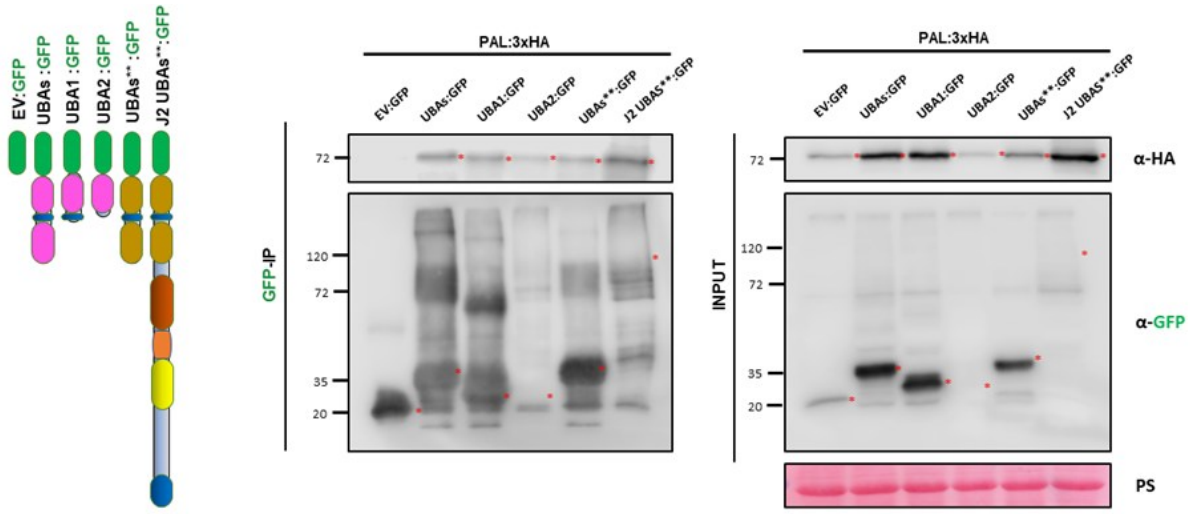

Figure 3.8: PAL is able to bind the UBA domains of Joka2, irrespectively of ubiquitin binding ability. A) Cartoon representation of the domain organisation of GFP tagged

proteins used to pull down HA-tagged PAL. B) In planta co-immunoprecipitation of HA tagged PAL and GFP tagged Joka2 and Joka2 UBA domains. Proteins were expressed in 4 week old *N .benthamiana* plants and samples were extracted 2 days post inoculation with *A. tumefasciens*. Immunoprecipitation (IP) was obtained by using anti-GFP antiserum and total protein extracts were immunoblotted with appropriate anti-HA and anti-GFP antisera. Red asterisks indicate protein bands of the expected molecular weight.

In order to verify our results I then proceeded to expose PAL to different Joka2 domains to see if there is any other binding activity. I included maltose binding protein as a secondary control in order to check that PAL is not 'sticky', meaning that it binds to any other protein it is exposed to (Figure 3.9). The results show that only the UBA domain of Joka2 is able to bind PAL, supporting our previous hypothesis that the UBA domains are the only domains responsible for the binding of PAL.

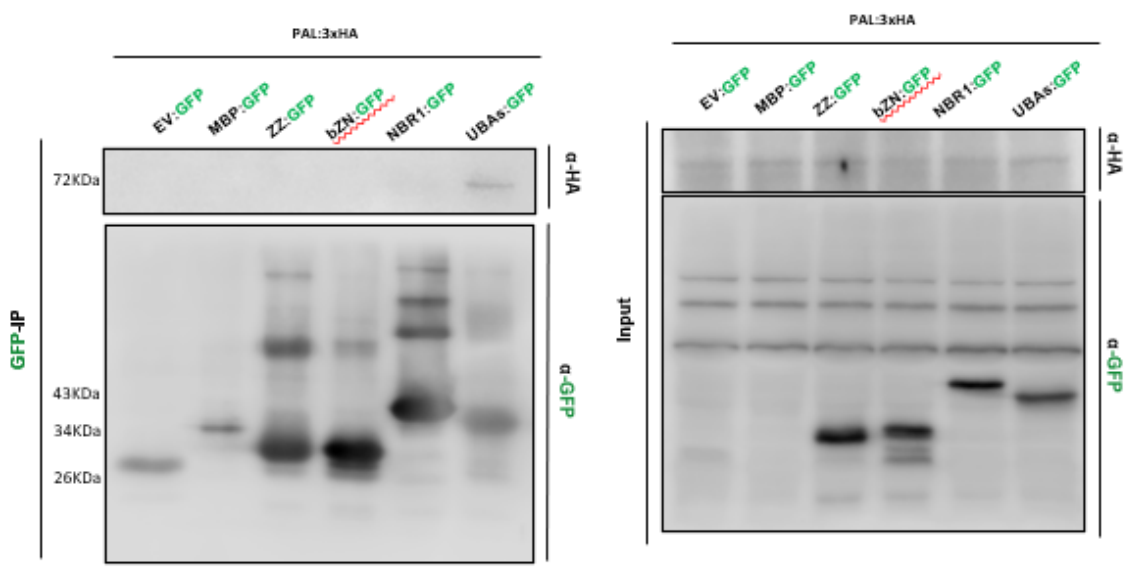

Figure 3.9: PAL is unable to bind any other domain of Joka2 besides the UBA domain. In planta co-immunoprecipitation of HA tagged PAL and GFP tagged EV and MBP controls and Joka2 domains. Proteins were expressed in 4 week old *N .benthamiana* plants and samples were extracted 2 days post inoculation with *A. tumefasciens*. Immunoprecipitation (IP) was

obtained by using anti-GFP antiserum and total protein extracts were immunoblotted with appropriate anti-HA and anti-GFP antisera. Red asterisks indicate protein bands of the expected molecular weight.

Finally and as an additional control, I tried to see if a truncate of Joka2 that did not contaoin the UBA domain was still able to bind PAL, to our surprise, it was able to bind PAL. I hypothesised that this is due to the aggregation of Joka2 proteins within cells, as they are often found in large insoluble aggregates and since our protein still had the ability to oligomerize with wild type Joka2 still present within the cell, PAL would still be able to be pulled down irrespective of the presence or absence of the UBA domains. In order to confirm this, I decided to perform another co-ip, this time with a truncate that both lacked the Uba domains as well as the PB1 oligomerization domain to see if this was true (Figure 3.10). However, as it can be seen from the Co-ip, Joka2 was still able to bind this protein with restricted oligomerization ability, leading us to believe that the mutant is still able to partially oligomerize with the wild type Joka2, or that PAL binds into a disordered region of Joka2.

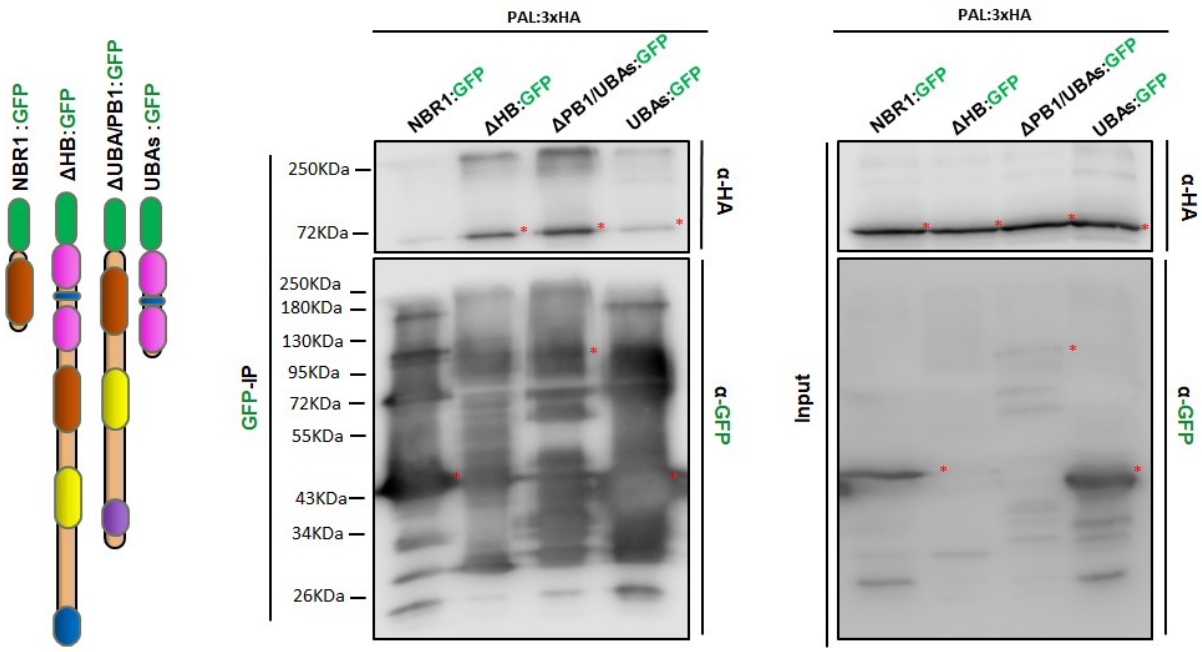

Figure 3.10: PAL is able to bind both ΔHB and ΔPB1/UBA. In planta co-immunoprecipitation of HA tagged PAL and GFP tagged EV and MBP controls and Joka2 domains. Proteins were expressed in 4 week old *N .benthamiana* plants and samples were extracted 2 days post inoculation with *A. tumefasciens*. Immunoprecipitation (IP) was obtained by using anti-GFP antiserum and total protein extracts were immunoblotted with appropriate anti-HA and anti-GFP antisera. Red asterisks indicate protein bands of the expected molecular weight.

3.4 Discussion

Joka2 is known for its role as a cargo receptor in autophagy. However, it also plays an important role in the defense against pathogens, although its role in the immune response is not yet well understood. Preliminary data showing its association with members of the MAPK family and PAL demonstrated Joka2 interacted with them, but they were not cargo, since interaction did not result in degradation (Tumtas *et al*, Unpublished). As a result, I decided to investigate this association further.

I first decided to start by validating previous claims that the NBR1 domain was responsible for MAPK3 binding to Joka2. Confocal microscopy of different Joka2 truncates and MAPK3 did not show any difference between the colocalization of different truncates with Joka2 or the number of puncta that Joka2 was able to form, with the exception of ΔPB1 (Figure 3.1, Figure 3.2). The lack of puncta from the ΔPB1 mutant can be explained since PB1 is the domain that allows for the oligomerization of Joka2 (Zientara-Rytter & Sirko, 2014) and lack of this domain resulted in only the presence of soluble Joka2, which was unable to form puncta. On the other hand, the presence of Joka2 positive puncta from the ΔNBR1 mutant was surprising, since the preliminary data from western blotting had shown that the NBR1 domain was responsible for the binding of Joka2 (Tumtas *et al*, Unpublished). This opened the door to other domains being responsible for this association, although the possibility of intrinsically expressed Joka2, whilst at a much lower level than that of the fluorescently tagged ΔNBR1, could have oligomerized with our truncate resulting in the aforementioned results.

After this, I proceeded to check whether this association was also true for MAPK6. I co-expressed MAPK6 alongside all of Joka2's individual domains and subsequently co-immunoprecipitated them in order to check for binding (Figure 3.3). Both the ZZ and NBR1 domains as well as the bZN region showed binding to Joka2. This was then verified through the reverse co-immunoprecipitation that was done with Joka2 truncates rather than the domains themselves, as removal of any one of the three individual domains could not result in the loss of binding to MAPK6 (Figure 3.4). This result is surprising to an extent, since MAPK3 and MAPK6 in *N. benthamiana* share a very high (>80%) similarity and often function redundantly of each other when phosphorylating enzymes (Savary et al., 2012).

Following this, I deemed it logical to see if this region was also important for the binding of the upstream component of both MAPK6 and MAPK3 MEK2 (Jonak et al., 2002). However, MEK2 poses a problem for performing co-immunoprecipitations, as in its native form it causes a high degree of cell death when infiltrated into *N. benthamiana* plants, I therefore had to design a new MEK2 enzyme that was actively dead. To do this I decided to introduce a single amino acid mutation (K to R) into MEK2, however, to test this mutation had no adverse effects on expression or binding to Joka2, I first introduced this mutation into MAPK3 in order to verify it. As I observed no change in MAPK3kr expression or binding to Joka2 compared to the wild type (Figure 3.5) I decided to continue and test MEK2kr with the individual domains of Joka2. Results from the subsequent co-immunoprecipitation yielded similar results to those of MAPK6, with MEK2 showing affinity for all three of the ZZ, NBR1 and bZN regions (Figure 3.6).

The close proximity of the domains involved in the binding for all three of MAPK3, MAPK6 and MEK2 pointed towards the possibility of Joka2 acting as a scaffolding protein for the MAPK family. To test this, I removed the NBR1 domain from Joka2 and tested the level of phosphorylation of MAPK6 when co-expressed with the truncate and the full-length protein. (Figure 3.7). Removal of the NBR1 domain caused a decrease in phosphorylation, however MAPK6 is able to bind ΔNBR1 as much as Joka2 (Figure 3.4). This, alongside the information that the NBR1 domain is responsible for the increased resistance to *P. infestans* and that increased Joka2 concentration does not lead to MAPK depletion, leads me to believe that Joka2's interaction with the MAP kinase family of proteins is as a scaffolding protein, positioning them for easier phosphorylation of their downstream elements.

The proposed role of Joka2 as a scaffolding protein for the MAP kinase family aligns closely with the established functions of its mammalian ortholog, p62 (SQSTM1) (Moscat, Diaz-Meco & Wooten, 2007). In mammalian systems, p62 acts as a critical scaffold in the MEK-ERK cascade, facilitating the efficient phosphorylation of ERK by MEK (Moscat, Diaz-Meco & Wooten, 2007). My findings suggest a similar mechanism in N. benthamiana, where Joka2 facilitates the interaction between MEK2 and MAPK6/3. Beyond its role in MAPK signaling, p62 is recognized as a multi-functional signaling hub that regulates apoptosis and oxidative stress (Agas et al., 2022). The association of Joka2 with the MAPK family, without targeting them for autophagic degradation, suggests that Joka2 has evolved to be a central integrator of plant defense signaling, much like p62 is in animals

Another finding in this study is the redundancy of binding sites for MAPK6 and MEK2, both of which showed affinity for the ZZ, NBR1, and bZN regions of Joka2. The involvement of the bZN region is particularly noteworthy, since scaffolding proteins often utilize such intermediate regions as Intrinsically Disordered Regions (IDRs) (Cortese, Uversky & Dunker, 2008). These flexible linkers allow the protein to wrap around multiple partners (Cortese, Uversky & Dunker, 2008), positioning MEK2 and MAPK6 in the optimal spatial orientation for enzymatic turnover. However, binding redundancy does not imply functional redundancy, while MAPK6 can still bind to a Joka2 truncate lacking the NBR1 domain, its phosphorylation is significantly decreased, suggesting that while the ZZ and bZN regions may act as primary tethers, the NBR1 domain is specifically required to facilitate the catalytic efficiency of the MAPK cascade.

In this chapter, I also decided to investigate what the binding site of PAL was. Preliminary data pointed towards the UBA domains of Joka2 being responsible for this interaction. The UBA domains are also responsible for ubiquitin binding, ubiquitin is a protein tag often used to mark proteins that need to be sent for degradation (Hagai & Levy, 2010), so there could be possibility that the association between Joka2 and PAL could be explained as the latter being cargo of the first one, tagged with ubiquitin to be degraded, so I decided to coexpress PAL with both a full length Joka2 and an UBA domain pair that both had no ubiquitin binding ability. However, PAL was still able to bind (Figure 3.8). Interestingly, PAL was able to bind Joka2 regardless of which of the

two UBA domains was present , as it showed affinity to both the UBA1 and UBA2 domains.

To see that this result was not because PAL was a protein that was “sticky” and binded non-specifically to other proteins, I exposed PAL to the ZZ and NBR1 domains as well as the bZN region to see if there was any binding to them. I also included another negative control in the form of maltose binding protein (Figure 3.8). No binding was seen to the other regions of Joka2 or to the extra control, so I assumed that the binding I saw previously was not non-specific.

As an alternate way to verify this result, I decided to do an inverse co-immunoprecipitation, where I pulled down PAL after co-expressing it with a Joka2 truncate lacking the UBA domain. However, removal of the UBA domain did not result in lack of binding (Figure 3.8). I hypothesised this could be due to some of the native Joka2 interacting with our construct, more specifically associations between the PB1 of both native Joka2 and our transgenic construct, so I repeated this experiment whilst also removing the PB1 domain. At this time, one of our collaborators had discovered a new domain within Joka2 known as the helical bundle (HB) domain (Ibrahim *et al*, Unpublished), as a result I tested whether or not it was also important for the binding of PAL. As I can see for figure 3.9, neither removal of the UBA and PB1 domains nor the HB domain resulted in loss of binding to Joka2. This result is surprising since the lack of UBA or PB1 domains should have resulted in a complete loss of binding, and since I had already established PAL as a non-sticky protein, I was inclined to believe that this was not non-specific binding. As a result, I conclude that PAL has at least two binding sites within Joka2, one of which is the UBA domains, but the other is yet unknown.

The proposal that PAL possesses multiple binding sites within Joka2 suggests a robust physical association that likely serves a purpose beyond simple autophagic clearance, possibly involving Joka2 once again acting as a scaffold to PAL and possibly other enzymes involved in phenylpropanoid synthesis.

This mirrors the scaffolding role I observed with the MAPK family. If Joka2 is indeed a dual-purpose scaffold, it may serve to bridge the gap between pathogen perception, through the MAPK cascade, and the metabolic response, through PAL-mediated phenylpropanoid synthesis. This would position Joka2 as a central coordination hub in the N. benthamiana immune response, synchronizing signaling and metabolism to ensure a rapid and localized defense against pathogens like P. infestans.

In conclusion, since the discovery that Joka2 associates with members of the MAP kinase family as well as other enzymes involved in plant defence, I have investigated which domains of Joka2 are responsible for this interaction. In this chapter I have shown that the ZZ and NBR1 domains as well as the region between them is essential for the binding of MAPK6 and MEK2. I have also demonstrated that the phosphorylation ability of MEK2 and MAPK3 is not necessary for them to maintain binding affinity, and that the removal of the NBR1 domain decreases the phosphorylation of MAPK6, leading me to propose the role of Joka2 as a scaffolding protein for the MAPKs.

I also showed that PAL binds to both of the UBA domains and it does so independently of their ubiquitin binding affinity. However, removal of the UBA domains is not sufficient

to eliminate the affinity PAL has for Joka2, so I propose PAL has multiple binding sites within Joka2. Further research still needs to be done regarding both of these topics. Firstly, co-immunoprecipitation experiments should be performed on the upstream component of MEK2, to determine if it also binds on proximity to the other members of the MAPK family. Secondly, it should also be determined if there is also a lack of phosphorylation of both MAPK3 and MEK2 when the NBR1 domain of Joka2 is removed. Finally further co-immunoprecipitations should be performed to determine the other binding sites of PAL in Joka2.

Chapter 4 - The effect of redox on Joka2 solubility

4.1 Introduction

4.1.1 Redox signaling in plant immunity and stress responses

Plants employ complex redox signaling networks to respond to both biotic and abiotic stresses. These networks rely primarily on reactive oxygen species (ROS), which serve as crucial signaling molecules.

The production of ROS occurs in multiple cellular compartments, with chloroplasts being the main site of singlet oxygen formation (Fischer, Hideg & Krieger-Liszkay, 2013), while ROS generation through molecular oxygen reduction, resulting in the production of peroxides and superoxides, occurs at several subcellular and extracellular sites, including mitochondria and peroxisomes as well as NADPH oxidases located within the plasma membrane (Foyer & Noctor, 2016). During pathogen infection, ROS production happens in two steps, first an early and weaker ROS production happens during PTI followed by a stronger and more prolonged ROS burst during ETI (Liu, C., Liu & Mou, 2024).

The complexity of redox signaling extends beyond single cells, as ROS signals are closely involved with another of the plant's defence mechanisms known as systemic acquired resistance (SAR) (Wang, C. et al., 2014). During SAR, ROS production by membrane-associated NADPH oxidases in one cell triggers similar responses in neighboring cells, enabling rapid transmission of defence signals from infection sites to distal tissues. However, ROS are not the only mobile signals associated with SAR, it has also been shown that ROS function in parallel with the salicylic acid (SA) signalling pathway in the establishment of SAR (Wang, C. et al., 2014; Wang, C. et al., 2018).

Besides SA, redox signaling also exhibits extensive cross-talk with other signaling pathways, particularly those involving reactive nitrogen species (RNS) such as nitric oxide (NO). These interactions add another layer of regulation to plant immune responses, with NO modulating ROS production through the S-nitrosylation of key proteins like the NADPH oxidase and RBOHD (Bleau & Spoel, 2021).

This intricate interplay between different reactive species allows for fine-tuned responses to various stresses while preventing excessive ROS accumulation that could damage cellular components. Other examples of ROS regulation include pigments like carotenoids, and secondary compounds like flavonoids (Noctor, Reichheld & Foyer, 2018).

4.1.2 Thiols and their role in redox control and signaling

Besides the aforementioned examples, thiols, particularly glutathione, also play a role in maintaining redox homeostasis and transmitting oxidative signals. Glutathione is the most abundant low molecular thiol present within the cell, it is usually found in its reduced form (GSH) and acts as an antioxidant through the absorption of excess ROS, resulting in the formation of glutathione disulphide (GSSG) (Queval et al., 2011).

Glutathione’s role in redox signalling involves conjugation to cysteine residues of proteins in a process known as S-glutathionylation, an example of which can be seen with the enzyme glyceraldehyde-3-phosphate dehydrogenase, where S-glutathionylation of the cysteine residue within the catalytic site leads to enzyme inhibition (Zaffagnini et al., 2007).

Complementing the role of glutathione, thioredoxins (TRX) and glutaredoxins (GRX) use the reducing power from GSH or NADPH to modify other proteins mostly by breaking down disulphide bridges back into their reduced -SH forms (Noctor, Reichheld & Foyer, 2018).

The thiol control system is characterized by significant crosstalk between the GSH/GRX and TRX pathways, providing redundancy that increases the robustness of the thiol network (Reichheld et al., 2007). Notably, the thiol network extends its influence to the nucleus, where specialized TRX and GRX systems interact with transcription regulators to modulate plant development, demonstrating the broad reach of redox regulation in plant cellular processes (Murmu et al., 2010; Ndamukong et al., 2007).

4.1.3 P62's s redox-dependent ability to aggregate is necessary for its function

p62, the human ortholog of Joka2, requires its ability to oligomerize in order to perform its function as a cargo receptor. This ability is driven by its PB1 domain and serves to better attach to both ubiquitinated cargo and LC3, since, by attaching many p62 proteins together, more ubiquitin binding domains and LIR motifs are available to interact with both the cargo and the autophagosome (Wurzer et al., 2015). This oligomeric state is crucial for the phase-transition of p62 and the subsequent formation of p62 bodies, who play a role in both autophagy and stress responses (Feng et al., 2023).

p62's oligomerization state is linked to its sensitivity to changes in the redox conditions of the cell. Under high oxidative conditions, caused by the saturation of

ROS buffering systems, p62 oligomerizes, causing the formation of aggregates which then form p62 bodies. This is due to the oxidation of two very close by cysteine residues, resulting in the formation of a disulphide bridge, which causes a reduction in the overall protein solubility, causing it to precipitate (Carroll et al., 2018). Chemical methods such as verteporfin can also be used to replicate this behaviour (Donohue et al., 2014). These close-by cysteine residues have now only been reported in mammals. Insects do not have these residues, with the *Drosophila melanogaster* homolog of Joka2 exhibiting no change in solubility when exposed to changes in the redox environment of the cell (Carroll et al., 2018).

These oligomers are thought to play a role in the recruitment of the autophagosomal machinery and the formation of the autophagosome (Itakura & Mizushima, 2011), but they also play a role in the sequestration of signalling molecules like KEAP1, thereby modulating the NRF2 antioxidant response (Guo et al., 2021; Mukherjee et al., 2024).

4.2 Aims

In this chapter, my aim was to determine how changes to the redox environment of the cell affect Joka2's solubility and to identify if Joka2 also undergoes a phase transition similarly to how p62 does and if so to identify the region responsible for this change. Plants, as part of their defence strategy, release a large number of reactive oxygen species upon pathogen detection. This, combined with the redox sensitivity of p62 has led me to believe that Joka2 might be able to phase shift, which in turn

could have implications in signalling, similarly to how p62 alters signalling by changing its solubility.

4.3 Results

4.3.1 Joka2 responds to different oxidation states by changing solubility

The human ortholog of Joka2, p62, has been previously reported to respond to oxidative changes within the cell. As a result, I wanted to investigate if the same is also true for Joka2. As a first step, I started by altering the concentration of reducing agent used in the extraction buffer when trying to isolate Joka2 that had been expressed *in planta* through *A. tumefaciens* infiltration. Joka2 and a control EV were exposed to different concentrations of DTT and beta-mercaptoethanol in order to change the overall oxidative state (Figure 4.1). Whilst the overall signal from the EV stayed constant regardless of the reducing agent used, Joka2's signal increased when the amount of DTT was reduced from 10 to 2 mM of DTT. with this overall signal being indicative of the soluble fraction present within the solution.

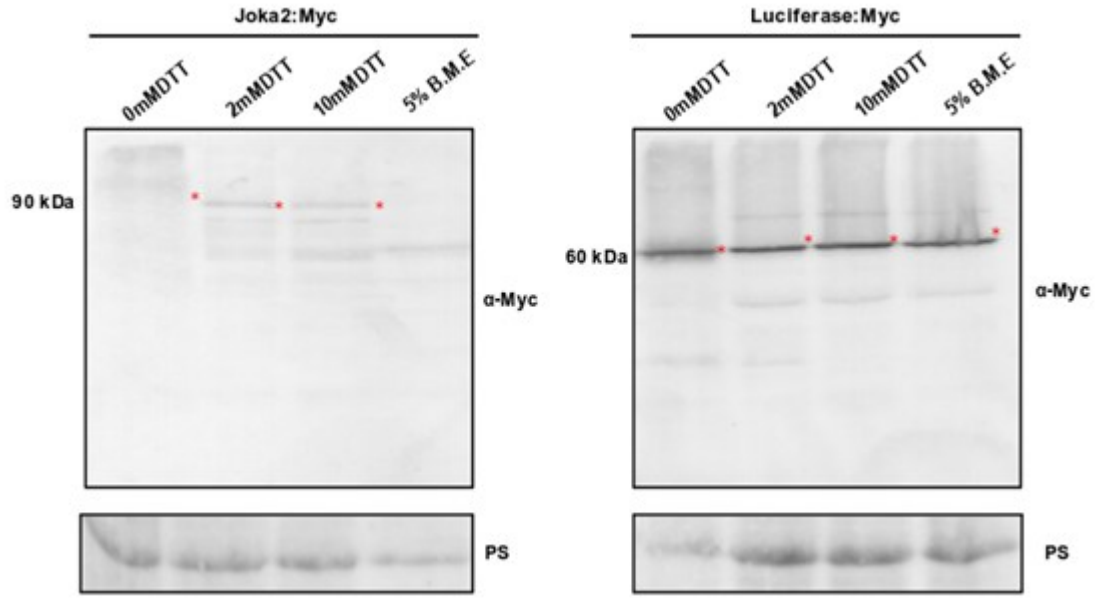

Figure 4.1: Joka2 shows an increased solubility when exposed to media containing a lower amount of reducing agent. *In planta* western blot of Myc tagged Joka2 and luciferase. Proteins were expressed in 4 week old *N. benthamiana* plants and samples were extracted 2 days post inoculation with *A. tumefasciens*. Red asterisks represent bands of expected size.

In order to verify that the change in solubility was caused due to the nature of Joka2 rather than due to the tag that I had decided to use, a further western blot was performed where the tag was changed from MYC to GFP whilst comparing Joka2 to a control EV (Figure 4.2). Once again, the reduction from 10mM to 2 mM DTT caused the Joka2 band to become thicker, whilst the EV band remained the same.

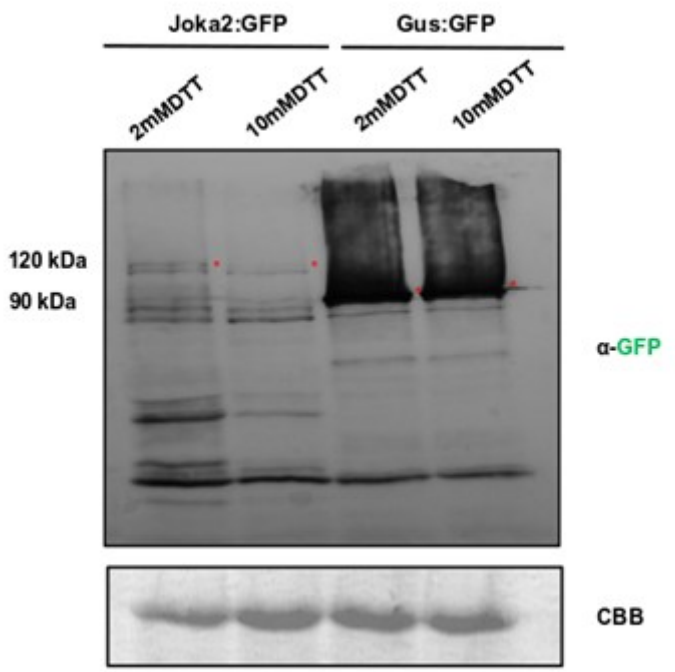

Figure 4.2:Joka2 shows an increased solubility when exposed to media containing a lower amount of reducing agent. *In planta* western blot of GFP tagged Joka2 and GUS. Proteins were expressed in 4 week old *N. benthamiana* plants and samples were extracted 2 days post inoculation with *A. tumefasciens*. Red asterisks represent bands of expected size.

To identify the domains responsible for Joka2's redox-dependent solubility, a systematic analysis of domain deletion mutants was performed. Initial investigations focused on the PB1 domain, which has been previously implicated in Joka2 oligomerization. A ΔPB1 mutant was generated and its solubility was assessed under varying DTT concentrations. Western blot analysis revealed that the ΔPB1 mutant retained the wild-type pattern of increased solubility under low DTT conditions (Figure 4.3), indicating that the PB1 domain is not essential for redox-dependent behavior.

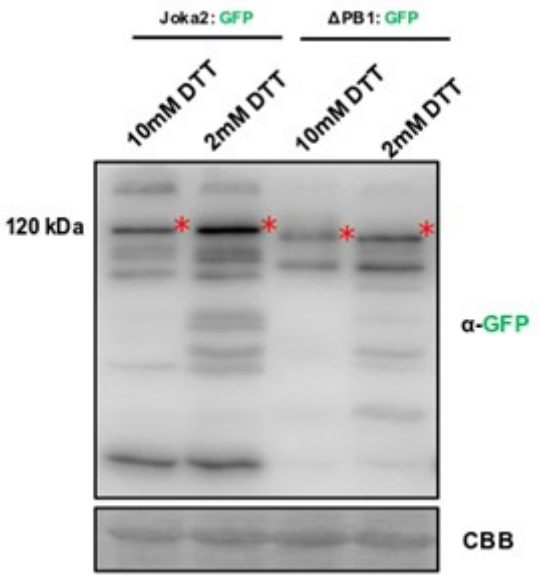

Figure 4.3:The change in solubility the Joka2 experiences is not linked to the HB domain of Joka2. *In planta* western blot of GFP tagged Joka2 and ΔHB. Proteins were expressed in 4 week old *N. benthamiana* plants and samples were extracted 2 days post inoculation with *A. tumefasciens*. Red asterisks represent bands of expected size.

Based on previous studies suggesting that cysteine residues often mediate protein responses to oxidative conditions, attention was directed to the ZZ domain, which contains two conserved cysteine residues. Concurrently, a novel protein region, designated as the HB domain, was identified in Joka2. To evaluate the potential contributions of these domains to redox sensitivity, ΔZZ and ΔHB truncation mutants were generated and analyzed under varying redox conditions (Figure 4.4).

Unexpectedly, the ΔZZ mutant exhibited wild-type solubility patterns despite the loss of two cysteine residues, suggesting that the ZZ domain is not the primary mediator of redox sensitivity. However, deletion of the newly identified HB domain, which contains two cysteine residues, produced a striking phenotype: the ΔHB mutant

displayed an inverse response to DTT concentration, with increased band intensity observed at higher (10 mM) rather than lower (2 mM) DTT concentrations. This finding suggests that the HB domain plays a critical role in determining Joka2's redox-dependent solubility properties.

These results reveal an unexpected complexity in Joka2's redox regulation, with the newly identified HB domain, rather than the cysteine-rich ZZ domain, appearing to be the key determinant of its oxidation-dependent behavior.

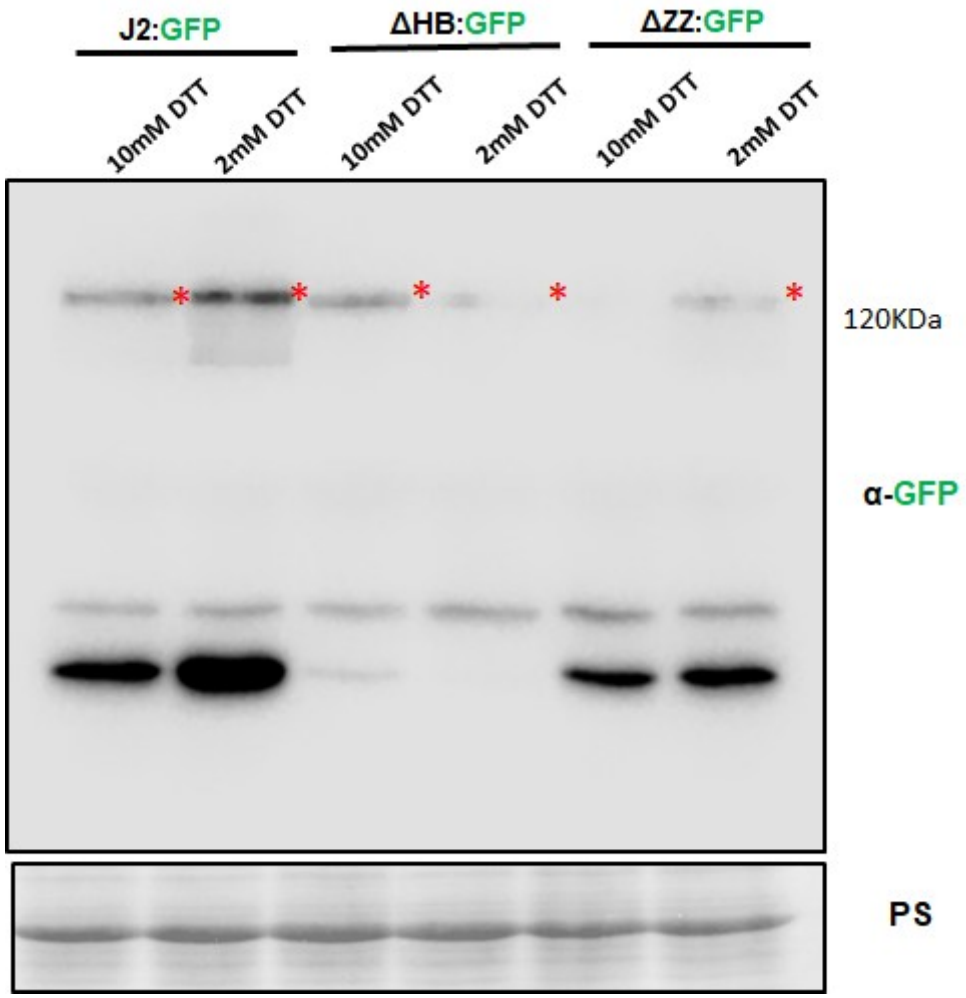

Figure 4.4: The shift in Joka2 is linked to the HB domain but not to the ZZ domain of Joka2. *In planta* western blot of GFP tagged Joka2, ΔZZ and ΔHB. Proteins were

expressed in 4 week old *N. benthamiana* plants and samples were extracted 2 days post inoculation with *A. tumefasciens*. Red asterisks represent bands of expected size.

4.3.2 Hydrogen peroxide exposure enhances Joka2 solubility

To further characterize Joka2's redox-dependent behavior, experiments were conducted to determine whether direct oxidation could replicate the effects observed under reduced DTT conditions. Hydrogen peroxide (H2O2) was selected as the oxidizing agent based on its established use in *Arabidopsis* redox studies and its physiological relevance as a cellular oxidant.

Protein extracts from *N. benthamiana* leaves expressing Joka2:GFP or GUS:GFP (control) were subjected to either 100 µM H2O2 or a mock treatment (water) for 60 minutes prior to SDS-PAGE analysis and immunoblotting. Western blot analysis revealed that H2O2 treatment significantly increased the intensity of the Joka2:GFP band compared to mock treatment, indicating enhanced protein solubility under oxidizing conditions (Figure 4.5). In contrast, GUS:GFP protein levels remained constant regardless of treatment, demonstrating that the observed effect was specific to Joka2 rather than a general response to oxidative conditions.

These results demonstrate that direct oxidation through H2O2 treatment recapitulates the effects observed with reduced DTT concentrations, providing further evidence that Joka2's solubility is specifically regulated by cellular redox conditions. The parallel responses to both decreased reducing agent and increased oxidizing agent suggest that this behavior reflects a physiologically relevant mechanism for regulating Joka2 function in response to cellular oxidative state.

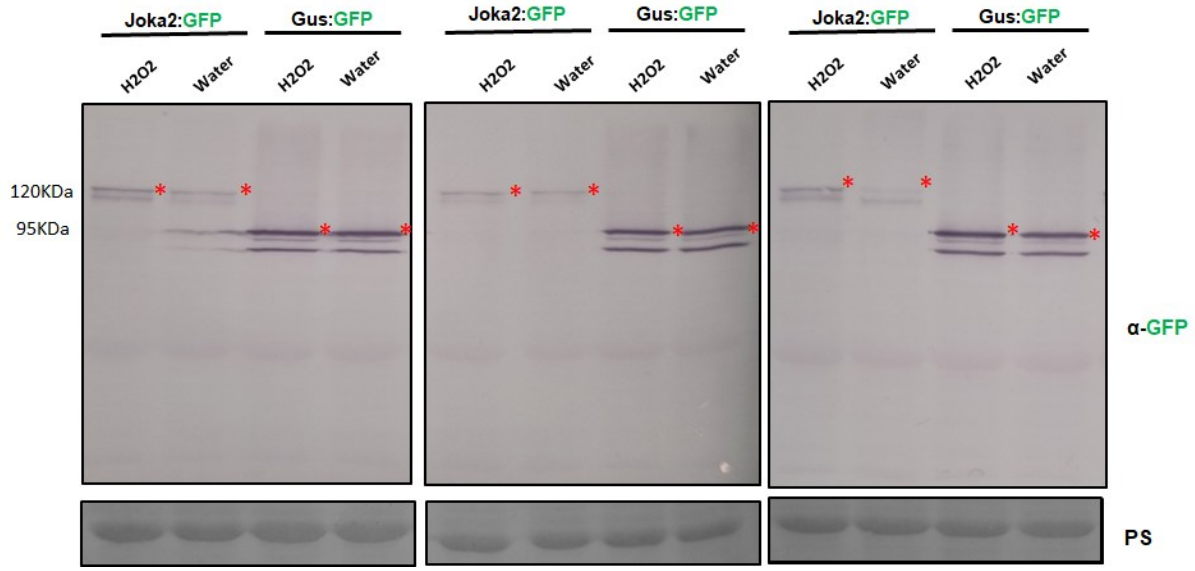

Figure 4.5: Joka2 shows an increased solubility when exposed to media containing a higher amount of oxidizing agent. *In planta* western blot of GFP tagged Joka2 and GUS. Proteins were expressed in 4 week old *N. benthamiana* plants and samples were extracted 2 days post inoculation with *A. tumefasciens*. Three biological repeats shown.

4.3.3 Redox-dependent solubility of Joka2 is independent of the ZZ domain

To further explore the potential role of cysteine residues in Joka2's redox-responsive behavior, the ΔZZ truncation mutant was subjected to H2O2 treatment and analyzed by Western blot. This experiment was designed to determine whether the cysteine-containing ZZ domain was necessary for the observed increase in Joka2 solubility under oxidizing conditions.

Consistent with the previous findings using reduced DTT concentrations (Figure 4.2), the ΔZZ mutant retained the wild-type pattern of enhanced solubility in response to H2O2 exposure (Figure 4.6). Western blot analysis revealed increased band intensity for the ΔZZ mutant under oxidizing conditions compared to mock treatment, demonstrating that the ZZ domain is not required for redox-dependent changes in Joka2 solubility.

These findings provide compelling evidence that the redox-responsive properties of Joka2 are not dependent on the cysteine residues within the ZZ domain, despite their potential to form redox-sensitive disulfide bonds. This observation suggests the existence of alternative molecular mechanisms governing Joka2's response to cellular oxidation state, potentially involving other structural elements or regulatory domains within the protein.

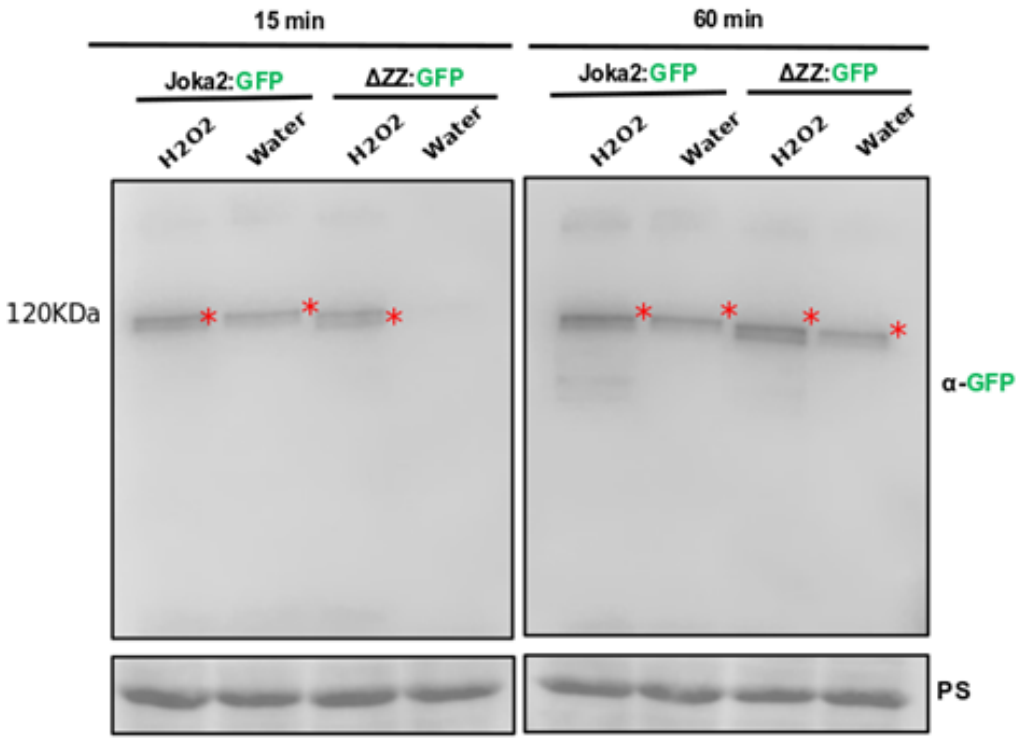

Figure 4.6: The ZZ domain is not responsible for the shift in solubility when under increased oxidation conditions. *In planta* western blot of GFP tagged Joka2 and ΔZZ. Proteins were expressed in 4 week old *N. benthamiana* plants and samples were extracted 2 days post inoculation with *A. tumefasciens*. Red asterisks represent bands of expected size.

4.3.4 The HB domain mediates Joka2's temporal response to oxidative conditions

Having established the HB domain's role in DTT-dependent solubility changes, its contribution to H2O2-mediated effects was investigated. The ΔHB truncation mutant was transiently expressed in *N. benthamiana* through *Agrobacterium*-mediated infiltration, and protein extracts were subjected to H2O2 treatment. To characterize

the temporal dynamics of this response, samples were analyzed at both early (15 minutes) and late (60 minutes) timepoints following oxidative treatment (Figure 4.7).

Western blot analysis revealed that deletion of the HB domain resulted in an inverse response to oxidative conditions compared to wild-type Joka2. The ΔHB mutant exhibited decreased solubility under oxidizing conditions, consistent with the reversed pattern previously observed in DTT experiments. This inverse relationship between oxidation and solubility was evident at both timepoints, with the effect being particularly pronounced at 15 minutes post-treatment.

These results further establish the HB domain as a critical determinant of Joka2's redox-dependent behavior. The consistent inverse response observed across both reducing (DTT) and oxidizing (H_2O_2) conditions suggests that the HB domain plays a fundamental role in coupling Joka2's solubility state to cellular redox conditions. The enhanced clarity of the response at 15 minutes indicates that this regulation occurs rapidly following changes in cellular redox state, suggesting it may represent an early response mechanism to oxidative stress.

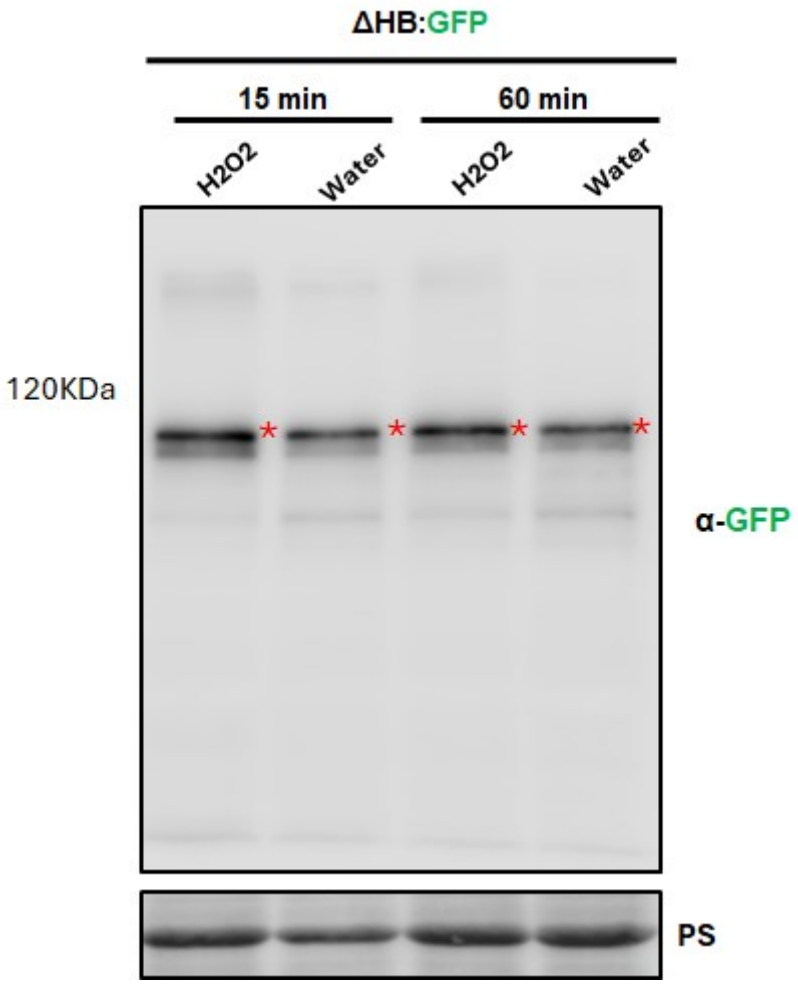

Figure 4.7: Removal of the HB domain eliminates the solubility shift seen under increased oxidation conditions. *In planta* western blot of GFP tagged ΔHB. Proteins were expressed in 4 week old *N. benthamiana* plants and samples were extracted 2 days post inoculation with *A. tumefasciens*. Red asterisks represent bands of expected size.

4.3.5 Recovery of insoluble Joka2 from pellet fractions under oxidizing conditions

Given the relatively low yield of soluble Joka2 compared to other proteins, experiments were conducted to investigate whether the protein's redox-dependent solubility could be exploited to recover additional protein from insoluble fractions. Initial observations suggested that a significant proportion of Joka2 might remain in the pellet fraction following standard extraction procedures.

To test this hypothesis, a sequential extraction protocol was developed where *N. benthamiana* leaves expressing Joka2 through *Agrobacterium*-mediated infiltration were processed using standard extraction procedures, but the post-centrifugation pellet was retained. The pellet was divided equally and resuspended in fresh extraction buffer containing either H_2O_2 or a water control. Following incubation at 4°C for one hour with constant agitation, the supernatant was collected. This extraction process was repeated three times, and all fractions were analyzed by Western blot (Figure 4.8).

Initial experiments using standard extraction buffer containing DTT showed no significant difference in Joka2 recovery between H2O2 and water treatments (Figure 4.8). However, when the protocol was modified to exclude DTT from the extraction buffer, H2O2 treatment resulted in significantly increased recovery of soluble Joka2 compared to the water control (Figure 4.9). This enhanced recovery under oxidizing conditions was consistent with previous observations of Joka2's redox-dependent solubility.

The discrepancy between results obtained with and without DTT suggests that the reducing agent likely neutralized the oxidizing effects of H2O2, preventing the redox-dependent solubilization of Joka2. These findings not only provide additional evidence for Joka2's redox-sensitive behavior but also establish a practical method for improving protein recovery from insoluble fractions. Furthermore, these results highlight the importance of considering buffer composition when studying redox-dependent protein properties, as reducing agents can potentially mask or interfere with oxidation-dependent effects.

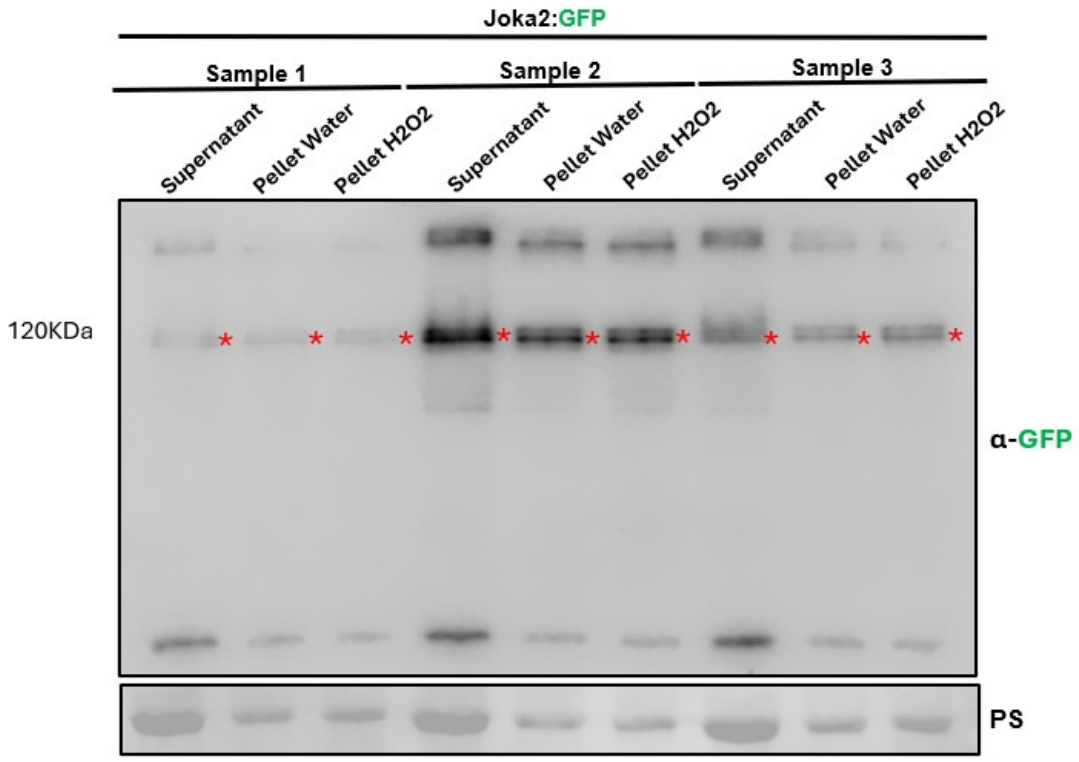

Figure 4.8: When there is DTT present within the extraction media, pellets extracted with hydrogen peroxide or water exhibit no difference in the amount of Joka2 present. *In planta* western blot of GFP tagged ΔHB. Proteins were expressed in 4 week

old *N. benthamiana* plants and samples were extracted 2 days post inoculation with *A. tumefasciens*. Joka2 pellet shows no difference in recovery levels regardless of the presence of hydrogen peroxide, when in the presence of reducing agents in the extraction media such as DTT. This is possibly due to a reaction between the oxidizing and reducing agents leading to no change in the redox potential.

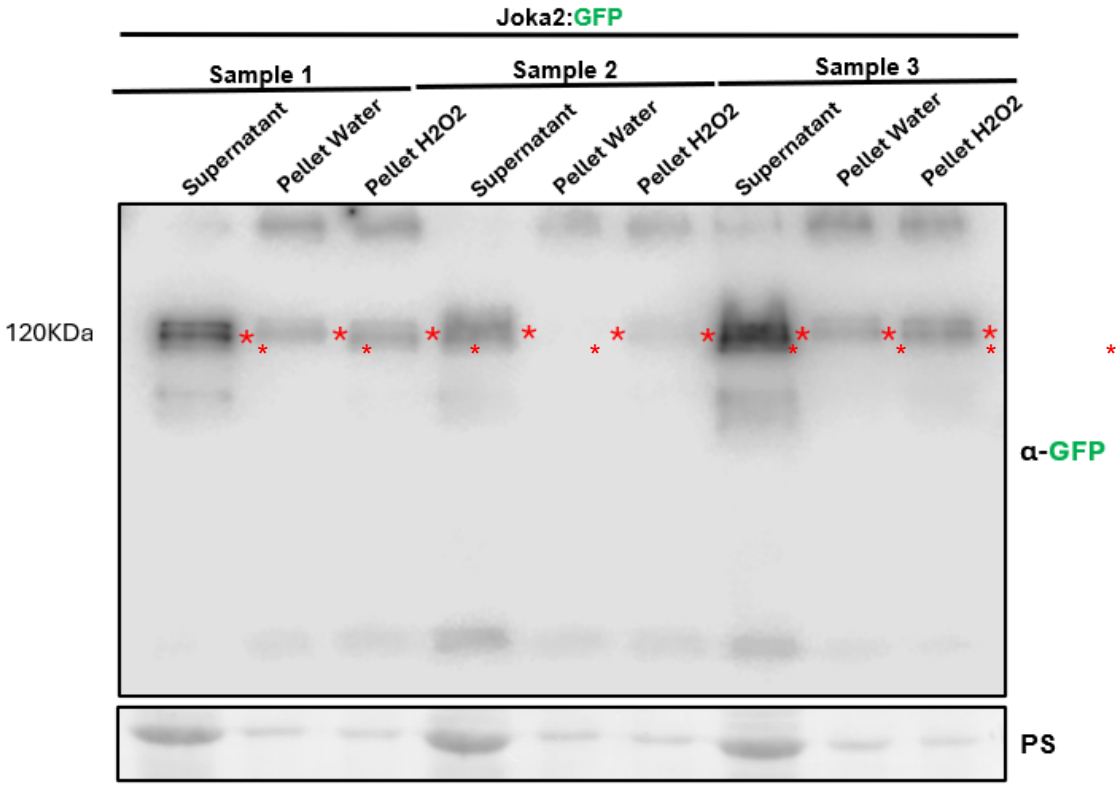

Figure 4.9: Upon removal of DTT from the extraction media, there is a significant difference in the band size when pellets are exposed to either water or hydrogen peroxide. *In planta* western blot of GFP tagged ΔHB. Proteins were expressed in 4 week old *N. benthamiana* plants and samples were extracted 2 days post inoculation with *A. tumefasciens*. Joka2 pellet exhibits distinct protein recovery levels when hydrogen peroxide is present in the recovery medium compared to when a mock water medium is used.

4.3.6 Microscopic analysis confirms time-dependent changes in Joka2 puncta formation under oxidative stress

To validate and quantitatively assess the biochemical findings, confocal microscopy analysis was employed to monitor Joka2 behavior in living cells. This approach offered several advantages, including the ability to perform quantitative analysis and capture temporal dynamics of Joka2 redistribution. However, it should be noted that the lack of suitable control proteins that form cytoplasmic puncta presented a limitation to this experimental approach, as conventional controls such as empty vector or maltose binding protein constructs exhibit purely diffuse cytoplasmic localization.

N. benthamiana leaves expressing fluorescently-tagged Joka2 or the ΔZZ truncate were treated with either H_2O_2 or water (mock), and confocal images were captured at 10 and 60 minutes post-treatment. Quantitative image analysis assessed both the number and size of Joka2 puncta (Figure 4.10). Both full length Joka2 and ΔZZ showed a significant increase in puncta number ($p<0.0001$) and decrease in puncta size ($p<0.01$) when exposed to PAMP treatment, whilst showing no significant difference when exposed to water treatment.

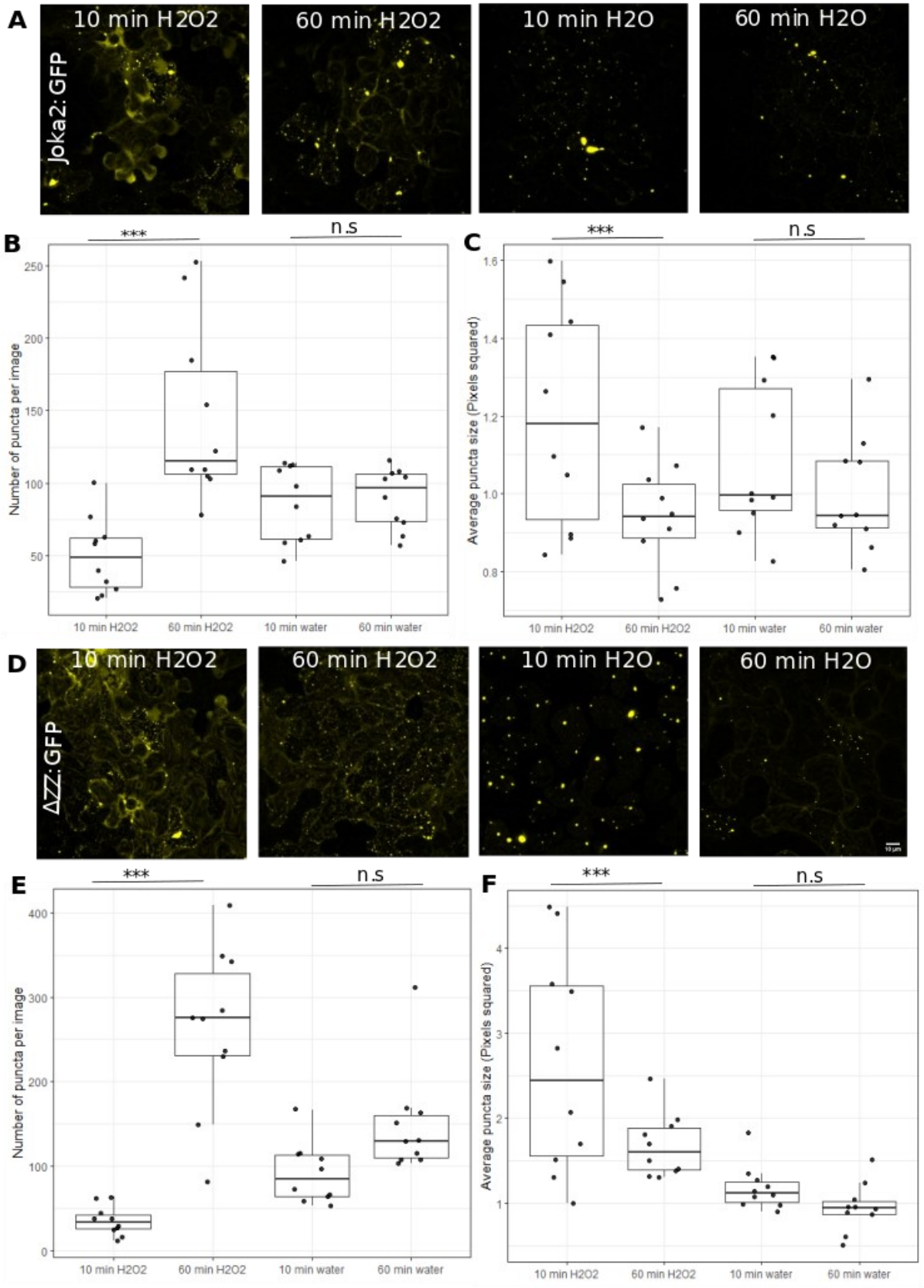

Figure 4.10: Full length Joka2 and ΔZZ both respond to hydrogen peroxide with an increase in puncta numbers and a decrease in puncta size. (A)

Representative images of Joka2:GFP at different timepoints and conditions. (B-C) Scatter plot graph showing 8 independent replicates, asterisks denote statistical significance (student's T-test) between groups.(D) Representative images of ΔZZ:GFP at different timepoints and conditions. (E-F) Scatter plot graph showing 8 independent replicates, asterisks denote statistical significance (student's T-test) between groups. Both Joka2 and ΔZZ show an increase in the number of puncta and a decrease in puncta size after 60 minutes under H_2O_2 treatment, but show no significant differences when exposed to the control water treatment.

These observations suggest that oxidative stress induces a time-dependent reorganization of Joka2 structures, potentially reflecting the protein's transition between different oligomeric states or cellular compartments.

Based on these temporal dynamics, the 60-minute time point was established as the standard for subsequent microscopy experiments with additional Joka2 variants. These microscopy results provide independent confirmation of Joka2's redox-dependent behavior and reveal additional aspects of its regulation that were not apparent from biochemical analyses alone.

Following this result, I also decided to test whether the results previously obtained through western blotting of ΔHB could also be replicated through microscopy in a similar fashion to those obtained with full length Joka2 (Figure 4.11).
Whilst Joka2 showed a significant increase in puncta numbers ($p=0.0024$) and a significant decrease in puncta size ($p=0.0461$), ΔHB did not show any of these differences, mimicking the results obtained from western blotting

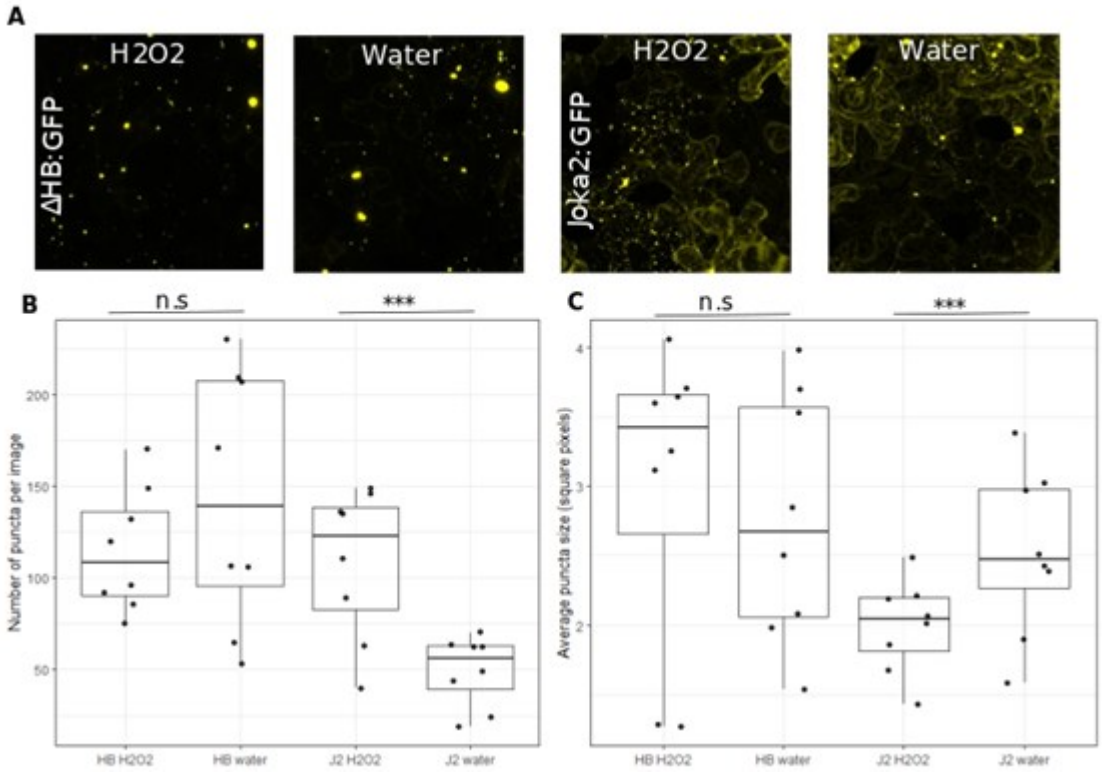

Figure 4.11: ΔHB puncta size and number do not change when exposed to hydrogen peroxide. (A) Representative images of Joka2:GFP and ΔHB:GFP (B-C) Scatter plot graph showing 8 independent replicates, asterisks denote statistical significance (student's T-test) between groups. Joka2 shows an increase in puncta numbers and a decrease in puncta size when PAMP treatment is compared to water treatment, however ΔHB does not show any significant difference.

4.3.7 Joka2 and NPR1 exhibit distinct responses to oxidative stress and salicylic acid

Following the characterization of Joka2's redox-dependent solubility, comparative analysis was undertaken with NPR1, a well-characterized *Arabidopsis thaliana* protein known to undergo oligomerization in response to salicylic acid (SA) during

systemic acquired resistance. This comparison was initiated to investigate potential parallels between pathogen-responsive oligomerization mechanisms.

Initially, NPR1's SA-dependent oligomerization was validated in the *N. benthamiana* system using Western blot analysis (Figure 4.12). Following successful reproduction of the previously reported NPR1 behavior, a comparative analysis of Joka2 and NPR1 responses to both H2O2 and SA treatments was performed (Figure 4.13). Western blot analysis revealed Joka2 exhibited increased solubility in response to H2O2 treatment, with no detectable response to SA, whilst NPR1 showed an oligomerized state exclusively in response to SA treatment, remaining unaffected by H2O2 exposure.

These findings demonstrate that despite both proteins showing condition-dependent changes in oligomerization state, their regulatory mechanisms are highly specific and independent. The lack of Joka2 response to SA is particularly noteworthy, as SA production typically follows the initial pathogen-induced ROS burst. This observation suggests that Joka2's redox-dependent behavior is specifically linked to early oxidative stress responses rather than downstream SA-mediated defense signaling.

The distinct response patterns of Joka2 and NPR1 highlight the precise regulation of defense-related protein oligomerization in plants, with different proteins responding to specific signals within the complex cascade of pathogen-induced cellular responses.

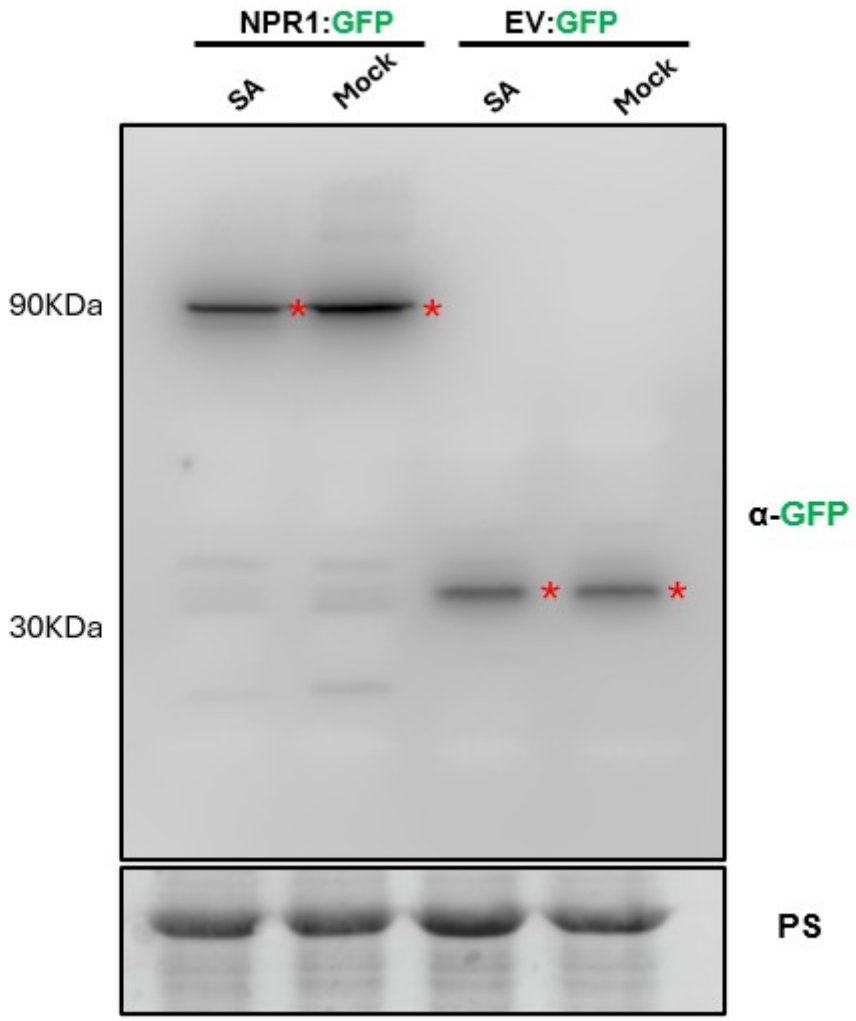

Figure 4.12: NPR1 oligomerizes in response to exposure to salicylic acid. *In planta* western blot of GFP tagged NPR1. Proteins were expressed in 4 week old *N. benthamiana* plants and samples were extracted 2 days post inoculation with *A. tumefasciens*. NPR1 shows increased aggregation as seen by the decrease in protein levels seen on the western blot.

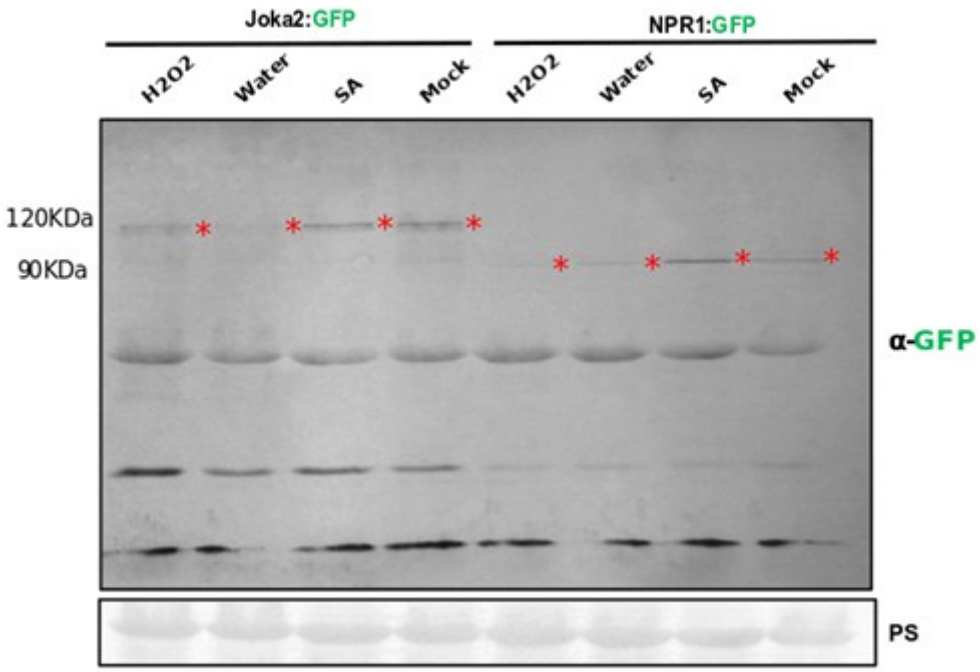

Figure 4.13: Joka2 does not oligomerize upon exposure to salicylic acid. *In planta* western blot of GFP tagged NPR1 and GFP tagged Joka2 . Proteins were expressed in 4 week old *N. benthamiana* plants and samples were extracted 2 days post inoculation with *A. tumefasciens*. Changes in solubility triggered by either SA or H2O2 seem to be exclusive to NPR1/Joka2 respectively as no significant change in protein concentrations can be seen when exposed to the other chemical.

4.3.8 PAMP-triggered immunity induces Joka2 reorganization in a HB domain-dependent manner

Given Joka2's sensitivity to H2O2 and the established role of ROS burst in early plant immune responses, the relationship between PAMP-triggered immunity (PTI) and Joka2 behavior was investigated. Initial biochemical analyses using Western

blot examined changes in Joka2 solubility following PAMP treatment (Figure 4.14). While some shifts in Joka2 solubility were observed, the results showed variable consistency, possibly due to the relatively modest amplitude of PAMP-induced ROS burst compared to direct H_2O_2 treatment. Notably, the ΔHB mutant showed no detectable response to PAMP treatment in these biochemical assays

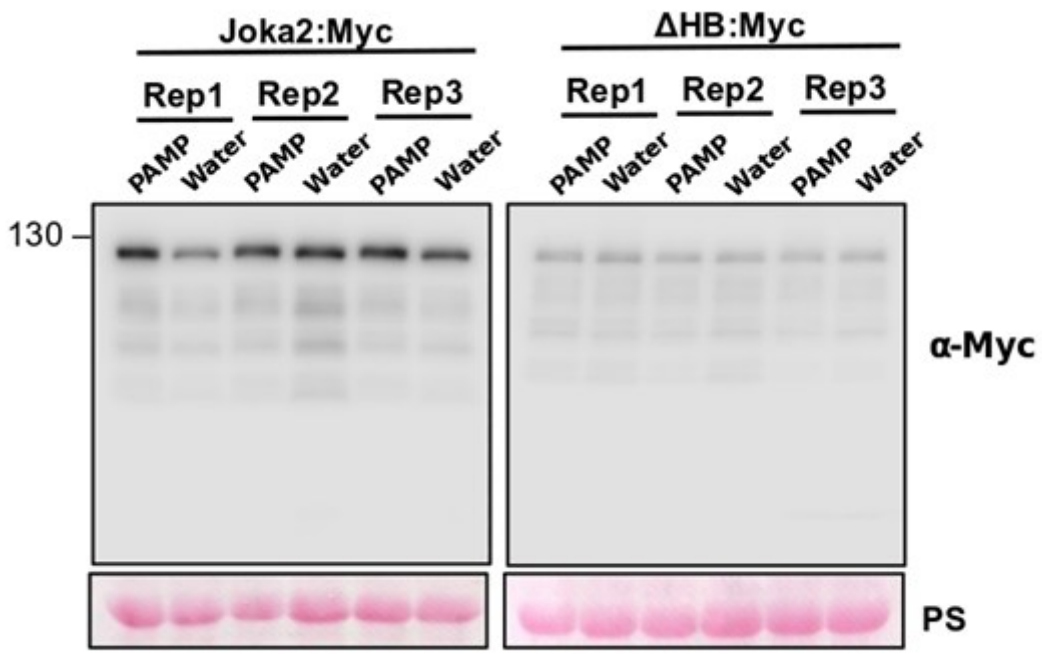

FIG 4.14:Joka2's response to PAMP extract cannot be determined using western blotting. *In planta* western blot of GFP tagged Joka2. Proteins were expressed in 4 week old *N. benthamiana* plants and samples were extracted 2 days post inoculation with *A. tumefasciens*. Three independent biological repeats are shown for both Joka2:Myc and ΔHB:Myc. Joka2:Myc seems to exhibit different behaviour to PAMP treatment with repeats 1 and 3 showing increased protein levels under PAMP treatment and repeat 2 showing no change/lower protein levels under PAMP treatment. No repeats show any significant changes in protein levels for ΔHB:Myc. Results obtained with the help of Cecilia Longoni

To achieve higher resolution analysis of these subtle changes, confocal microscopy was employed to examine both wild-type Joka2 and the ΔHB mutant following PAMP treatment (Figure 4.15). Quantitative image analysis revealed that wild-type Joka2 responded to PAMP treatment with an increased number of puncta ($p=9.3x10^{-5}$) and decreased average puncta size (p=0.00374), matching the response pattern previously observed with H2O2 treatment. In contrast, the ΔHB mutant showed no significant changes in either puncta number or size, demonstrating a complete loss of PAMP responsiveness.

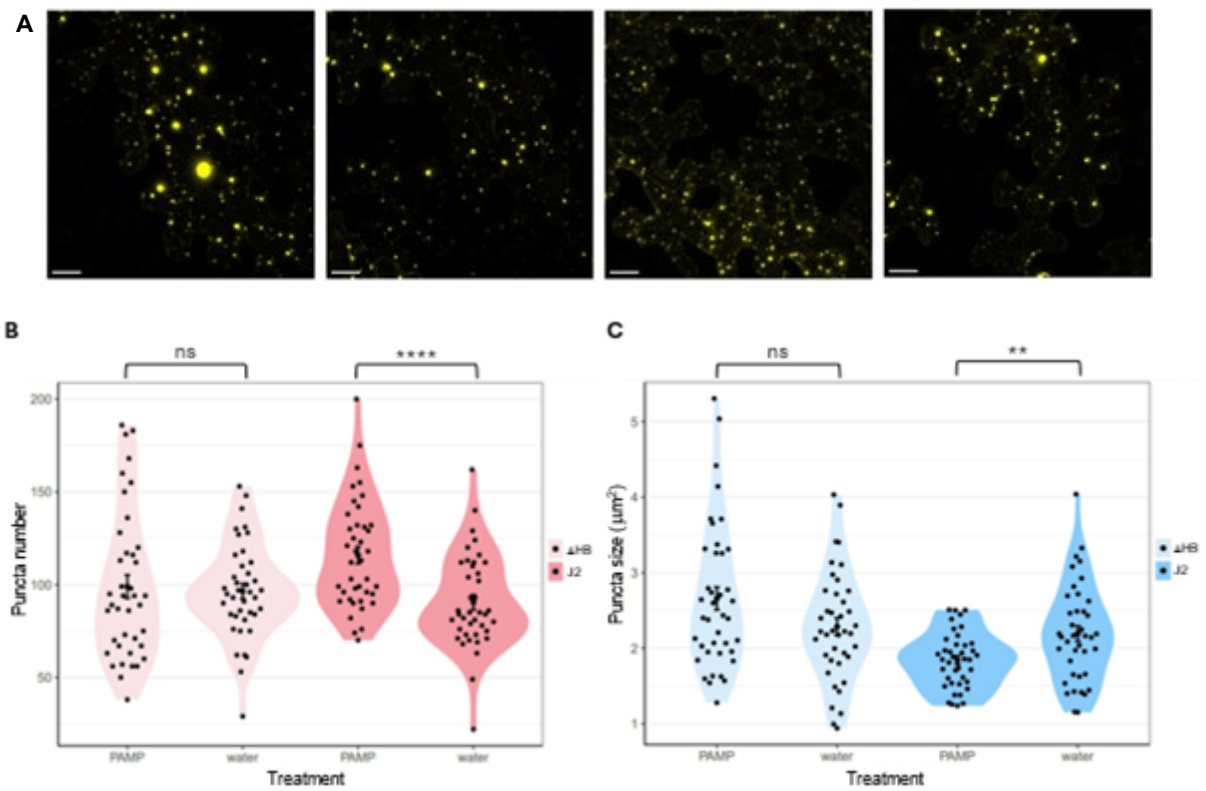

Figure 4.15:: Full length Joka2 and ΔHB both respond to PAMP treatment with an increase in puncta numbers and a decrease in puncta size (A) Representative images of Joka2:GFP and ΔHB:GFP (B) Violin plot showing puncta number for overexpressed

DHB (light pink) and full length Joka2 (dark pink). (C) Violin plot showing puncta size (mm^2) for overexpressed DHB (light blue) and full length Joka2 (blue). Results obtained with the help of Cecilia Longoni

These microscopy results demonstrate that PAMP treatment induces reorganization of Joka2 structures in a manner similar to direct oxidative stress, suggesting that Joka2 responds to the PTI-associated ROS burst. The complete absence of response in the ΔHB mutant further establishes the HB domain as a critical mediator of Joka2's integration into early immune responses. The enhanced sensitivity of microscopy-based analysis enabled detection of these PAMP-induced changes that were less apparent in biochemical assays, likely due to the more moderate nature of physiological ROS production compared to external H2O2 treatment.

4.3.9 Fluorescence Recovery After Photobleaching reveals altered Joka2 mobility under oxidative conditions

To quantitatively assess changes in Joka2 mobility and solubility, Fluorescence Recovery After Photobleaching (FRAP) analysis was employed as a complementary approach to puncta quantification. FRAP provides a direct measure of protein dynamics in living cells by monitoring the rate at which fluorescent molecules repopulate a photobleached region.

In FRAP experiments, specific Joka2 puncta were targeted with high-intensity laser illumination, causing irreversible photobleaching of the fluorophore within the defined region of interest. The subsequent recovery of fluorescence intensity occurs through the diffusion of unbleached fluorescent proteins from the surrounding cytoplasm into

the bleached area. The rate of this recovery serves as a quantitative measure of protein mobility: highly soluble proteins exhibit rapid recovery due to unrestricted diffusion, while proteins in aggregates or large complexes show delayed recovery due to limited mobility.

To investigate whether oxidative conditions affect Joka2 mobility, FRAP analysis was performed on Joka2-expressing *N. benthamiana* leaves treated with either H2O2 or water (mock). Individual puncta were photobleached and their fluorescence recovery was monitored over time (Figure 4.16). This approach provided a direct measurement of Joka2's dynamic behavior under different redox conditions, complementing the previous biochemical and microscopic analyses of its solubility state.

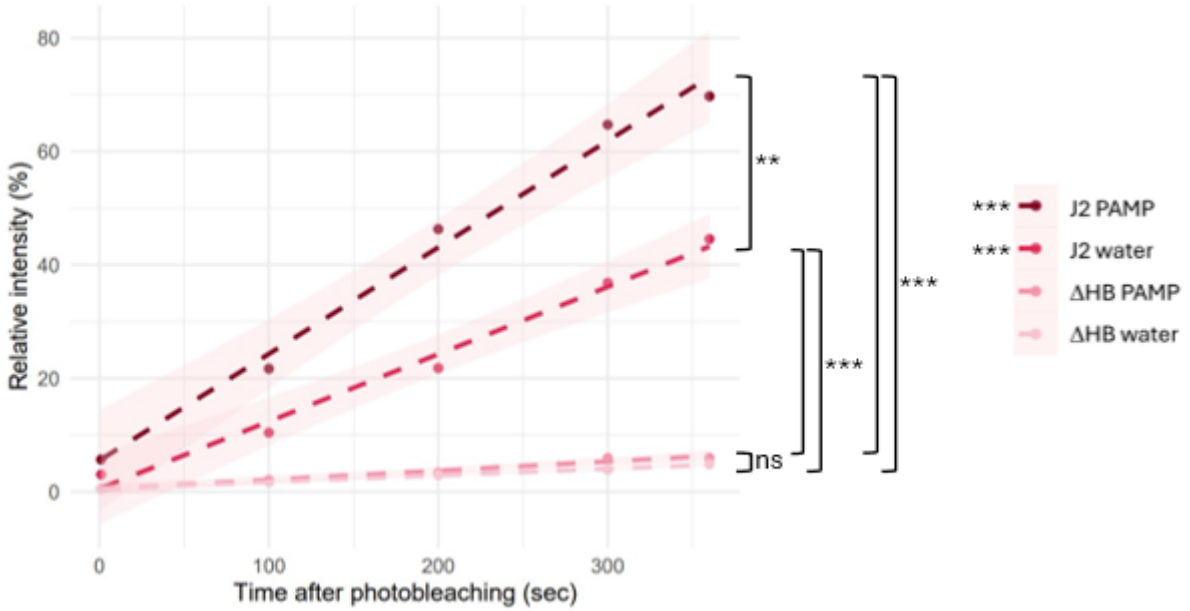

Figure 4.16: PAMP extract causes Joka2 puncta to recover faster after photobleaching but has no effect on ΔHB puncta recovery. Linear regression model of recovery over time. Recovery is measured as relative intensity, calculated from average grayscale value across puncta and maximum fluorescence (from t=0). Each data

point is the average of 6 independent repeats. Error bars are represented by pale pink shading around regression lines. Results obtained with the help of Cecilia Longoni

Statistical analysis of the FRAP reveals there is a significant difference in recovery of Joka2 between t=0 and t=360 in both water(p=1.08e-11) and PAMP(p=<2e-16), although in the presence of PAMP extract Joka2 recovers at a significantly faster rate(p=0.00158). ΔHB on the other hand, not only does not show any significant recovery in fluorescence, but also does not show a significant difference between treatments. There is also no significant difference between the y-intercepts of the slopes, meaning all punctas were bleached to the same extent regardless of treatment.

4.3.10 The ΔHB mutant retains ATG8-binding functionality

To address whether the altered redox sensitivity of the ΔHB mutant resulted from protein misfolding rather than specific domain function, ATG8-binding capacity was assessed. While Joka2 lacks established functional assays and its cargo specificity remains undefined, its interaction with ATG8 serves as a critical indicator of proper protein folding and functionality.

Co-immunoprecipitation experiments were performed comparing ATG8 binding among wild-type Joka2, the ΔHB mutant, and empty vector control (Figure 4.17). Western blot analysis demonstrated that both wild-type Joka2 and the ΔHB mutant successfully co-immunoprecipitated with ATG8, while no interaction was detected with the empty vector control. This preserved ATG8-binding capability of the ΔHB mutant indicates that the protein remains properly folded and maintains essential

molecular interactions, suggesting that its altered redox response represents a specific loss of HB domain function rather than general protein dysfunction.

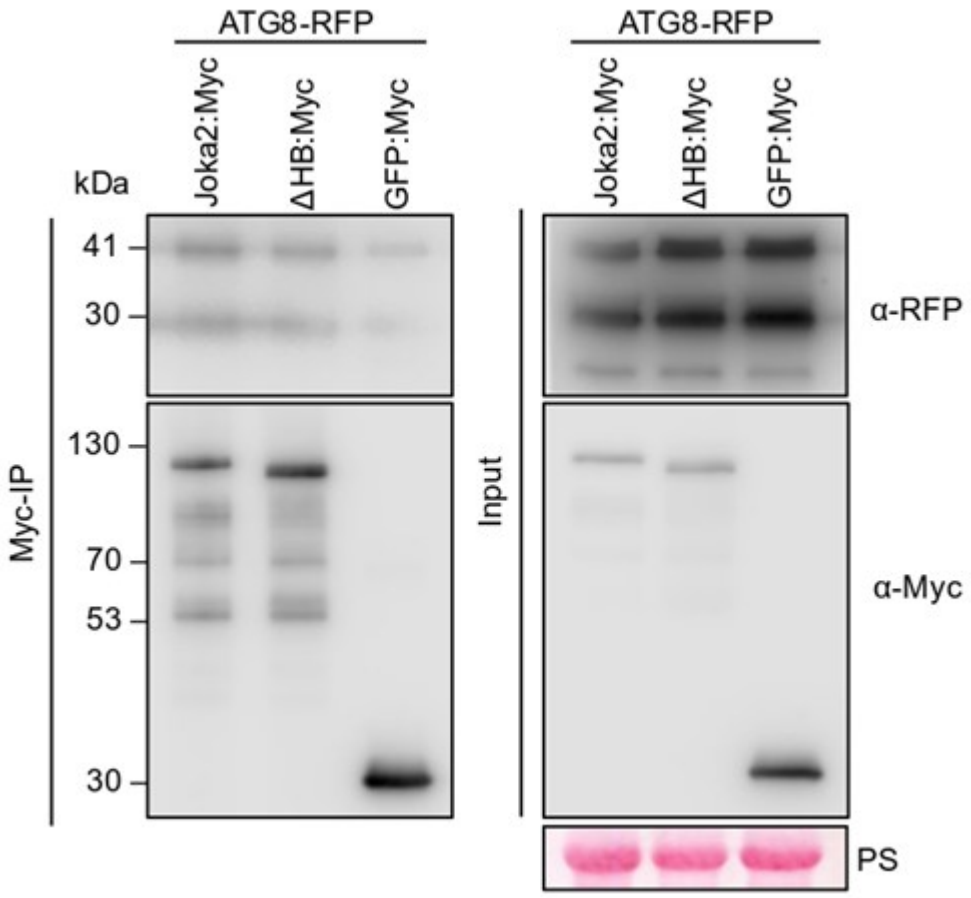

Figure 4.17: ΔHB is still able to bind ATG8 similarly to full length Joka2. *In planta* western blot of MYC tagged Joka2, ΔHB and GFP with RFP tagged ATG8. Proteins were expressed in 4 week old *N. benthamiana* plants and samples were extracted 2 days post inoculation with *A. tumefasciens*. Results obtained with the help of Cecilia Longoni

4.4 Discussion

While p62 has been relatively well characterized in the literature, its plant homolog Joka2 remains largely unexplored despite its important role in autophagy. The discovery that p62's function is regulated by redox conditions led me to investigate whether Joka2 shares this redox sensitivity.

As a first step, I started by changing the levels of DTT present within the solution used to extract proteins from leaf extract after agroinfiltration (Figure 4.1) Reduction of DTT causes an increase in the oxidative state of the solution and an increase in the soluble fraction of Joka2, as seen by the stronger intensity of the bands on the western blot. In order to verify that this was not because of the protein tag associated with the protein, I repeated this experiment with another tag (Figure 4.2) and it yielded the same results, a lower reducing agent concentration led to an increase in Joka2 solubility.

Once this shift had been established, I decided to further investigate which domain was responsible for this shift in solubility. I decided to start with the PB1 domain since that has been described as the domain responsible for the oligomerization of Joka2 (Zientara-Rytter & Sirko, 2014), and so it could be related to the change in solubility, however, removing the PB1 domain did not result in any changes to Joka2 solubility when exposed to different redox conditions (Figure 4.3). I then decided to test whether the ZZ domain was responsible, since it has the most cysteines of any Joka2 domain with 2, and cysteines are prone to changes under altered redox conditions that can be used for signalling (Van Der Reest et al., 2018). However its removal also resulted in no change, only with the removal of the newly discovered

HB domain did the exposure to an increased oxidative environment not yield an increase in Joka2 solubility (Figure 4.4). These results indicated that unlike p62, Joka2's redox dependent oligomerization was not PB1 dependent but rather HB dependent. The ZZ domain also appeared to not be involved although it contained the highest number of cysteines within any of the Joka2 domains.

As a way to verify the previous experiments, rather than decreasing the amount of DTT within the extraction buffer, I decided to add hydrogen peroxide, to test it was not that an increase in DTT was causing aggregation, but rather that it was linked to the redox potential of the environment. As expected, an increase in hydrogen peroxide did yield an increase in Joka2 solubility (Figure 4.5). This shift in solubility was not affected by the removal of the ZZ domain (Figure 4.6) , but was completely eliminated with the removal of the HB domain (Figure 4.7).

After establishing that Joka2 responds to hydrogen peroxide, I decided to test whether this property could be utilized to recover insoluble Joka2 from the pellet formed during protein extraction. To test this, the pellet was washed with either water or H2O2, and the solubility of Joka2 was analyzed. Interestingly, the results show no discernible difference between water and H2O2 treatments (Figure 4.8). This outcome can be attributed to the presence of DTT in the extraction mixture, which neutralizes the H2O2 by reacting with it. When the experiment was repeated without DTT in the extraction mixture, a clear difference between water and H2O2 treatments was observed (Fig. 4.9). These findings confirm that Joka2's solubility can be modulated by H2O2 under conditions where reducing agents like DTT are

absent, providing a practical method for recovering insoluble Joka2 during protein extraction.

To verify that this process also occurred *in vivo*, as well as to corroborate the previous findings through an alternate method, confocal microscopy was performed on leaves that had been infiltrated with hydrogen peroxide. Both puncta number (Figure 4.10) and puncta size (Figure 4.11) measurements were taken at both 10 and 60 minutes post treatment. In these measurements, Joka2 exhibits a shift in puncta distribution, after being exposed to hydrogen peroxide, with an increase in the overall number of puncta. However, those puncta were significantly smaller than the ones in the control treatment, whilst ΔHB showed no differences between the control and water treatments. I believe that this change in distribution can be attributed to Joka2's solubility shift causing larger puncta to break down into smaller puncta after Joka2 becomes more soluble, causing it to not aggregate as much as when there is a more reducing environment.

Previous results indicate that Joka2 responds to ROS, which are known to play a key role in the plant immune response as signaling molecules. Salicylic acid (SA), another critical component of the plant immune system, is closely linked to ROS signaling, often acting downstream or in coordination to modulate defense responses (Noctor, Reichheld & Foyer, 2018). This raises the question: does Joka2 also respond to SA, and if so, how might this interaction contribute to the broader immune signaling network in plants? As a control for this, I decided to use the NPR1 protein that aggregates in response to salicylic acid (Mou, Fan & Dong, 2003). After validating that the change in solubility of NPR1 can be detected using a western blot

(Figure 4.13) I decided to expose both Joka2 and NPR1 to both SA and hydrogen peroxide (Figure 4.14). Neither the Joka2 reacted to the SA nor the NPR1 reacted to the hydrogen peroxide. This result was unexpected, given the well-established link between SA and ROS in plant immune signaling with their frequent coordination suggesting a high degree of interplay between the two pathways. The observed specificity, with Joka2 responding only to ROS and NPR1 only to SA, highlights a surprising level of functional divergence. Also, the lack of response of Joka2 to SA indicates that its interaction with ROS is highly specific and does not extend to other components of the immune signaling network, such as SA. This specificity suggests that Joka2 may have a distinct and targeted role within the plant immune response, independent of the broader SA-mediated pathways.

Joka2 has been shown to specifically respond to ROS, which are rapidly generated in plants as signaling molecules during the early stages of pathogen invasion. This ROS burst is a hallmark of the immune response and is closely associated with the activation of downstream defense mechanisms (Noctor, Reichheld & Foyer, 2018). PAMP treatment, which mimics infection by triggering immune signaling pathways, induces ROS production. Therefore, I investigated whether or not, PAMP treatment was sufficient to induce a change in the solubility of Joka2. At first I tried using the same western blot technique that I used for the hydrogen peroxide treatments (Figure 4.15). Whilst I obtained the results I expected for the HB domain, no difference between PAMP treatment and water, the results for Joka2 were inconsistent, possibly due to the more modest amount of ROS produced as a result of the PAMP treatment compared to the more potent hydrogen peroxide. Therefore, this method proved ineffective due to the low degree of definition in western blots,

and their lack of quantificaiton to perform statistics. Therefore I resorted to microscopy, as a way to quantify this effect. PAMP treated Joka2 showed an increase in puncta with smaller overall puncta size, whilst ΔHB showed no difference between treatments (Figure 4.16). The effect on the Joka2 puncta is what would be expected for an increase in solubility, with smaller puncta indicating that Joka2 shifts its localization from the puncta to the cytoplasmic fraction.

In order to further validate the microscopy, FRAP was performed on several of the Joka2 puncta, since FRAP can be used to determine the diffusion rate of a protein and to that extent, its solubility. Figure 12 indicates that by removing the HB domain from Joka2, the solubility shift caused by the PAMP treatment is also removed. This can be seen by the much slower recovery times, indicative of a reduced soluble fraction of Joka2 in the surrounding cytoplasm. Furthermore, when compared to mock treatment, ΔHB did not show a significant difference compared to PAMP, whilst the full length Joka2 did, leading me to conclude that the HB domain is the main domain responsible for the redox solubilization and phase transition of Joka2.

Finally, as a method of validation that the changes in solubility that were observed were not as a result of ΔHB being misfolded a co-immunoprecipitation was performed to determine if its ATG8 binding ability had been retained (Figure 4.18) ΔHB was able to pulldown ATG8 as efficiently as the control full-length Joka2.

The identification of the HB domain as the driver of redox sensitivity reveals a functional divergence between Joka2 and its mammalian homolog, p62. While oxidative stress triggers p62 aggregation via disulfide bond formation (Otten et al., 2018) my results demonstrate that both ROS and PAMPs conversely promote Joka2

solubilization. This dynamic aligns with recent models of Liquid-Liquid Phase Separation (LLPS) in autophagy, where phase transitions are used to regulate reaction kinetics and protein availability (Noda, Wang & Zhang, 2020)

The independence of these changes from the SA pathway, however, is striking since SA is linked to cellular redox signaling most often through the glutathione pool (Kuźniak et al., 2013). One emerging theory is that of the redox rheostat, where different thresholds of redox intensities must be crossed for different pathways to be active. By using this model, the plant would be able to distinguish between the different immune phases. More specifically, it would differentiate between the smaller redox shifts associated with SA signaling compared to the larger ROS burst at the active infection site (Liu, Liu & Mou, 2024; Lukan & Coll, 2022)ensuring Joka2 is only mobilized at immediate sites of infection.
This redox rheostat model has also been reported in epithelial stem cell development (Chen et al., 2025)

The identification of the HB domain as a cysteine-dependent sensor suggests that Joka2 functions via a redox switch mechanism, a strategy widely employed by plant immune regulators. This is analogous to the behavior of TGA transcription factors, which utilize conserved cysteine residues to sense cellular redox potential and modulate their DNA-binding capacity during the immune response (Herrera-Vásquez et al., 2020). Similarly, the NPR1 protein relies on cysteine reduction to switch between oligomeric storage and monomeric active forms (Zavaliev et al., 2020). However, Joka2 presents a unique variation on this theme. While TGA and NPR1 utilize redox switches primarily to control nuclear translocation or transcriptional

activity (Zavaliev & Dong, 2024), the HB domain appears to couple with cysteine oxidation directly to phase transition and solubility.

In this chapter I have explored how changes in the redox potential of the environment affect Joka2 solubility and which domains are responsible for this change. Interestingly it was not the PB1 domain which had been previously documented as the domain responsible for changes in p62, nor was it the ZZ domain which contained the highest amount of cysteine residues, but rather it was the newly discovered HB domain the one responsible for these changes. Although the shift in solubility can be seen clearly with the use of hydrogen peroxide, PAMP treatment, which causes an immune response within the plant and therefore a ROS burst within the cells, is sufficient for this shift to occur, although to a lesser extent than the hydrogen peroxide treatment.

I believe the reason for this shift, similarly to that of p62, is due to the cysteine residues within Joka2. Cysteine residues can oxidize in two different ways, depending on whether or not there is a second cysteine residue nearby. If there is, both cysteines form a disulphide bridge between the residues, leading to a less soluble state, which is what happens in p62 (Poole & Nelson, 2008). I propose that in Joka2, cysteine residues behave differently and oxidize without a secondary cysteine being present, leading to the formation of sulfonic and sulfenic acid, both of which are highly polar, causing the protein to become more soluble. Verification of this hypothesis needs further investigation, with one key experiment being the substitution of the cysteine residue within the HB domain of Joka2 with an alanine, to eliminate its function.

Chapter 5 - The role of Joka2 on gene expression and signalling

5.1 Introduction

5.1.1 Transcriptional regulation of plant defense

Transcriptional reprogramming is a fundamental aspect of plant immunity that orchestrates complex defense responses against pathogens. This reprogramming involves multiple regulatory layers that control the expression of defense-related genes through both direct transcriptional regulation and protein-protein interactions that affect signaling cascades (Aerts et al., 2022).

Transcriptional regulation involves proteins whose function is modulated by cellular redox states. A well-characterized example is NPR1 (Non-expresser of PR genes 1), which serves as a master regulator of defense gene expression. Under normal conditions, NPR1 exists as oligomers in the cytoplasm, held together by disulfide bridges (Mou, Fan & Dong, 2003). During pathogen attack, changes in cellular redox status lead to NPR1 monomerization and nuclear translocation, where it acts as a transcriptional co-activator through interaction with TGA transcription factors to activate defense genes (Zhou, Jun-Ma et al., 2000).

Modulation of the function of transcription factors can also be done through post-translational modification. MAPKs play an important role through the phosphorylation of transcription factors such as WRKY33, responsible for the production of camalexin in response to *Botritis cinerea* infection in *A. thaliana* (Mao et al., 2011). Although other kinases such as calcium-dependent kinases have also been shown to play a role in transcription factor phosphorylation (Zhou, Jinggeng et al., 2020).

Besides phosphorylation, ubiquitination is also important as a method of protein level control, such as in the case of ORA59, a transcription factor that is ubiquitinated after

the detection of increased levels of salicylic acid, resulting in its degradation through the 26S proteasome pathway (Van der Does et al., 2013).

5.1.2 The role of p62 and NBR1 in signalling and gene expression

The human orthologs of Joka2, NBR1 and p62, play an important role in signalling in addition to autophagy. More specifically, both proteins have been found to play a role in defence against cancer cells. p62 has been shown to upregulate several transcription factors such as Nrf2 and NF-κB (Tang et al., 2021). This first transcription factor is involved in the expression of antioxidant and cytoprotective genes and the latter is a well known regulator of the immune response and inflammation related genes. p62 also associates with the multi protein complex HIF1α, which in turn regulates many genes involved in glucose metabolism and angiogenesis, although it can also modulate glucose metabolism by direct association with either HK2 or GLUT (Glucose transporter) proteins (Chen et al., 2016). Human NBR1 also plays a role in signalling, by interacting with Interferon regulatory factor 3 (IRF3) and promoting its degradation through autophagy, reducing the expression of interferon stimulated genes during innate immunity (Cai, Y. et al., 2022). NBR1 also interacts with the interleukin subunits IL12A and IL12B leading to regulation of genes involved in T-cell response and inflammation (Yang, J. et al., 2010).

The plant NBR1 also plays a role in signalling, with the arabidopsis NBR1 affecting the expression of absisic acid (ABA) genes (Yang, J. et al., 2010). In poplar on the other hand, NBR1 accelerates antioxidant system activity through gene modulation to enhance salt stress tolerance (Yang, J. et al., 2010).

5.2 Aim

In previous chapters, I have established how Joka2 both interacts with members of the MAP kinases and changes solubility in a redox dependent manner. In this chapter, I investigate whether either of these are connected to Joka2's role in immunity. My approach to this is manyfold, first I aimed to investigate whether Joka2 plays a role a scaffolding protein by establishing whether its absence leads to a reduction in defence gene expression, I then aimed to see if this is MAPK related by trying to rescue the phenotype using truncates that lack some of the domains responsible for MAPK binding. Secondly I also aimed to investigate whether removal of the HB domain results in a loss of immunity against *P. infestans* similarly to the NBR1 domain. Finally, I aimed to see if the solubility shift of Joka2 makes it associate less with ATG8 and more with members of the MAPK family signifying a shift from its autophagic role into a scaffolding and signalling role.

5.3 Results

5.3.1 Joka2 is responsible for the upregulation of certain genes associated with defence

Since I believe that Joka2 could have a role in the signaling of the MAPKs by serving as a scaffolding protein, I decided to see if any genes were active downstream of Joka2.

To accomplish this, we started by silencing opposite sides of the same leaf with either a Joka2 RNAi construct or a control GUSRNAi. Once the leaves had been appropriately silenced, they were fully exposed to either PAMP treatment obtained form *P. infestans* or a water control (Figure 5.1.A). RNA-seq was then performed of 3 replicates of each contruct labled (J1-12). Results were then STAR (Spliced transcripts alignment to a reference) mapped to the reference genome (Citation needed). As a quality control measure PCA (principal component analysis) plots were performed on the normalized gene counts for all samples, as seen in figure 5.1.B. The variance between repetitions was higher than that of the different RNAi constructs, therefore facilitating a direct comparison between the two treatments. Following these quality controls we then moved on to select wich genes were differentially expressed. In order to decide this, we needed to set some boundaries for both the p-adjusted values and the log fold counts. After carefull consideration we decided to use p-adjusted values that were smaller than 0.05 and log fold counts that were bigger than 1 (Figure 5.1.C and 5.1.D). We then filtered though te datatsets to obtain genes that met these condions whilst PAMP- treated but not whilst control-

treated when GUS was silenced and viceversa when Joka2 was silenced. The results of this are shown in table 5.1. 6 genes were found to fit the criteria

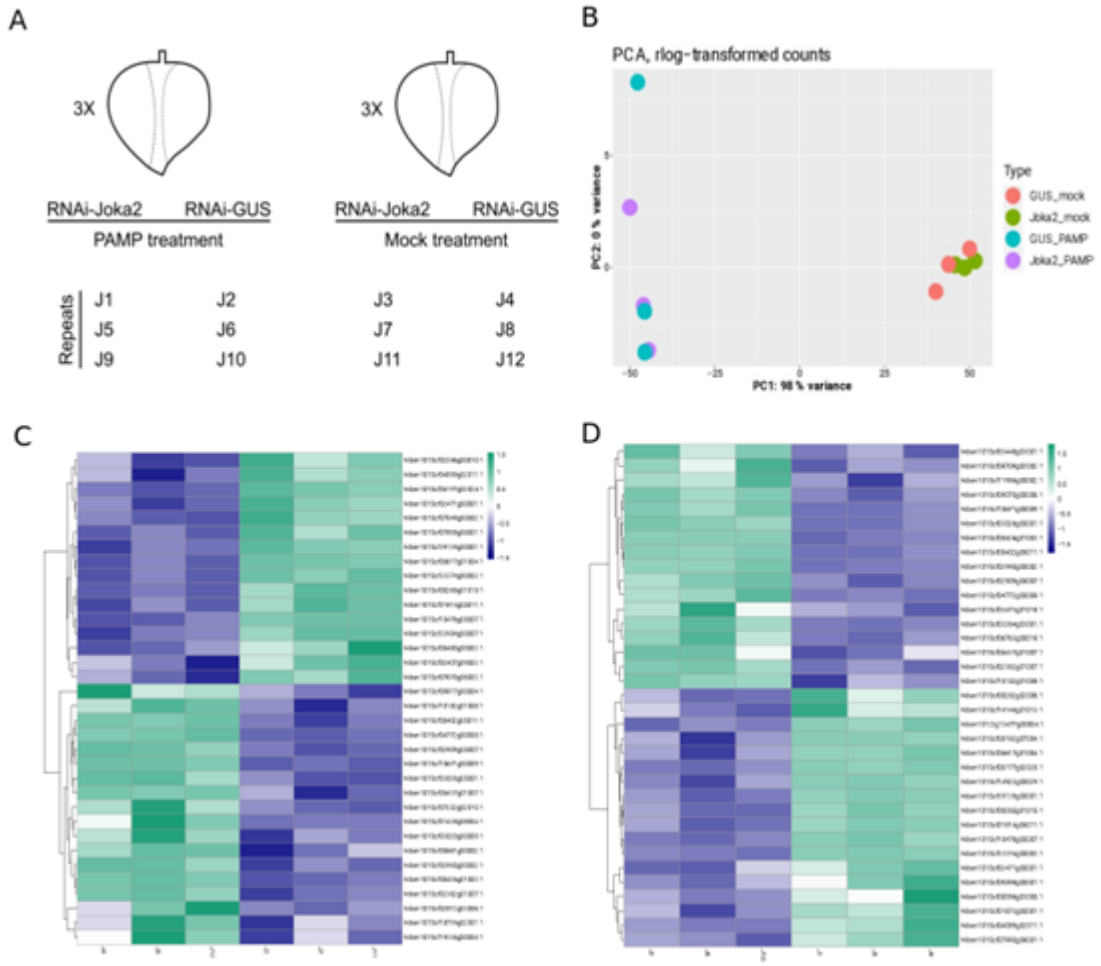

Figure 5.1: Joka2 alters gene expression when *N. benthamiana* is exposed to PAMP treatment. (A) Schematic representation of the experimental design. (B) Principal component analysis (PCA) plot for the twelve tested samples. (C-D) Heatmaps representing changes in gene expression organised through hiererchical clustering by euclidean distances. Results obtained with the help of Yasin Tumtas and Alan Wanke.

	DEGs Mock [RNAi-GUSi vs RNAi-Joka2]			DEGs PAMP [RNAi-GUS RNAi-Joka2]			
Gene name	baseMean	Log2FC	Padj value	baseMean	Log2FC	Padj value	Solgenomics ID
Outer arm dynein light chain 1	153.45	-0.34	1.00	38.62	1.55	0.05	Ctg13477g00004.1
Plastid lipid-associated protein	22.58	0.13	1.00	22.52	2.53	0.05	Scf00096g03005.1
Ethylene-responsive transcriptior factor 10	72.42	0.55	1.00	184.96	1.54	0.00	Scf00282g02006.1
GRAS family transcriptior factor	1.67	0.84	NA	201.22	1.35	0.00	Scf03473g01018.1
Actin-related protein 5	249.01	-0.45	1.00	143.76	1.00	0.03	Scf08709g02002.1
Conserved hypothetica protein (unknown function)	27.99	0.85	1.00	113.09	1.58	0.00	Scf14144g01013.1

Table 5.1: Selected genes that are significantly upregulated by Joka2 during PAMP treatment. Genes were chosen based on two criteria. During mock treatment changes in the following crieria between GUS and Joka2 silenecing: Log2 fold change in gene expression (Log2FC) < 1.00 and the p-adjacent value > 0.05. During PAMP treatment changes in the following crieria between GUS and Joka2 silenecing: Log2FC > 1.00 and the p-adjacent value < 0.05.

5.3.2 Joka2 regulates several genes during the exposure of *N. benthamiana* to PAMP treatment.

To validate the results obtained from the RNA-seq analysis, I performed quantitative real-time PCR (qPCR). Plants under the same conditions were collected, and RNA was extracted from them. The extracted RNA was then reverse-transcribed into cDNA, and after verification using NanoDrop spectrophotometry, I conducted qPCR

on the samples. As shown in Figure 5.2, a significant difference could be observed between Joka2-silenced and GUS-silenced PAMP-treated samples for two of the genes tested: Outer arm dynein light chain 1 ($p<0.0001$) and Ethylene responsive transcription factor 10 ($p=0.0113$) , while no difference was detected between the water-treated samples.

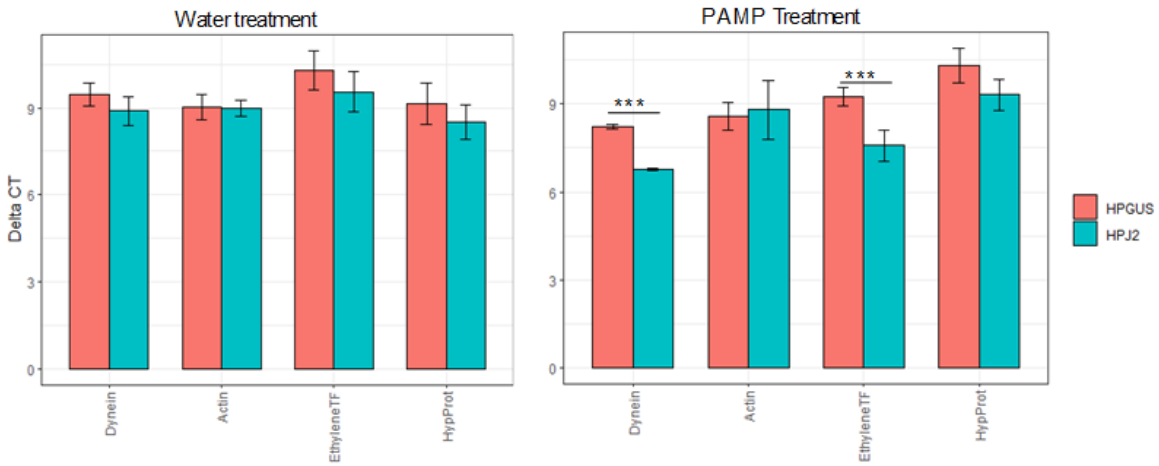

Figure 5.2: Silencing of Joka2 causes differences in gene expression levels during PAMP treatment. Bar graphs representing gene expression levels normalised to the housekeeping gene GAPDH (Dynein: Outer arm dynein light chain 1, Actin: Actin related protein 5, EthyleneTF: Ethylene responsive transcription factor 10, HypProt: Conserved hypothetical protein). Under PAMP treatment two of the four tested genes showed significantly different expression levels when normalised to GAPDH, dependent on the gene that was silenced, with Joka2 exhibiting lower gene expression levels. Stars indicate significance ($p < 0.05$) student's T-test

5.3.3 ΔNBR1 is not able to rescue gene levels after being infiltrated into Joka2 silence plants

I then decided that as an extra validation I was going to see if I could "rescue" the gene levels by supplying the Joka2 silenced plants with Joka2 proteins. I

hypothesised that by doing this I could restore the levels of the genes back to their unsilenced counterparts. As a control, these plants would also be “rescued” with ΔNBR1 to see if there was any difference, since it has been shown that The NBR1 domain is the key part between Joka2 and MAK6 and MAK3. (Figures 5.3 and 5.4)

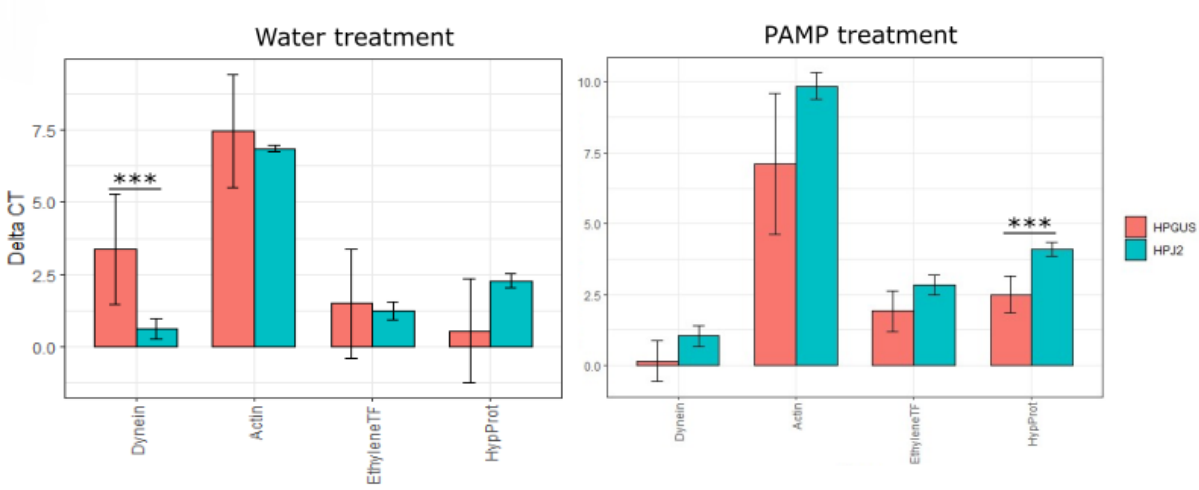

Figure 5.3: Agroinfiltration of Joka2 is able to restore gene expression levels so there is no significant difference between GUS and Joka2 silenced plants during PAMP treatment except for the protein of unknown function. Bar graphs representing gene expression levels normalised to the housekeeping gene GAPDH (Dynein: Outer arm dynein light chain 1, Actin: Actin related protein 5, EthyleneTF: Ethylene responsive transcription factor 10, HypProt: Conserved hypothetical protein). Stars indicate significance ($p < 0.05$) student’s T-test.

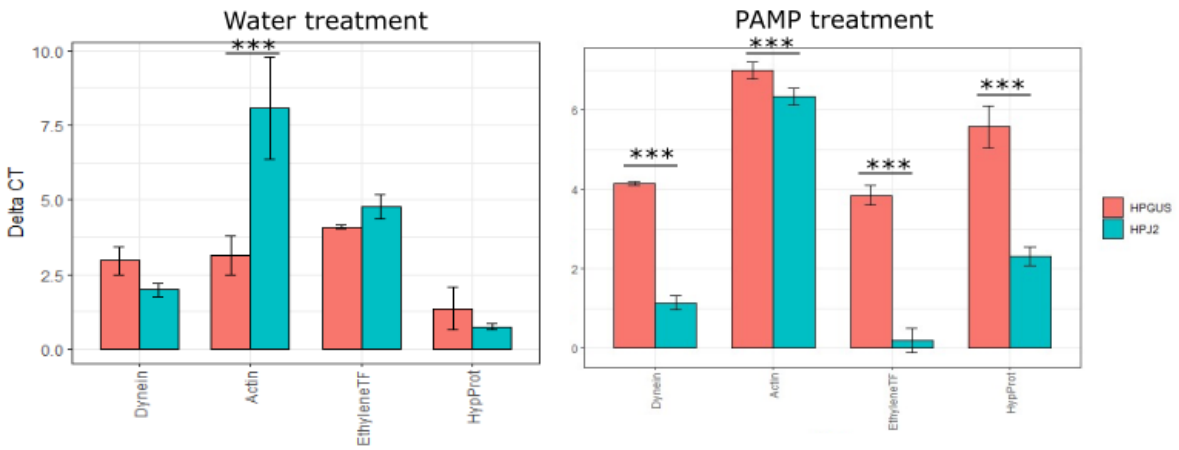

Figure 5.4: Agroinfiltration of ΔNBR1 is not able to restore gene expression levels so there is a significant difference between GUS and Joka2 silenced plants during PAMP treatment. Bar graphs representing delta CT normalised to the housekeeping gene GAPDH (Dynein: Outer arm dynein light chain 1, Actin: Actin related protein 5, EthyleneTF: Ethylene responsive transcription factor 10, HypProt: Conserved hypothetical protein). Stars indicate significance ($p < 0.05$) student's T-test.

Results from figures 5.3 and 5.4 show that whilst Joka2 was able to rescue the levels from silenced plants back to those of unsilenced plants, ΔNBR1 was not able to except for the hypothetical protein of unknown function . This can be seen in the significant difference between gene expression levels in plants that underwent PAMP treatment and were agroinfiltrated with NBR1, all of the tested genes showed significantly smaller expression levels when Joka2 was silenced. These results point us in the direction that the NBR1 domain is essential for the gene regulation activity of Joka2.

5.3.4 Removal of the HB domain does not decrease resistance towards *P. infestans*

After the discovery that the HB domain was instrumental in the redox capabilities of Joka2, I decided to investigate if this resulted in increased resistance to *P. infestans* infection. To test this, several *N. benthamiana* plants with several truncates of Joka2, including ΔHB and ΔNBR1 as a negative control, as well as full length Joka2 as a positive control were infected with *P. infestans* and the areas the necrotic lesions were measured (Figure 5.5).

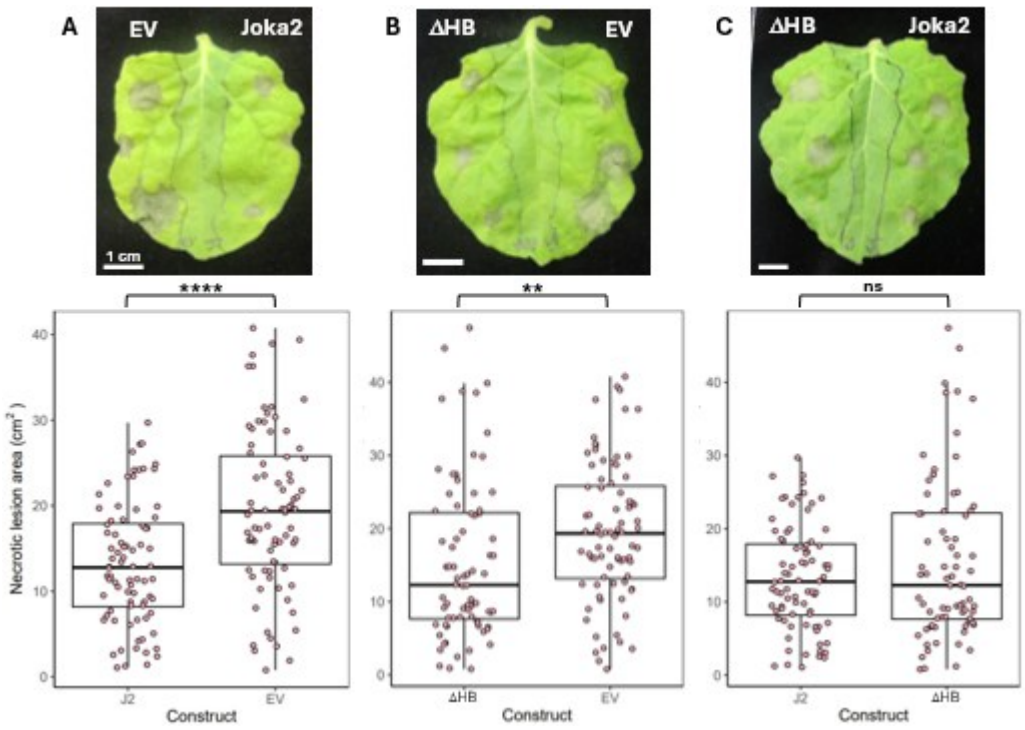

Figure 5.5: Removal of the HB domain does not reduce resistance to *P. infestans*. (A-C) Representative images and boxplot of *P. infestans* infection assay comparing necrotic lesion size at 2dpi when overexpressing Joka2, ΔHB-Joka2 or EV tagged with GFP. Results obtained with the help of Cecilia Longoni

Here we can see that there is no significant difference between either the EV control or the ΔNBR1 truncate, but both the ΔHB truncate and the full length Joka2 show a significant increase in resistance.

5.3.5 None of the conserved phosphorilated residues in Joka2 have an effect on resistance.

Preliminary data from our collaborators in the Üstun lab had uncovered that during *Xanthomonas campestris*, the homolog of Joka2 in tomato (NBR1), was phosphorylated at several key sites. Joka2's association with the MAP kinases, lead me to hypothesise that Joka2 could also be phosphorylated, as such I performed phylogenetic analysis and sequence alignment to determine which of these residues are conserved within the Solanaceae family (Figure 5.6). Results indicated that 5 residues were conserved: 4 serineresidues located at positions 106, 123, 732 and 734 as well as a tyrosine residue located at position 107.

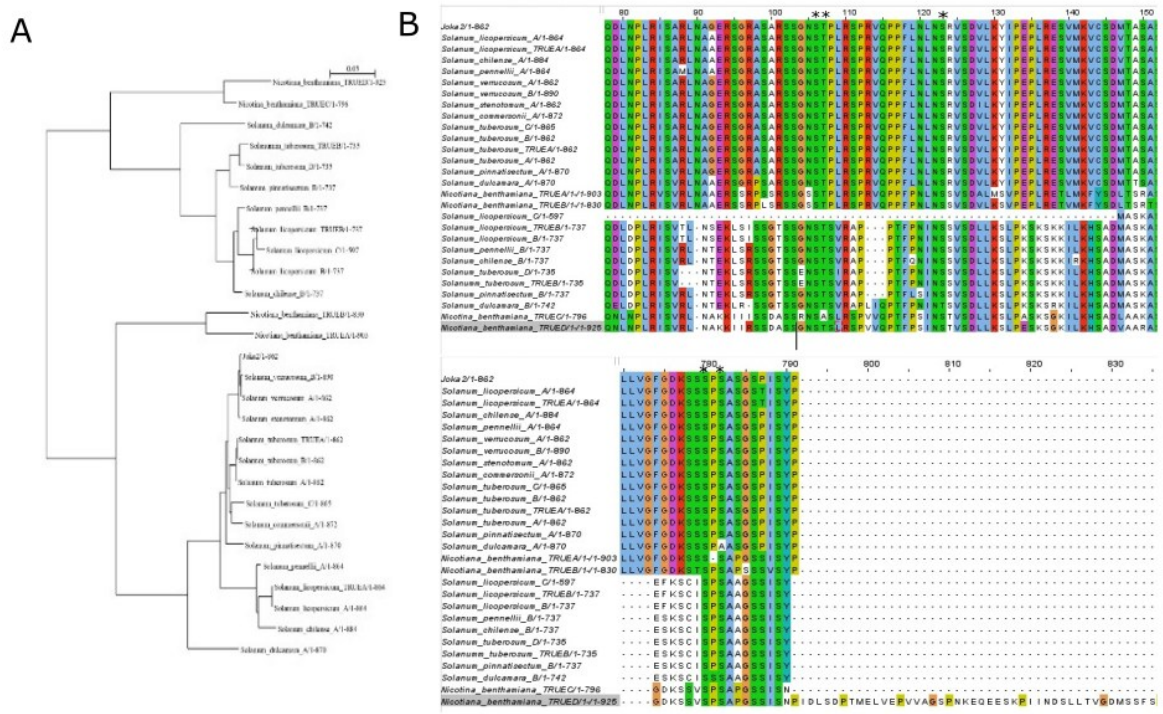

Figure 5.6: Joka2 and its homologs share 5 phosphorylation residues. (A) Phylogenetic tree of Joka2 orthologs from the Solanaceae family. (B) Aminoacid sequence of the Joka2 orthologs, asterisks indicate the 5 conserved residues that are phosphorylated during *Xanthomonas campestris* infection in tomato (S 106, T 107, S 123, S 732 and S 734)

After identification of the conserved residues, I then proceeded to mutate all of those conserved residues into alanine, in order to eliminate any function that they still had. The resulting Joka2 construct (5xA) was then agroinfiltrated into *N. benthamiana* plants that were then infected with *P. infestans* zoospores and the resulting necrosis was measured. (Figure 5.7)

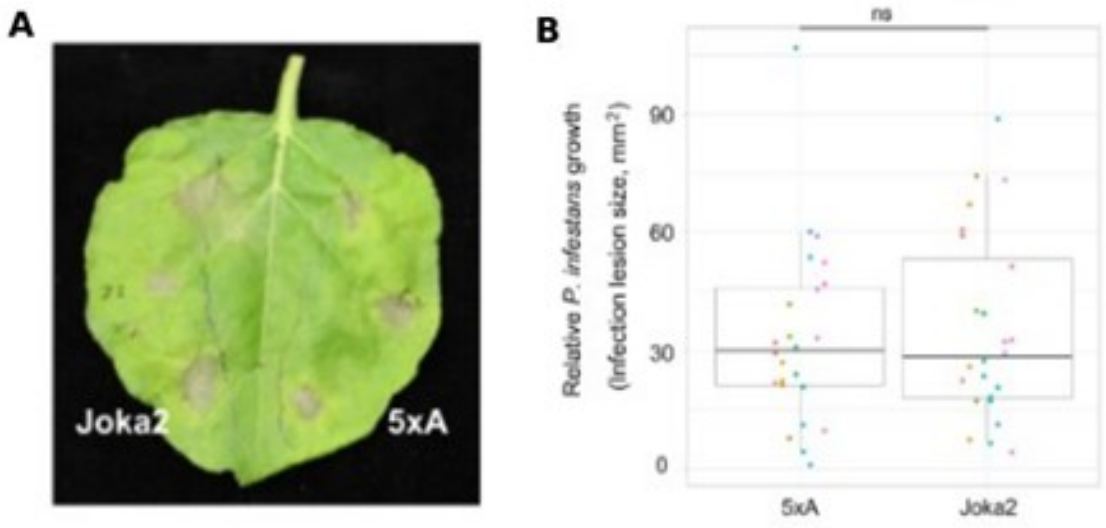

Figure 5.7: Mutation of conserved phosphorylated residues did not result in lower necrosis levels upon P. infestans infection. (A) N. benthamiana leaves were agroinfiltrated with either Joka2 or the 5xA construct and subsequently infected with P. infestans and pathogen growth was determined by measuring infection lesion size eight days post-inoculation. (B) Boxplot illustrating the extent of lesion size after 8 days of growth.

Results show no significant difference between Joka2 and 5xA. Results obtained with the help of XinYi Yang

As we can see, there is no significant difference between the 5xA construct or the full length Joka2, whilst both of them show an increased resistance when compared to the EV control, meaning that the five conserved residues are not necessary for the defence of Joka2 against *P. infestans*

5.3.6 PAMP treatment does not cause a shift in the colocalization of Joka2 between MAPK6 and ATG8

Since the reason for the shift in solubility of Joka2 was still unclear I hypothesised it could be a way of using Joka2 to go from its role in autophagy bound to ATG8 to its role in signalling when it associates with the MAPK6. To test this, confocal microscopy was performed on *N. benthamiana* leaves that had been infiltrated with fluorescently tagged Joka2, ATG8 and MAPK6. Half of the leaf had been infiltrated with PAMP treatment and the other half with a water control. Puncta numbers and percentage puncta colocalization were then obtained to determine if there was a shift in the behaviour of Joka2. (Figure 5.8)

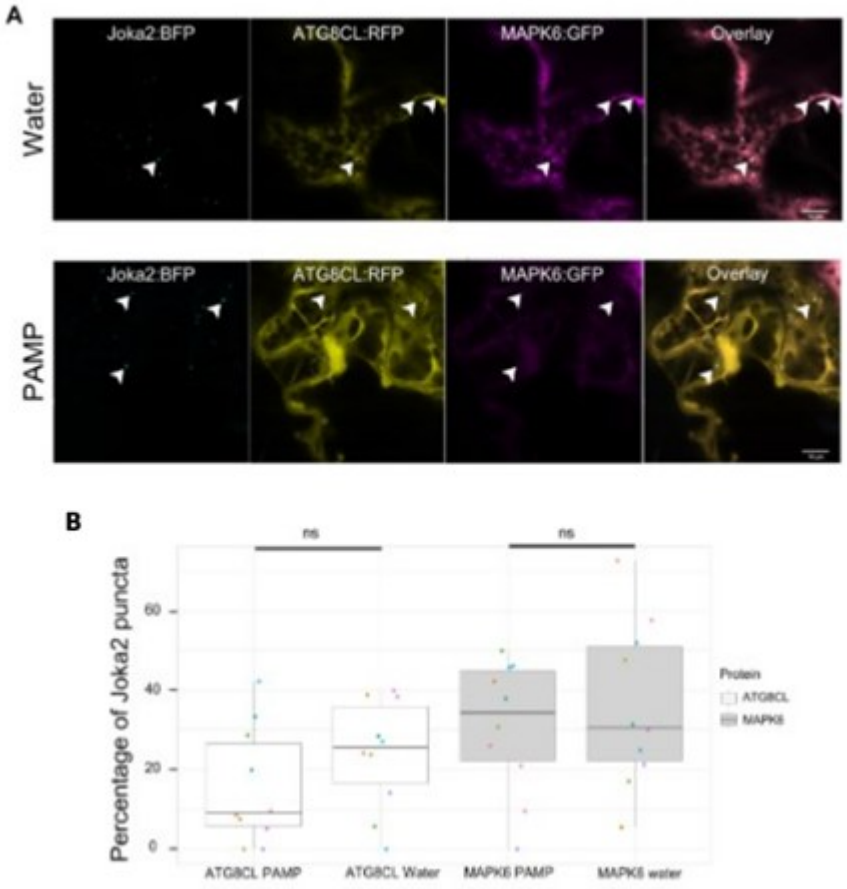

Figure 5.8: Joka2 does not associate differently between ATG8 and MAPK6 when exposed to PAMP treatment. (A) Representative images of Joka2:BFP, ATG8CL:RFP and MAPK6:GFP under both PAMP and water treatments. (B) Boxplots representing overall association of Joka2 puncta with either ATG8CL and MAPK6 under both water and PAMP treatments. Joka2 does not differentially associate with either ATG8CL or MAPK6 irrespectively of the presence of PAMPs Results obtained with the help of XinYi Yang

Results show, there is no significant change between the percentage colocalization of Joka2 puncta and either of ATG8 or MAPK6 irrespective of the presence of PAMP treatment, this suggests that both the autophagic and the signalling functions of Joka2 work during normal and defence conditions.

5.3 Discussion

In this chapter, I have investigated whether Joka2 plays a role in the upregulation of defence genes during immunity. I also tried to establish a link between Joka2's role in immunity and its interaction with the MAP kinases, as well as its ability to change solubility depending on the redox status of the cell.

As a first step, RNA-seq was performed on both PAMP and water treated plants that had either Joka2 or a control gene silenced (Figure 5.1). from this I obtained a list of candidate genes that Joka2 could be modulating (Table 5.1). Of the identified genes, it is worth highlighting the presence of two important defence related transcription factors, an ethylene induced transcription factor and a GRAS type transcription factor that forms part of the scarecrow subfamily. Both of these have been shown to be upregulated in the context of defence and are responsible for the upregulation of defence related genes (Yang, J. et al., 2010)

qPCR primers were then designed for the candidate genes of which I was able to perform qPCR onr four of those genes and two of them were validated to be upregulated in the presence of Joka2. (Figure 5.2). As a further validation step, I then tried to rescue the phenotype by agroinfiltrating either full-length Joka2 or ΔNBR1 into the silenced plants to see if I could eliminate the difference in gene expression between the different treatments (Figs 5.3 and 5.4). Infiltration of the full-length Joka2 did remove the difference in gene expression between silencing

treatments, but infiltration of the ΔNBR1 construct did not recover the difference. The inability of the ΔNBR1 mutant to rescue defense gene expression suggests that Joka2 likely functions as a molecular scaffold, physically facilitating the phosphorylation of the necessary MAP kinases to activate these transcription factors. This mirrors the scaffolding role of mammalian p62, which organizes MEKK3 and ERK signaling complexes to drive transcription (Moscat, Diaz-Meco & Wooten, 2007), and implies that Joka2 is a direct participant in the signal transduction chain upstream of these transcription factors.

Phosphorylation is known to stabilize transcription factors, such as the ethylene transcription factor that we found Joka2 upregulates, preventing their turnover and allowing them to drive defense gene expression (Wang et al., 2022). My data suggests that Joka2 may be the missing link in this process potentially recruiting the MAPK to the vicinity of the TF or facilitating its nuclear entry thereby ensuring the robust activation of downstream defense genes. This mechanic, would mimic other plant proteins such as GBPL3 have also been shown to regulate defence gene expression after pathogen invasion through liquid-liquid phase separation (Huang et al., 2021)

As a next step, I decided to see if the presence of the HB domain affected the resistance that Joka2 conferred to *N. benthamiana* plants by measuring how the infected area size compared between full-length and ΔHB (Figure 5.5). Both full length Joka2 and ΔHB showed no significant difference in the size of the infected area. This means that whilst the HB domain is essential for the solubilization of Joka2, it is not important for the immunity Joka2 confers against *P. infestans*. This was somewhat unexpected since the change in solubility is important for the signalling role p62 plays in humans (Yang, J. et al., 2010).

One other important factor was whether or not Joka2's phosphorylation plays a role in defence. As a way to verify this, I did some phylogenetic analysis on the Solanaceae family to look for conserved phosphorylated residues and I then mutated them into alanines in order to verify that the change was not affecting the resistance towards *P. infestans* (Fig. 5.7). The resulting mutant (5xA) did not show any significant difference compared to the full length Joka2, indicating that phosphorylated residues do not play a role in immunity.

Finally, I wanted to investigate whether or not the shift in Joka2 solubility led to a stronger association with the MAP kinases, since I hypothesised that the solubility shift was necessary for the association between Joka2 and the kinases. I also hypothesised that the shift in association with the kinases would result in a lower association with ATG8, since Joka2 would not be performing its autophagic role when associated with members of the MAPK family. Confocal microscopy was performed between Joka2, MAPK6 and ATG8 to understand if their colocalization patterns changed in response to PAMP treatment (Fig. 5.8). Results show that there is no significant difference in the number of Joka2-ATG8 puncta between water and PAMP treatments, there is also no difference between the number of Joka puncta associating with ATG8 and MAPK6 during either of water or PAMP treatments. This was rather surprising since I was hypothesising a possible shift in Joka2 function from its defence autophagy role into a more signalling heavy role, although the results rather show Joka2 acting simultaneously on both autophagy and signalling.

In this chapter, I have demonstrated that Joka2 plays a role in the upregulation of defence-related genes during immunity and investigated its relationship with cellular redox status, phosphorylation, and MAP kinase signaling. Through RNA-seq analysis, I identified several defence-related genes that are modulated by Joka2, including two important transcription factors involved in defence responses: an ethylene-induced transcription factor and a grass-type transcription factor from the scarecrow subfamily. I validated these findings through qPCR and showed that the NBR1 domain is essential for this gene regulation, as demonstrated by the rescue experiments where only full-length Joka2, but not ΔNBR1, could restore normal gene expression patterns in silenced plants.

I have also shown that while the HB domain is important for Joka2's solubility changes, it is not essential for its role in immunity against P. infestans. This was demonstrated through infection assays with the ΔHB construct, which showed no significant difference in resistance compared to full-length Joka2. Similarly, mutation of conserved phosphorylation sites (Figure 5.7) did not affect Joka2's role in immunity, suggesting that neither solubility changes nor phosphorylation are critical for its defence function.

Finally, I investigated the relationship between Joka2's roles in autophagy and MAP kinase signaling through colocalization studies. Contrary to our initial hypothesis, I found that Joka2 maintains consistent associations with both ATG8 and MAPK6 regardless of PAMP treatment, suggesting it can simultaneously perform both its autophagy and signaling functions rather than switching between them.

Further research is needed to fully understand the mechanisms by which Joka2 regulates defence gene expression and how this relates to its dual role in autophagy

and MAP kinase signaling. Additionally, investigation into other potential post-translational modifications of Joka2 could reveal new aspects of its regulation in immunity. Finally, it would be valuable to examine how Joka2 coordinates its simultaneous roles in autophagy and signaling, and whether there are additional factors that influence this balance.

Chapter 6 – General Discussion and future perspectives

Autophagy is a conserved eukaryotic mechanism that not only plays a role in the maintenance of cell homeostasis, but also is important towards immunity (Sertsuvalkul, DeMell & Dinesh-Kumar, 2022). Reduction or lack of autophagy in eukaryotic organisms can lead to severe illness. In plants, due to their lack of an adaptive immune system, autophagy serves as one of the main layers of defence against pathogens and as a result could prove useful as a new method of biocontrol for plant pathogens. As the autophagic process became more studied, it was uncovered that it was not a bulk degradation process, but rather a highly specialised system dependent on the use of autophagy cargo receptors, which line the inside of the autophagosome conferring specificity (Gatica, Lahiri & Klionsky, 2018).

Joka2 is one such cargo receptor, although its cargo is unknown, it has been shown to confer resistance to *N. benthamiana* against the pathogen *P. infestans* (Dagdas et al., 2018). Its mammalian ortholog, NBR1, has also been shown to help against neurodegenerative diseases (Odagiri et al., 2012). In plants *P. infestans* counteracts the immunity of Joka2 through the production of the effector protein PexRD54, through direct competition for the binding of the AIM motif (Dagdas et al., 2016).

Throughout this study I have focused on the role Joka2 plays in immunity, with a specific focus on its binding to the MAP kinases. I have also studied how changes in redox affect its solubility and finally I have tried to see if either of these are related to each other. A summary of the main findings of this study can be found in figure 6.1.

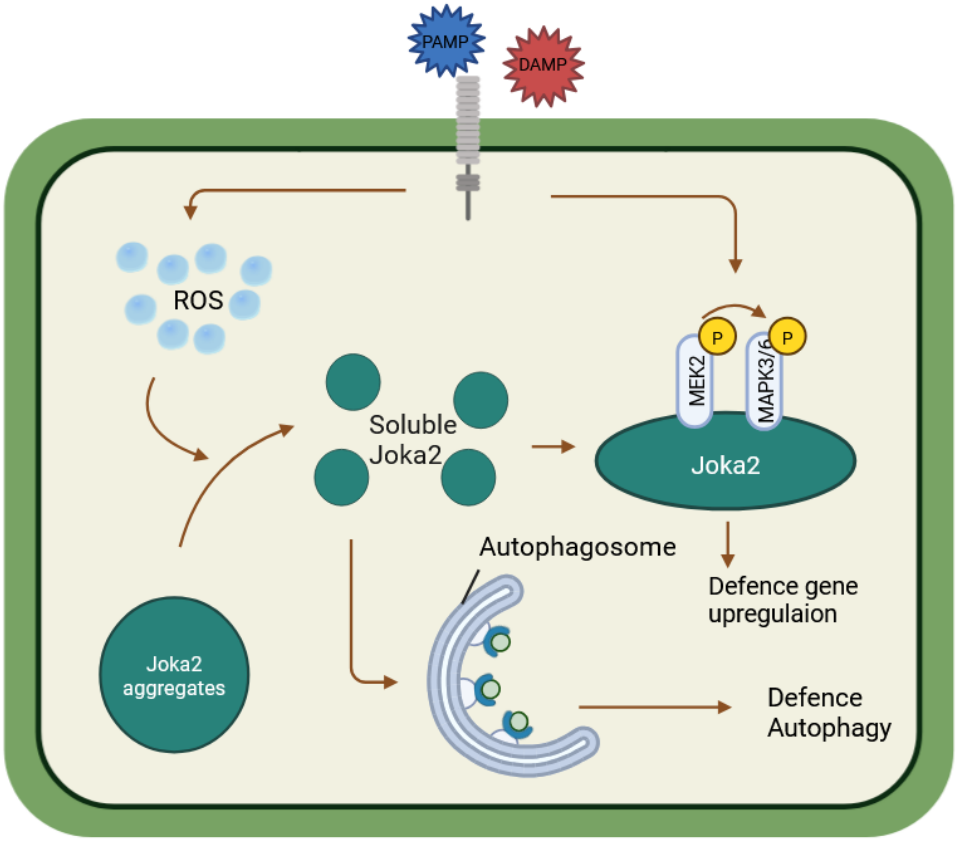

Figure 6.1: Summary figure of the role of Joka2 during immunity. Recognition of PAMPs or DAMPs through PRR receptors, causes several molecular signals to be emitted. Some of these result in the association of Joka2 with members of the MAP kinase family, this interaction is mediated through the NBR1/bZN/ZZ area. Simultaneously, plant cells produce reactive oxygen species (ROS) that cause a change in the redox potential of the cell, causing Joka2 aggregates to solubilize, resulting in more readily available Joka2 for both MAPK signalling and defence autophagy.

As a first step, I decided to further investigate the binding of Joka2 to MAP kinase 6 and the upstream component of both MAPK6 and MAPK3, MEK2 (Chapter3). I first started validating the claim that the NBR1 domain was necessary for the binding of Joka2 to MAPK3 through confocal microscopy, although the results I obtained pointed towards more than one domain being responsible for the binding, since

removal of the individual domains lead to no significant decrease in binding. Results obtained from co-immunoprecipitation of MAPK6 and Joka2 truncates, also pointed towards Joka2 using multiple domains for binding, more specifically the NBR1 and ZZ domains as well as the region that interconnects them (bZN). I also investigated the role of the NBR1 domain in the phosphorylation of MAPK6, co-immunoprecipitation assays revealed that the NBR1 domain was at least partially necessary for the phosphorylation of MAPK6 with its removal causing a decrease in phosphorylation levels. This then prompted me to investigate the upstream component, MEK2, which after checking that its function does not affect binding to Joka2, It was uncovered that it binds to the ZZ,bZN and NBR1 areas similarly to MAPK6. This mimics how other MAPK scaffolds work, such as kinase suppressor of Ras1 (KSR1), who utilizes its CA5 and C1 domains to bind RAF, MEK and ERK (Paniagua et al., 2022) Finally, I also investigated how PAL binds Joka2. I discovered that it does so through the UBA domains, It is capable of binding both UBA domains irrespectively of their ubiquitin binding abilities although further testing revealed that the UBA domains whilst sufficient are not necessary for binding and PAL binds to another domain of Joka2, however the details of this binding are unclear.

As the next step in my investigation I decided to investigate how redox affects Joka2's solubility, since the function of the human ortholog of Joka2 seems to be affected by its ability to change solubility (Carroll et al., 2018) (Chapter 4). Firstly, I determined that Joka2 was affected by changes in solubility, by exposing it to reducing agents, and after verifying this process was independent of the tag used, I started exposing different truncates to the changed redox conditions leading to the discovery that the HB domain is responsible for the changes in solubility. This

process was later also repeated with an oxidizing agent rather than a reducing agent and the same result of an increased oxidizing environment leading to an increase in solubility was achieved. Finally, I was able to successfully rescue some of the insoluble Joka2 found at the pellet obtained during extraction. Next, I wanted to see if I could also see the solubility shift using confocal microscopy. An increase in puncta number and a decrease in puncta size of Joka2 was observed, whilst those changes were not seen with truncates lacking the HB domain. This switch in solubility is consistent with other autophagy proteins that can undergo liquid-liquid phase separation which allows them to start the autophagosome formation process (Noda, Wang & Zhang, 2020) yet in Joka2's case I hypothesized that this solubility change was responsible for its interactions with the MAP kinases.

As a next step, I wanted to see if I could trigger the solubility changes seen in Joka2 in other ways, since the production of ROS species is part of the immune response, I hypothesised that Salicylic acid (SA) could also induce the solubility change of Joka2, I compared it to NPR1, a protein already known to solubilize in the presence of salicylic acid, however Joka2 did not exhibit any changes in solubility. This was stricking since SA, is linked to redox signalling through the glutathione pool (Liu, Liu & Mou, 2024), yet it was ultimately independent firm Joka2 solubilization possibly since the levels of ROS produced by SA are significantly smaller than those produced by direct PAMP injections. The other hypothesis I had was that by triggering an immune response through the use of PAMP extract ROS production could also be triggered within the plant and as a result we could also trigger the change in solubility of Joka2. In order to accomplish this, I performed co-immunoprecipitations, which demonstrated the change in solubility but once again ni change without the HB domain, I then proceeded to perform confocal microscopy and fluorescence recovery

after photobleaching which also demonstrated that PAMP extract indices a change in Joka2 solubility but ΔHB is not affected by the change in redox conditions.

In the final chapter, I sought to uncover the nature of Joka2's contributions to immunity, through the use of RNA-seq and subsequent validation through qPCR (Chapter 5). I uncovered that Joka2 does in fact cause the upregulation of several defence associated genes after beeing exposed to PAMP treatment. The upregulation of these genes is dependent however, on the presence of the NBR1 domain, as experiments where I tried to rescue the gene levels after silencing Joka2 did not result in the reestablishing of the gene expression levels when the ΔNBR1 construct was utilized. This gene modulation is similar to what has been reported in p62, who after binding MAPK members, is able to induce expression of certain antioxidant genes such as *Gstm5*, and *Gpx2* (Li, Jiang & Wu, 2020)

Then I investigated whether other causes besides the NBR1 domain were essential for Joka2 dependent immunity. I first removed the HB domain thinking that the solubilization of Joka2 might play a role in defence, but it resulted in no significant difference. I then shifted focus onto the possible phosphorylation of Joka2, with the help of preliminary data from our collaborators, I performed some phylogenetic analysis on Joka2 and identified 5 conserved residues that are phosphorylated during *X. campestris* invasion in tomato and mutated those residues into alanines to eliminate their function. However, results showed that the new alanine mutant did not have decreased resistance when compared to full length Joka2.

Finally I decided to investigate if this change in solubility leads to a change in the localization of Joka2 between its two known roles as an autophagy cargo receptor and as a scaffold for the MAP kinases. However I was unable to prove that PAMP

treatment causes a change in the localization of Joka2 within the cell, so that it associates more favourably with ATG8 or MAPK6.

In conclusion, this project has revealed multiple facets of Joka2's role in plant immunity. Firstly, I demonstrated that Joka2 functions as a scaffolding protein for the MAP kinase signaling cascade, with MAPK3, MAPK6, and MEK2 all binding to a specific region encompassing the NBR1, bZN, and ZZ domains. This scaffolding function appears to be critical for defence gene activation during pathogen attack, as demonstrated by the requirement of a functional NBR1 domain for proper defence gene expression. Second, I uncovered a novel redox-dependent property of Joka2 mediated by its HB domain, whereby oxidative conditions increase its solubility. This behavior differs markedly from its mammalian ortholog p62, likely due to different mechanisms of cysteine oxidation. While this redox sensitivity suggests a potential regulatory mechanism, the removal of the HB domain did not affect Joka2's immune functions. Furthermore, contrary to our initial hypothesis, PAMP treatment did not alter Joka2's relative association with ATG8 or MAP kinases, suggesting it maintains both autophagy and signaling functions simultaneously rather than switching between them.

Future investigations should focus on several key areas to better understand Joka2's complex role in plant immunity. First, a comprehensive analysis of Joka2's interactions with the complete MAPK cascade, including MAPKKKs, would reveal whether it serves as a universal scaffold for MAPK signaling. Future investigations should utilize yeast two-hybrid (Y2H) screens or bimolecular fluorescence complementation (BiFC), as other forms of validation, besides western blots. Second, examining whether ΔHB mutants retain the ability to upregulate PAMP-

responsive genes would help clarify the relationship between Joka2's redox sensitivity and its defence functions. Additionally, structural studies of the HB domain and its cysteine residues would provide insight into the molecular mechanism of Joka2's redox-dependent solubility changes. Finally, investigation of the temporal dynamics of Joka2's interactions with both autophagy and MAPK pathway components during immune responses could reveal subtle regulatory mechanisms that coordinate these dual functions. Together, these studies would provide a more complete understanding of how Joka2 integrates multiple cellular responses during plant immunity.

A promising direction for further research would be to also investigate whether Joka2 also interacts with any members of the thioredoxin (TRX) family of proteins, who are responsible for the reduction of oxidized proteins and have been known to act after the initial ROS burst present after infection (Sevilla et al., 2023) Besided this, we should probe whether these mechanisms are part of the PTI or the ETI response using purified *P. infestans* PAMPs, such as arachidonic acid and effectors such as PexRD54.

Appendix

R code

qPCR Analysis:

```
# ----------------------------------------------------
# 1) Load libraries
# ----------------------------------------------------
library("dplyr")
library("ggplot2")
library("readxl")
# ----------------------------------------------------
# 2) Import the data
# ----------------------------------------------------
Data <- read_excel(file.choose())
data2 <- subset(Data, Sample.Name == "HPGUS" | Sample.Name == "HPJ2")
# ----------------------------------------------------
# 3) Organize factor levels
# ----------------------------------------------------
data2$Rep <- as.factor(data2$Rep)
data2$Sample.Name <- factor(data2$Sample.Name, levels = c("HPGUS","HPJ2"))
data2$Target.Name <- factor(data2$Target.Name, levels = c("GAPDH", "Dynein", "Actin",
"EthyleneTF", "HypProt"))
# ----------------------------------------------------
# 4) Plot CT values (violin + jitter)
# ----------------------------------------------------
pCT <- ggplot(data2, aes(x = Target.Name, y = CT, color = Rep)) +
  geom_violin(position = position_dodge(width = 0.75),
              size = 1, width = 1,
              fill = "grey80", color = NA) +
  geom_jitter()
pCT +
  facet_wrap(vars(Sample.Name)) +
  theme_bw() +
  theme(axis.text.x = element_text(angle = 90, vjust = 0.5, hjust = 1))
# ----------------------------------------------------
# 5) Calculate delta CT
# ----------------------------------------------------
Avr_data <- data2 %>%
  group_by(Sample.Name, Target.Name, Rep) %>%
  summarize(mean_CT = CT)
```

```
DeltaCT <- Avr_data %>%
  group_by(Sample.Name, Rep) %>%
  mutate(delta_CT = mean_CT - mean_CT[which(Target.Name=="GAPDH")])
# ---------------------------------------------------------
# 6) Summarize mean deltaCT (+ SD and SE) for error bars
# ---------------------------------------------------------
stats_deltaCT <- DeltaCT %>%
  group_by(Sample.Name, Target.Name) %>%
  summarize(
          avr_DeltaCT = mean(delta_CT),
          sd_DeltaCT  = sd(delta_CT),
          se_DeltaCT  = sd(delta_CT) / sqrt(n())
  )

# Remove GAPDH from the final bar plot dataset
stats_deltaCT <- subset(stats_deltaCT, Target.Name != "GAPDH")

# (Optional) If you really want absolute-value deltaCT:
stats_deltaCT$avr_DeltaCT <- abs(stats_deltaCT$avr_DeltaCT)
# Note: keep in mind how you want to treat the error bars if forcing abs().
# ---------------------------------------------------------
# 7) Plot with bars and error bars
# ---------------------------------------------------------
p2 <- ggplot(stats_deltaCT,
          aes(x = Target.Name,
                    fill = Sample.Name,
                    y = avr_DeltaCT,
                    width = 0.7)) +
  geom_bar(stat = "identity",
          color = "black",
          position = position_dodge()) +
  # Add error bars:
  geom_errorbar(aes(
          ymin = avr_DeltaCT - se_DeltaCT,
          ymax = avr_DeltaCT + se_DeltaCT),
          width = 0.2,
          position = position_dodge(width = 0.7)) +
  labs(x = "Gene",
          y = "Delta CT",
          fill = "") +
  theme_bw() +
  theme(axis.text.x = element_text(angle = 90,
                                   vjust = 0.5,
                                   hjust = 1))

p2
```

Fiji Macros

Puncta count and colocalization:

```
macro "Background subtraction [F5]" {
wait(100);
open();
run("Subtract Background...", "rolling=6");
run("Despeckle");
run("Split Channels");
//run("Threshold...");
waitForUser("");
run("Convert to Mask");
saveAs("Tiff", "Green.tif");
close();
setAutoThreshold("RenyiEntropy dark");
//run("Threshold...");
waitForUser("");
run("Convert to Mask");
saveAs("Tiff", "Red.tif");
close();
  open();
open();
run("Merge Channels...", "red=Red.tif green=Green.tif blue=*None* gray=*None* create");
run("Stack to RGB");
run("Split Channels");
run("Colocalization ", "channel_1=[Composite (RGB) (red)] channel_2=[Composite (RGB)
(green)] ratio=30 threshold_channel_1=15 threshold_channel_2=15 display=255
colocalizated");
selectWindow("Colocalizated points (8-bit) ");
run("Make Binary");
run("Analyze Particles...", "size=3-1000 circularity=0.00-1.00 show=Outlines display
summarize");
selectWindow("Composite (RGB) (green)");
run("Make Binary");
run("Analyze Particles...", "size=3-1000 pixel circularity=0.00-1.00  show=Outlines display
summarize");
selectWindow("Composite (RGB) (red)");
run("Make Binary");
run("Analyze Particles...", "size=3-1000 pixel circularity=0.00-1.00  show=Outlines
        display summarize")
```

References

Adriaenssens, E., Ferrari, L. & Martens, S. (2022) Orchestration of selective autophagy by cargo receptors. *Current Biology.* 32 (24), R1357–R1371.

Aerts, N., Chhillar, H., Ding, P. & Van Wees, S. C. (2022) Transcriptional regulation of plant innate immunity. *Essays in Biochemistry.* 66 (5), 607–620.

Agas, D., Gabai, V., Sufianov, A. A., Shneider, A. & Sabbieti, M. G. (2022) P62/SQSTM1 enhances osteogenesis and attenuates inflammatory signals in bone marrow microenvironment. *General and Comparative Endocrinology.* 320 114009.

Anand, G. & Rajeshkumar, K. C. (2022) Challenges and threats posed by plant pathogenic fungi on agricultural productivity and economy. In: Anonymous *Fungal diversity, ecology and control management.* , Springer. pp. 483–493.

Baldrich, P., Rutter, B. D., Karimi, H. Z., Podicheti, R., Meyers, B. C. & Innes, R. W. (2019) Plant extracellular vesicles contain diverse small RNA species and are enriched in 10-to 17-nucleotide “tiny” RNAs. *The Plant Cell.* 31 (2), 315–324.

Bleau, J. R. & Spoel, S. H. (2021) Selective redox signaling shapes plant–pathogen interactions. *Plant Physiology.* 186 (1), 53–65.

Block, A. & Alfano, J. R. (2011) Plant targets for Pseudomonas syringae type III effectors: virulence targets or guarded decoys? *Current Opinion in Microbiology.* 14 (1), 39–46.

Boddey, J. A., O’Neill, M. T., Lopaticki, S., Carvalho, T. G., Hodder, A. N., Nebl, T., Wawra, S., Van West, P., Ebrahimzadeh, Z. & Richard, D. (2016) Export of malaria proteins requires co-translational processing of the PEXEL motif independent of phosphatidylinositol-3-phosphate binding. *Nature Communications.* 7 (1), 10470.

Bozkurt, T. O., Richardson, A., Dagdas, Y. F., Mongrand, S., Kamoun, S. & Raffaele, S. (2014) The plant membrane-associated REMORIN1. 3 accumulates in discrete perihaustorial domains and enhances susceptibility to Phytophthora infestans. *Plant Physiology.* 165 (3), 1005–1018.

Bozkurt, T. O., Schornack, S., Banfield, M. J. & Kamoun, S. (2012) Oomycetes, effectors, and all that jazz. *Current Opinion in Plant Biology.* 15 (4), 483–492.

Bronkhorst, J., Kots, K., de Jong, D., Kasteel, M., van Boxmeer, T., Joemmanbaks, T., Govers, F., van der Gucht, J., Ketelaar, T. & Sprakel, J. (2022) An actin mechanostat ensures hyphal tip sharpness in Phytophthora infestans to achieve host penetration. *Science Advances.* 8 (23), eabo0875.

Cai, Q., He, B., Wang, S., Fletcher, S., Niu, D., Mitter, N., Birch, P. R. & Jin, H. (2021) Message in a bubble: shuttling small RNAs and proteins between cells and

interacting organisms using extracellular vesicles. *Annual Review of Plant Biology.* 72 (1), 497–524.

Cai, Q., Qiao, L., Wang, M., He, B., Lin, F., Palmquist, J., Huang, S. & Jin, H. (2018) Plants send small RNAs in extracellular vesicles to fungal pathogen to silence virulence genes. *Science.* 360 (6393), 1126–1129.

Cai, Y., Zhu, Y., Zheng, J., Zhang, Y. & Chen, W. (2022) NBR1 mediates autophagic degradation of IRF3 to negatively regulate type I interferon production. *Biochemical and Biophysical Research Communications.* 623 140–147.

Caillaud, M., Wirthmueller, L., Sklenar, J., Findlay, K., Piquerez, S. J., Jones, A. M., Robatzek, S., Jones, J. D. & Faulkner, C. (2014) The plasmodesmal protein PDLP1 localises to haustoria-associated membranes during downy mildew infection and regulates callose deposition. *PLoS Pathogens.* 10 (11), e1004496.

Carroll, B., Otten, E. G., Manni, D., Stefanatos, R., Menzies, F. M., Smith, G. R., Jurk, D., Kenneth, N., Wilkinson, S. & Passos, J. F. (2018) Oxidation of SQSTM1/p62 mediates the link between redox state and protein homeostasis. *Nature Communications.* 9 (1), 256.

Chen, K., Zeng, J., Xiao, H., Huang, C., Hu, J., Yao, W., Yu, G., Xiao, W., Xu, H. & Ye, Z. (2016) Regulation of glucose metabolism by p62/SQSTM1 through HIF1α. *Journal of Cell Science.* 129 (4), 817–830.

Chen, X., Raghunathan, K., Bao, B., Ngwa, E., Kwong, A., Wu, Z., Babcock, S., Baek, C., Ye, G. & Muppirala, A. (2025) A niche-dependent redox rheostat regulates epithelial stem cell fate. *Nature Communications.*

Colcombet, J. & Hirt, H. (2008) Arabidopsis MAPKs: a complex signalling network involved in multiple biological processes. *Biochemical Journal.* 413 (2), 217–226.

Contreras, M. P., Lüdke, D., Pai, H., Toghani, A. & Kamoun, S. (2023) NLR receptors in plant immunity: making sense of the alphabet soup. *EMBO Reports.* 24 (10), e57495.

Coomber, A., Saville, A. & Ristaino, J. B. (2024) Evolution of Phytophthora infestans on its potato host since the Irish potato famine. *Nature Communications.* 15 (1), 6488.

Cortese, M. S., Uversky, V. N. & Dunker, A. K. (2008) Intrinsic disorder in scaffold proteins: getting more from less. *Progress in Biophysics and Molecular Biology.* 98 (1), 85–106.

Cristina, M. S., Petersen, M. & Mundy, J. (2010) Mitogen-activated protein kinase signaling in plants. *Annual Review of Plant Biology.* 61 (1), 621–649.

Csorba, T., Lózsa, R., Hutvágner, G. & Burgyán, J. (2010) Polerovirus protein P0 prevents the assembly of small RNA-containing RISC complexes and leads to degradation of ARGONAUTE1. *The Plant Journal.* 62 (3), 463–472.

Cui, H., Tsuda, K. & Parker, J. E. (2015) Effector-triggered immunity: from pathogen perception to robust defense. *Annual Review of Plant Biology.* 66 (1), 487–511.
D'Agostino, C., Nogalska, A., Cacciottolo, M., King Engel, W. & Askanas, V. (2011) Abnormalities of NBR1, a novel autophagy-associated protein, in muscle fibers of sporadic inclusion-body myositis. *Acta Neuropathologica.* 122 627–636.

Dagdas, Y. F., Belhaj, K., Maqbool, A., Chaparro-Garcia, A., Pandey, P., Petre, B., Tabassum, N., Cruz-Mireles, N., Hughes, R. K. & Sklenar, J. (2016) An effector of the Irish potato famine pathogen antagonizes a host autophagy cargo receptor. *Elife.* 5 e10856.

Dagdas, Y. F., Pandey, P., Tumtas, Y., Sanguankiattichai, N., Belhaj, K., Duggan, C., Leary, A. Y., Segretin, M. E., Contreras, M. P. & Savage, Z. (2018) Host autophagy machinery is diverted to the pathogen interface to mediate focal defense responses against the Irish potato famine pathogen. *Elife.* 7 e37476.

Dahale, S. K., Ghosh, D., Ingole, K. D., Chugani, A., Kim, S. H. & Bhattacharjee, S. (2021) HopA1 effector from pseudomonas syringae pv syringae strain 61 affects NMD processes and elicits effector-triggered immunity. *International Journal of Molecular Sciences.* 22 (14), 7440.

Djamei, A., Pitzschke, A., Nakagami, H., Rajh, I. & Hirt, H. (2007) Trojan horse strategy in Agrobacterium transformation: abusing MAPK defense signaling. *Science.* 318 (5849), 453–456.

Dodds, P. N. & Rathjen, J. P. (2010) Plant immunity: towards an integrated view of plant–pathogen interactions. *Nature Reviews Genetics.* 11 (8), 539–548.

Donohue, E., Balgi, A. D., Komatsu, M. & Roberge, M. (2014) Induction of covalently crosslinked p62 oligomers with reduced binding to polyubiquitinated proteins by the autophagy inhibitor verteporfin. *PloS One.* 9 (12), e114964.

Felix, G., Duran, J. D., Volko, S. & Boller, T. (1999) Plants have a sensitive perception system for the most conserved domain of bacterial flagellin. *The Plant Journal.* 18 (3), 265–276.

Feng, X., Sun, D., Li, Y., Zhang, J., Liu, S., Zhang, D., Zheng, J., Xi, Q., Liang, H. & Zhao, W. (2023) Local membrane source gathering by p62 body drives autophagosome formation. *Nature Communications.* 14 (1), 7338.

Fischer, B. B., Hideg, É & Krieger-Liszkay, A. (2013) Production, detection, and signaling of singlet oxygen in photosynthetic organisms. *Antioxidants & Redox Signaling.* 18 (16), 2145–2162.

Foyer, C. H. & Noctor, G. (2016) Stress-triggered redox signalling: what's in pROSpect? *Plant, Cell & Environment.* 39 (5), 951–964.

Gatica, D., Lahiri, V. & Klionsky, D. J. (2018) Cargo recognition and degradation by selective autophagy. *Nature Cell Biology.* 20 (3), 233–242.

Giraldo, M. C., Dagdas, Y. F., Gupta, Y. K., Mentlak, T. A., Yi, M., Martinez-Rocha, A. L., Saitoh, H., Terauchi, R., Talbot, N. J. & Valent, B. (2013) Two distinct secretion systems facilitate tissue invasion by the rice blast fungus Magnaporthe oryzae. *Nature Communications.* 4 (1), 1–12.

Giraldo, M. C. & Valent, B. (2013) Filamentous plant pathogen effectors in action. *Nature Reviews Microbiology.* 11 (11), 800–814.

Golovkine, G. R., Roberts, A. W., Morrison, H. M., Rivera-Lugo, R., McCall, R. M., Nilsson, H., Garelis, N. E., Repasy, T., Cronce, M. & Budzik, J. (2023) Autophagy restricts Mycobacterium tuberculosis during acute infection in mice. *Nature Microbiology.* 8 (5), 819–832.

Gómez-Gómez, L. & Boller, T. (2000) FLS2: an LRR receptor–like kinase involved in the perception of the bacterial elicitor flagellin in Arabidopsis. *Molecular Cell.* 5 (6), 1003–1011.

Gondor, O. K., Janda, T., Soós, V., Pál, M., Majláth, I., Adak, M. K., Balázs, E. & Szalai, G. (2016) Salicylic acid induction of flavonoid biosynthesis pathways in wheat varies by treatment. *Frontiers in Plant Science.* 7 1447.

Guo, C., Zhang, Y., Nie, Q., Cao, D., Wang, X., Wan, X., Liu, M., Cui, J., Sun, J. & Bai, Y. (2021) SQSTM1/p62 oligomerization contributes to Aβ-induced inhibition of Nrf2 signaling. *Neurobiology of Aging.* 98 10–20.

Hafrén, A., Macia, J., Love, A. J., Milner, J. J., Drucker, M. & Hofius, D. (2017) Selective autophagy limits cauliflower mosaic virus infection by NBR1-mediated targeting of viral capsid protein and particles. *Proceedings of the National Academy of Sciences.* 114 (10), E2026–E2035.

Hafrén, A., Üstün, S., Hochmuth, A., Svenning, S., Johansen, T. & Hofius, D. (2018) Turnip mosaic virus counteracts selective autophagy of the viral silencing suppressor HCpro. *Plant Physiology.* 176 (1), 649–662.

Hagai, T. & Levy, Y. (2010) Ubiquitin not only serves as a tag but also assists degradation by inducing protein unfolding. *Proceedings of the National Academy of Sciences.* 107 (5), 2001–2006.

Hamel, L., Nicole, M., Sritubtim, S., Morency, M., Ellis, M., Ehlting, J., Beaudoin, N., Barbazuk, B., Klessig, D. & Lee, J. (2006) Ancient signals: comparative genomics of plant MAPK and MAPKK gene families. *Trends in Plant Science.* 11 (4), 192–198.

Herrera-Vásquez, A., Fonseca, A., Ugalde, J. M., Lamig, L., Seguel, A., Moyano, T. C., Gutiérrez, R. A., Salinas, P., Vidal, E. A. & Holuigue, L. (2020) Transcription factor TGA2 is essential for UV-B stress tolerance controlling oxidative stress in Arabidopsis. *Biorxiv.* 2020.05. 24.113589.

Hofius, D., Munch, D., Bressendorff, S., Mundy, J. & Petersen, M. (2011) Role of autophagy in disease resistance and hypersensitive response-associated cell death.

Cell Death & Differentiation. 18 (8), 1257–1262.

Huang, J., Gu, M., Lai, Z., Fan, B., Shi, K., Zhou, Y., Yu, J. & Chen, Z. (2010) Functional analysis of the Arabidopsis PAL gene family in plant growth, development, and response to environmental stress. *Plant Physiology.* 153 (4), 1526–1538.

Huang, S., Zhu, S., Kumar, P. & MacMicking, J. D. (2021) A phase-separated nuclear GBPL circuit controls immunity in plants. *Nature.* 594 (7863), 424–429.

Huang, X., Chen, S., Yang, X., Yang, X., Zhang, T. & Zhou, G. (2020) Friend or enemy: a dual role of autophagy in plant virus infection. *Frontiers in Microbiology.* 11 736.

Itakura, E. & Mizushima, N. (2011) p62 Targeting to the autophagosome formation site requires self-oligomerization but not LC3 binding. *Journal of Cell Biology.* 192 (1), 17–27.

Ivanov, A. A., Ukladov, E. O. & Golubeva, T. S. (2021) Phytophthora infestans: an overview of methods and attempts to combat late blight. *Journal of Fungi.* 7 (12), 1071.

Jonak, C., Ökrész, L., Bögre, L. & Hirt, H. (2002) Complexity, cross talk and integration of plant MAP kinase signalling. *Current Opinion in Plant Biology.* 5 (5), 415–424.

Kim, D. S. & Hwang, B. K. (2014) An important role of the pepper phenylalanine ammonia-lyase gene (PAL1) in salicylic acid-dependent signalling of the defence response to microbial pathogens. *Journal of Experimental Botany.* 65 (9), 2295–2306.

Kirkin, V., Lamark, T., Sou, Y., Bjørkøy, G., Nunn, J. L., Bruun, J., Shvets, E., McEwan, D. G., Clausen, T. H. & Wild, P. (2009) A role for NBR1 in autophagosomal degradation of ubiquitinated substrates. *Molecular Cell.* 33 (4), 505–516.

Kobayashi, M., Seo, S., Hirai, K., Yamamoto-Katou, A., Katou, S., Seto, H., Meshi, T., Mitsuhara, I. & Ohashi, Y. (2010) Silencing of WIPK and SIPK mitogen-activated protein kinases reduces tobacco mosaic virus accumulation but permits systemic viral movement in tobacco possessing the N resistance gene. *Molecular Plant-Microbe Interactions.* 23 (8), 1032–1041.

Kraft, C., Peter, M. & Hofmann, K. (2010) Selective autophagy: ubiquitin-mediated recognition and beyond. *Nature Cell Biology.* 12 (9), 836–841.

Krysan, P. J. & Colcombet, J. (2018) Cellular complexity in MAPK signaling in plants: Questions and emerging tools to answer them. *Frontiers in Plant Science.* 9 1674.

Kuźniak, E., Kaźmierczak, A., Wielanek, M., Głowacki, R. & Kornas, A. (2013) Involvement of salicylic acid, glutathione and protein S-thiolation in plant cell death-mediated defence response of Mesembryanthemum crystallinum against Botrytis

cinerea. *Plant Physiology and Biochemistry.* 63 30–38.

Lange, S., Xiang, F., Yakovenko, A., Vihola, A., Hackman, P., Rostkova, E., Kristensen, J., Brandmeier, B., Franzen, G. & Hedberg, B. (2005) The kinase domain of titin controls muscle gene expression and protein turnover. *Science.* 308 (5728), 1599–1603.

Li, P., Lu, Y., Chen, H. & Day, B. (2020) The lifecycle of the plant immune system. *Critical Reviews in Plant Sciences.* 39 (1), 72–100.

Li, S., Xu, B., Niu, X., Lu, X., Cheng, J., Zhou, M. & Hooykaas, P. J. (2021) JAZ8 interacts with VirE3 attenuating Agrobacterium mediated root tumorigenesis. *Frontiers in Plant Science.* 12 685533.

Li, T., Jiang, D. & Wu, K. (2020) p62 promotes bladder cancer cell growth by activating KEAP1/NRF2-dependent antioxidative response. *Cancer Science.* 111 (4), 1156–1164.

Liu, C., Liu, Q. & Mou, Z. (2024) Redox signaling and oxidative stress in systemic acquired resistance. *Journal of Experimental Botany.* erae193.

Liu, G., Kang, G., Wang, S., Huang, Y. & Cai, Q. (2021) Extracellular vesicles: emerging players in plant defense against pathogens. *Frontiers in Plant Science.* 12 757925.

Liu, X., Lin, Y., Liu, D., Wang, C., Zhao, Z., Cui, X., Liu, Y. & Yang, Y. (2017) MAPK-mediated auxin signal transduction pathways regulate the malic acid secretion under aluminum stress in wheat (Triticum aestivum L.). *Scientific Reports.* 7 (1), 1620.

Liu, Y., Schiff, M., Czymmek, K., Tallóczy, Z., Levine, B. & Dinesh-Kumar, S. P. (2005) Autophagy regulates programmed cell death during the plant innate immune response. *Cell.* 121 (4), 567–577.

Lu, Y., Schornack, S., Spallek, T., Geldner, N., Chory, J., Schellmann, S., Schumacher, K., Kamoun, S. & Robatzek, S. (2012) Patterns of plant subcellular responses to successful oomycete infections reveal differences in host cell reprogramming and endocytic trafficking. *Cellular Microbiology.* 14 (5), 682–697.

Lukan, T. & Coll, A. (2022) Intertwined roles of reactive oxygen species and salicylic acid signaling are crucial for the plant response to biotic stress. *International Journal of Molecular Sciences.* 23 (10), 5568.

Mao, G., Meng, X., Liu, Y., Zheng, Z., Chen, Z. & Zhang, S. (2011) Phosphorylation of a WRKY transcription factor by two pathogen-responsive MAPKs drives phytoalexin biosynthesis in Arabidopsis. *The Plant Cell.* 23 (4), 1639–1653.

Mauch-Mani, B. & Slusarenko, A. J. (1996) Production of salicylic acid precursors is a major function of phenylalanine ammonia-lyase in the resistance of Arabidopsis to Peronospora parasitica. *The Plant Cell.* 8 (2), 203–212.

Mendgen, K. & Nass, P. (1988) The activity of powdery-mildew haustoria after feeding the host cells with different sugars, as measured with a potentiometric cyanine dye. *Planta.* 174 283–288.

Meng, X. & Zhang, S. (2013) MAPK cascades in plant disease resistance signaling. *Annual Review of Phytopathology.* 51 (1), 245–266.

Micali, C. O., Neumann, U., Grunewald, D., Panstruga, R. & O'Connell, R. (2011) Biogenesis of a specialized plant–fungal interface during host cell internalization of Golovinomyces orontii haustoria. *Cellular Microbiology.* 13 (2), 210–226.

Miya, A., Albert, P., Shinya, T., Desaki, Y., Ichimura, K., Shirasu, K., Narusaka, Y., Kawakami, N., Kaku, H. & Shibuya, N. (2007) CERK1, a LysM receptor kinase, is essential for chitin elicitor signaling in Arabidopsis. *Proceedings of the National Academy of Sciences.* 104 (49), 19613–19618.

Mohanta, T. K., Arora, P. K., Mohanta, N., Parida, P. & Bae, H. (2015) Identification of new members of the MAPK gene family in plants shows diverse conserved domains and novel activation loop variants. *BMC Genomics.* 16 1–20.

Moscat, J., Diaz-Meco, M. T. & Wooten, M. W. (2007) Signal integration and diversification through the p62 scaffold protein. *Trends in Biochemical Sciences.* 32 (2), 95–100.

Mou, Z., Fan, W. & Dong, X. (2003) Inducers of plant systemic acquired resistance regulate NPR1 function through redox changes. *Cell.* 113 (7), 935–944.

Mukherjee, R., Bhattacharya, A., Mello-Vieira, J., Kuncha, S. K., Hoffmann, M., Gonzalez, A., Rathore, R., Chadha, A., Shin, D. & Colby, T. (2024) Serine ubiquitination of SQSTM1 regulates NFE2L2-dependent redox homeostasis. *Autophagy.* 1–17.

Murmu, J., Bush, M. J., DeLong, C., Li, S., Xu, M., Khan, M., Malcolmson, C., Fobert, P. R., Zachgo, S. & Hepworth, S. R. (2010) Arabidopsis basic leucine-zipper transcription factors TGA9 and TGA10 interact with floral glutaredoxins ROXY1 and ROXY2 and are redundantly required for anther development. *Plant Physiology.* 154 (3), 1492–1504.

Ndamukong, I., Abdallat, A. A., Thurow, C., Fode, B., Zander, M., Weigel, R. & Gatz, C. (2007) SA-inducible Arabidopsis glutaredoxin interacts with TGA factors and suppresses JA-responsive PDF1. 2 transcription. *The Plant Journal.* 50 (1), 128–139.

Nicot, A., Lo Verso, F., Ratti, F., Pilot-Storck, F., Streichenberger, N., Sandri, M., Schaeffer, L. & Goillot, E. (2014) Phosphorylation of NBR1 by GSK3 modulates protein aggregation. *Autophagy.* 10 (6), 1036–1053.

Nishimura, T. & Tooze, S. A. (2020) Emerging roles of ATG proteins and membrane lipids in autophagosome formation. *Cell Discovery.* 6 (1), 32.

Noctor, G., Reichheld, J. & Foyer, C. H. (2018) ROS-related redox regulation and signaling in plants. *Seminars in cell & developmental biology.* , Elsevier. pp.3–12.

Noda, N. N., Wang, Z. & Zhang, H. (2020) Liquid–liquid phase separation in autophagy. *Journal of Cell Biology.* 219 (8), e202004062.

Odagiri, S., Tanji, K., Mori, F., Kakita, A., Takahashi, H. & Wakabayashi, K. (2012) Autophagic adapter protein NBR1 is localized in Lewy bodies and glial cytoplasmic inclusions and is involved in aggregate formation in α-synucleinopathy. *Acta Neuropathologica.* 124 173–186.

Otten, E. G., Stefanatos, R., Carroll, B. & Korolchuk, V. I. (2018) Oxidation of p62 as an evolutionary adaptation to promote autophagy in stress conditions. *Cell Stress.* 2 (4), 91.

Paniagua, G., Jacob, H. K., Brehey, O., García-Alonso, S., Lechuga, C. G., Pons, T., Musteanu, M., Guerra, C., Drosten, M. & Barbacid, M. (2022) KSR induces RAS-independent MAPK pathway activation and modulates the efficacy of KRAS inhibitors. *Molecular Oncology.* 16 (17), 3066–3081.

Poole, L. B. & Nelson, K. J. (2008) Discovering mechanisms of signaling-mediated cysteine oxidation. *Current Opinion in Chemical Biology.* 12 (1), 18–24.

Popa, C., Li, L., Gil, S., Tatjer, L., Hashii, K., Tabuchi, M., Coll, N. S., Ariño, J. & Valls, M. (2016) The effector AWR5 from the plant pathogen Ralstonia solanacearum is an inhibitor of the TOR signalling pathway. *Scientific Reports.* 6 (1), 27058.

Qin, L., Zhou, Z., Li, Q., Zhai, C., Liu, L., Quilichini, T. D., Gao, P., Kessler, S. A., Jaillais, Y. & Datla, R. (2020) Specific recruitment of phosphoinositide species to the plant-pathogen interfacial membrane underlies Arabidopsis susceptibility to fungal infection. *The Plant Cell.* 32 (5), 1665–1688.

Queval, G., Jaillard, D., Zechmann, B. & Noctor, G. (2011) Increased intracellular H2O2 availability preferentially drives glutathione accumulation in vacuoles and chloroplasts. *Plant, Cell & Environment.* 34 (1), 21–32.

Rakosy-Tican, E., Thieme, R., König, J., Nachtigall, M., Hammann, T., Denes, T., Kruppa, K. & Molnár-Láng, M. (2020) Introgression of two broad-spectrum late blight resistance genes, Rpi-Blb1 and Rpi-Blb3, from Solanum bulbocastanum Dun plus race-specific R genes into potato pre-breeding lines. *Frontiers in Plant Science.* 11 699.

Reichheld, J., Khafif, M., Riondet, C., Droux, M., Bonnard, G. & Meyer, Y. (2007) Inactivation of thioredoxin reductases reveals a complex interplay between thioredoxin and glutathione pathways in Arabidopsis development. *The Plant Cell.* 19 (6), 1851–1865.

Rogov, V. V., Nezis, I. P., Tsapras, P., Zhang, H., Dagdas, Y., Noda, N. N., Nakatogawa, H., Wirth, M., Mouilleron, S. & McEwan, D. G. (2023) Atg8 family

proteins, LIR/AIM motifs and other interaction modes. *Autophagy Reports.* 2 (1), 2188523.

Romeis, T., Tang, S., Hammond-Kosack, K., Piedras, P., Blatt, M. & Jones, J. D. (2000) Early signalling events in the Avr9/Cf-9-dependent plant defence response. *Molecular Plant Pathology: Original Articles.* 1 (1), 3–8.

Rutter, B. D. & Innes, R. W. (2017) Extracellular vesicles isolated from the leaf apoplast carry stress-response proteins. *Plant Physiology.* 173 (1), 728–741.

Savary, S., Ficke, A., Aubertot, J. & Hollier, C. (2012) Crop losses due to diseases and their implications for global food production losses and food security. *Food Security.* 4 (4), 519–537.

Sertsuvalkul, N., DeMell, A. & Dinesh-Kumar, S. P. (2022) The complex roles of autophagy in plant immunity. *FEBS Letters.* 596 (17), 2163–2171.

Sevilla, F., Martí, M. C., De Brasi-Velasco, S. & Jiménez, A. (2023) Redox regulation, thioredoxins, and glutaredoxins in retrograde signalling and gene transcription. *Journal of Experimental Botany.* 74 (19), 5955–5969.

Shahid, S., Kim, G., Johnson, N. R., Wafula, E., Wang, F., Coruh, C., Bernal-Galeano, V., Phifer, T., Depamphilis, C. W. & Westwood, J. H. (2018) MicroRNAs from the parasitic plant Cuscuta campestris target host messenger RNAs. *Nature.* 553 (7686), 82–85.

Shi, Y., Lu, S., Noda, T., Chiu, C. & Chiang-Ni, C. (2024) Capsule-deficient group A Streptococcus evades autophagy-mediated killing in macrophages. *Mbio.* 771.

Taj, G., Agarwal, P., Grant, M. & Kumar, A. (2010) MAPK machinery in plants: recognition and response to different stresses through multiple signal transduction pathways. *Plant Signaling & Behavior.* 5 (11), 1370–1378.

Tang, J., Li, Y., Xia, S., Li, J., Yang, Q., Ding, K. & Zhang, H. (2021) Sequestosome 1/p62: A multitasker in the regulation of malignant tumor aggression. *International Journal of Oncology.* 59 (4), 1–20.

Tonnessen, B. W., Manosalva, P., Lang, J. M., Baraoidan, M., Bordeos, A., Mauleon, R., Oard, J., Hulbert, S., Leung, H. & Leach, J. E. (2015) Rice phenylalanine ammonia-lyase gene OsPAL4 is associated with broad spectrum disease resistance. *Plant Molecular Biology.* 87 273–286.

Torrens-Spence, M. P., Matos, J. O., Li, T., Kastner, D. W., Kim, C. Y., Wang, Z., Glinkerman, C. M., Sherk, J., Kulik, H. J. & Wang, Y. (2024) Mechanistic basis for the emergence of EPS1 as a catalyst in salicylic acid biosynthesis of Brassicaceae. *Nature Communications.* 15 (1), 10356.

Üstün, S., Hafrén, A., Liu, Q., Marshall, R. S., Minina, E. A., Bozhkov, P. V., Vierstra, R. D. & Hofius, D. (2018) Bacteria exploit autophagy for proteasome degradation and enhanced virulence in plants. *The Plant Cell.* 30 (3), 668–685.

Van der Does, D., Leon-Reyes, A., Koornneef, A., Van Verk, M. C., Rodenburg, N., Pauwels, L., Goossens, A., Körbes, A. P., Memelink, J. & Ritsema, T. (2013) Salicylic acid suppresses jasmonic acid signaling downstream of SCFCOI1-JAZ by targeting GCC promoter motifs via transcription factor ORA59. *The Plant Cell.* 25 (2), 744–761.

Van Der Reest, J., Lilla, S., Zheng, L., Zanivan, S. & Gottlieb, E. (2018) Proteome-wide analysis of cysteine oxidation reveals metabolic sensitivity to redox stress. *Nature Communications.* 9 (1), 1581.

Wang, C., El-Shetehy, M., Shine, M. B., Yu, K., Navarre, D., Wendehenne, D., Kachroo, A. & Kachroo, P. (2014) Free radicals mediate systemic acquired resistance. *Cell Reports.* 7 (2), 348–355.

Wang, C., Liu, R., Lim, G., de Lorenzo, L., Yu, K., Zhang, K., Hunt, A. G., Kachroo, A. & Kachroo, P. (2018) Pipecolic acid confers systemic immunity by regulating free radicals. *Science Advances.* 4 (5), eaar4509.

Wang, R., Wang, G. & Ning, Y. (2019) PALs: emerging key players in broad-spectrum disease resistance. *Trends in Plant Science.* 24 (9), 785–787.

Wang, S., Boevink, P. C., Welsh, L., Zhang, R., Whisson, S. C. & Birch, P. R. (2017) Delivery of cytoplasmic and apoplastic effectors from Phytophthora infestans haustoria by distinct secretion pathways. *New Phytologist.* 216 (1), 205–215.

Wang, S., Welsh, L., Thorpe, P., Whisson, S. C., Boevink, P. C. & Birch, P. R. (2018) The Phytophthora infestans haustorium is a site for secretion of diverse classes of infection-associated proteins. *MBio.* 9 (4), 10.1128/mbio. 01216–18.

Wang, X., Meng, H., Tang, Y., Zhang, Y., He, Y., Zhou, J. & Meng, X. (2022) Phosphorylation of an ethylene response factor by MPK3/MPK6 mediates negative feedback regulation of pathogen-induced ethylene biosynthesis in Arabidopsis. *Journal of Genetics and Genomics.* 49 (8), 810–822.

Wawra, S., Trusch, F., Matena, A., Apostolakis, K., Linne, U., Zhukov, I., Stanek, J., Koźmiński, W., Davidson, I. & Secombes, C. J. (2017) The RxLR motif of the host targeting effector AVR3a of Phytophthora infestans is cleaved before secretion. *The Plant Cell.* 29 (6), 1184–1195.

Whisson, S. C., Boevink, P. C., Wang, S. & Birch, P. R. (2016) The cell biology of late blight disease. *Current Opinion in Microbiology.* 34 127–135.

Wurzer, B., Zaffagnini, G., Fracchiolla, D., Turco, E., Abert, C., Romanov, J. & Martens, S. (2015) Oligomerization of p62 allows for selection of ubiquitinated cargo and isolation membrane during selective autophagy. *Elife.* 4 e08941.

Yamamoto, H. & Matsui, T. (2024) Molecular mechanisms of macroautophagy, microautophagy, and chaperone-mediated autophagy. *Journal of Nippon Medical*

School. 91 (1), 2–9.

Yan, Y., Wang, P., He, C. & Shi, H. (2017) MeWRKY20 and its interacting and activating autophagy-related protein 8 (MeATG8) regulate plant disease resistance in cassava. *Biochemical and Biophysical Research Communications.* 494 (1-2), 20–26.

Yang, F., Kimberlin, A. N., Elowsky, C. G., Liu, Y., Gonzalez-Solis, A., Cahoon, E. B. & Alfano, J. R. (2019) A plant immune receptor degraded by selective autophagy. *Molecular Plant.* 12 (1), 113–123.

Yang, J., Liu, H., Diaz-Meco, M. T. & Moscat, J. (2010) NBR1 is a new PB1 signalling adapter in Th2 differentiation and allergic airway inflammation in vivo. *The EMBO Journal.* 29 (19), 3421–3433.

Yang, Z. & Klionsky, D. J. (2010) Eaten alive: a history of macroautophagy. *Nature Cell Biology.* 12 (9), 814–822.

Yoshida, K., Schuenemann, V. J., Cano, L. M., Pais, M., Mishra, B., Sharma, R., Lanz, C., Martin, F. N., Kamoun, S. & Krause, J. (2013) The rise and fall of the Phytophthora infestans lineage that triggered the Irish potato famine. *Elife.* 2 e00731.

Zaffagnini, M., Michelet, L., Marchand, C., Sparla, F., Decottignies, P., Le Maréchal, P., Miginiac-Maslow, M., Noctor, G., Trost, P. & Lemaire, S. D. (2007) The thioredoxin-independent isoform of chloroplastic glyceraldehyde-3-phosphate dehydrogenase is selectively regulated by glutathionylation. *The FEBS Journal.* 274 (1), 212–226.

Zavaliev, R. & Dong, X. (2024) NPR1, a key immune regulator for plant survival under biotic and abiotic stresses. *Molecular Cell.* 84 (1), 131–141.

Zavaliev, R., Mohan, R., Chen, T. & Dong, X. (2020) Formation of NPR1 condensates promotes cell survival during the plant immune response. *Cell.* 182 (5), 1093–1108. e18.

Zeng, Y., Xu, S., Wei, Y., Zhang, X., Wang, Q., Jia, Y., Wang, W., Han, L., Chen, Z. & Wang, Z. (2021) The PB1 protein of influenza A virus inhibits the innate immune response by targeting MAVS for NBR1-mediated selective autophagic degradation. *PLoS Pathogens.* 17 (2), e1009300.

Zhou, J., Wang, X., He, Y., Sang, T., Wang, P., Dai, S., Zhang, S. & Meng, X. (2020) Differential phosphorylation of the transcription factor WRKY33 by the protein kinases CPK5/CPK6 and MPK3/MPK6 cooperatively regulates camalexin biosynthesis in Arabidopsis. *Plant Cell.* 32 (8), 2621–2638.

Zhou, J., Trifa, Y., Silva, H., Pontier, D., Lam, E., Shah, J. & Klessig, D. F. (2000) NPR1 differentially interacts with members of the TGA/OBF family of transcription factors that bind an element of the PR-1 gene required for induction by salicylic acid. *Molecular Plant-Microbe Interactions.* 13 (2), 191–202.

Zhu, Y., Wu, C., Deng, Y., Yuan, W., Zhang, T. & Lu, J. (2024) Recent advances in virulence of a broad host range plant pathogen Sclerotinia sclerotiorum: a mini-review. *Frontiers in Microbiology.* 15 1424130.

Zientara-Rytter, K., Łukomska, J., Moniuszko, G., Gwozdecki, R., Surowiecki, P., Lewandowska, M., Liszewska, F., Wawrzyńska, A. & Sirko, A. (2011) Identification and functional analysis of Joka2, a tobacco member of the family of selective autophagy cargo receptors. *Autophagy.* 7 (10), 1145–1158.

Zientara-Rytter, K. & Sirko, A. (2014) Significant role of PB1 and UBA domains in multimerization of Joka2, a selective autophagy cargo receptor from tobacco. *Frontiers in Plant Science.* 5 13.

Zipfel, C., Kunze, G., Chinchilla, D., Caniard, A., Jones, J. D., Boller, T. & Felix, G. (2006) Perception of the bacterial PAMP EF-Tu by the receptor EFR restricts Agrobacterium-mediated transformation. *Cell.* 125 (4), 749–760.

Zvereva, A. S., Golyaev, V., Turco, S., Gubaeva, E. G., Rajeswaran, R., Schepetilnikov, M. V., Srour, O., Ryabova, L. A., Boller, T. & Pooggin, M. M. (2016) Viral protein suppresses oxidative burst and salicylic acid-dependent autophagy and facilitates bacterial growth on virus-infected plants. *New Phytologist.* 211 (3), 1020–1034.